

# **TNO Defence, Security and Safety**

**ONGERUBRICEERD**

Kampweg 5  
P.O. Box 23  
3769 ZG Soesterberg  
The Netherlands

[www.tno.nl](http://www.tno.nl)

T +31 34 635 62 11  
F +31 34 635 39 77  
[info-DenV@tno.nl](mailto:info-DenV@tno.nl)

**TNO-DV 2010 C435**

## **Mesopic vision and public lighting – A literature review and a face recognition experiment**

|                       |  |
|-----------------------|--|
| Date                  | December 2010  |
| Author(s)             | ing. J.W.A.M. Alferdinck<br>dr. M.A. Hogervorst<br>prof. dr. A.M.J. van Eijk<br>dr. J.T. Kusmierczyk |
| Assignor              | Ministry of Infrastructure and Environment (I&M), Den Haag ,<br>Netherlands                          |
| Project number        | 032.31561  |
| Classification report | Ongerubriceerd   |
| Title                 | Ongerubriceerd   |
| Abstract              | Ongerubriceerd   |
| Report text           | Ongerubriceerd   |
| Appendices            | Ongerubriceerd   |
| Number of pages       | 89 (incl. appendices)  |
| Number of appendices  | 3  |

All rights reserved. No part of this report may be reproduced and/or published in any form by print, photoprint, microfilm or any other means without the previous written permission from TNO.

All information which is classified according to Dutch regulations shall be treated by the recipient in the same way as classified information of corresponding value in his own country. No part of this information will be disclosed to any third party.

In case this report was drafted on instructions, the rights and obligations of contracting parties are subject to either the Standard Conditions for Research Instructions given to TNO, or the relevant agreement concluded between the contracting parties. Submitting the report for inspection to parties who have a direct interest is permitted.

© 2011 TNO

**ONGERUBRICEERD**



## Samenvatting

### Vraagstelling

Het Ministerie van Infrastructuur en Milieu (I&M) heeft in navolging van de adviezen van de - door haar in 2007 ingestelde - Taskforce Verlichting een onderzoek ingesteld om vast te stellen in hoeverre er in de openbare verlichting energie kan worden bespaard door onder andere toepassing van lichtbronnen die geoptimaliseerd zijn voor mesopisch zien. Aanleiding voor dit onderzoek is een recente CIE-publicatie over mesopisch zien en de opkomst van ledverlichting waarmee relatief eenvoudig spectra zijn te optimaliseren.

Het spectrum van verlichting dat geoptimaliseerd is voor mesopisch zien bevat relatief veel blauwachtig licht (hogere S/P-ratio) en is daardoor effectief voor perifere visuele taken bij mesopische lichtniveaus. Omdat de wetenschappelijke inzichten met betrekking tot mesopisch zien nog onvoldoende uitgekristalliseerd zijn voor het aanpassen van de huidige normen voor openbare verlichting, is een aantal vragen met betrekking tot mesopisch zien bij openbare verlichting onderzocht. We hebben een literatuuronderzoek uitgevoerd naar adaptatie, effect van leeftijd, atmosferische verstrooiing, en gezichtsherkenning. Daarnaast is er een gezichtsherkenningsexperiment uitgevoerd bij verschillende lichtspectra.

### Werkwijze

In het literatuuronderzoek hebben we ons gericht op het modeleren van adaptatieluminantie, het effect van leeftijd de waarnemer op S/P-ratio, de atmosferische verstrooiing en gezichtsherkenning bij lichtbronnen die geoptimaliseerd zijn voor mesopisch zien. In het gezichtsherkenningsexperiment hebben wij in een gesimuleerde woonstraat de gezichtsherkenningsafstand gemeten van doelpersonen op verschillende posities en bij verschillende lichtniveaus. Er werden zes verschillende lichtbronnen gebruikt voor de verlichting: een warmwitte fluorescentielamp (S/P=1.26), een hogedruk natrium lamp (S/P=0.52), twee witte ledlampen (3000 K, S/P=1,16 en 4500 K, S/P=1,61), en twee ledlampen met hoge S/P-ratio's van 2,73 en 3,16. Twee groepen (jong, gem.: 16,5 jaar; oud, gem.: 60,2 jaar) van in totaal 45 proefpersonen beoordeelden de herkenbaarheid van de gezichten van de doelpersonen. We hebben de verticale verlichtingssterkte en halfcilindrische verlichtingssterkte gemeten op de gezichten van de doelpersonen.

De mesopische verlichtingssterkten werden berekend met het CIE-model.

### Resultaten

#### Literatuuronderzoek

- Het visuele adaptatiesysteem is complex, maar er zijn modellen beschikbaar voor de berekening van het tijdsverloop van de adaptatie, dat tot 3 minuten kan duren voor de luminanties in de openbare verlichting ( $<2 \text{ cd/m}^2$ ). De adaptatie wordt beïnvloed door oogbewegingen en de maskerende verblinding (*disability glare*) en is nooit optimaal in praktische situaties. Er is geen betrouwbaar model dat rekening houdt met de oogbewegingen en de luminantieverdelingen in reële verkeerssituaties.
- Een lichtbron met een S/P-ratio van 3 verstrooit slechts 10% meer licht in een standaard atmosfeer dan een warmwitte lichtbron (S/P=1,23). Bij een lager meteorologisch zicht (heilig, mistig) is er geen verschil in verstrooiing tussen deze lichtbronnen.

- De effectieve S/P-ratio van lichtbronnen daalt met toenemende leeftijd van de waarnemer als gevolg van de vergeling van het oogmedia. Voor 80-jarige is de S/P-ratio van lichtbronnen voor openbare verlichting 10% tot 25% lager dan voor een 30-jarige.
- In enkele studies op het gebied van gezichtsherkenning wordt geconcludeerd dat een grotere kleurweergave-index leidt tot grotere herkenningsafstanden. Andere studies stellen dat kleur geen belangrijke rol speelt en dat alleen in situaties van zeer slechte beelden en bij de drempelniveaus de kleur een effect zou kunnen hebben.

#### Gezichtsherkenningsexperiment

In het experiment is er geen effect gevonden van de spectra van de zes lichtbronnen op de gezichtsherkenningsafstand. De herkenningsafstand is sterk afhankelijk van de verticale verlichtingssterkte op het gezicht van de doelpersonen en kan worden beschreven met een wortelfunctie in de vorm  $y = a \cdot x^{0,5}$ . De mesopische en de half-cilindrische verlichtingssterkte geven geen betere omschrijving voor de gezichtsherkenningsafstand dan de normale verticale fotopische verlichtingssterkte. De herkenningsafstand voor jongeren is gemiddeld een factor 1,7 groter dan voor ouderen.

#### Conclusie

Uit het literatuuronderzoek kunnen we concluderen dat er nuttige adaptatiemodellen bestaan, maar dat deze moeten worden verbeterd om rekening te houden met oogbewegingen en de luminantieverdelingen in reële verkeerssituaties. Voorlopig wordt geadviseerd de adaptatieluminantie gelijk te stellen aan de som van de gemiddelde luminantie van de scène en de sluiertiluminantie als gevolg van de maskerende verblinding. Het blijkt dat de toename van de lichtvervuiling als gevolg van lichtbronnen met S/P-ratio tot 3, kan worden verwaarloosd. Bij de toepassing verlichting voor mesopisch zien moet rekening gehouden worden met het effect van de leeftijd op de S/P-ratio. Er is nog discussie over de vraag of kleur een belangrijke rol speelt bij gezichtsherkenning.

Uit de resultaten van het gezichtsherkenningsexperiment kunnen we concluderen dat het spectrum van de lampen geen rol speelt bij gezichtsherkenning. Dat betekent dat lichtbronnen met een hoge S/P-ratio dus niet slechter of beter presteren dan de conventionele lichtbronnen (fluorescentie, hogedruk natrium) en witte ledlampen met een S/P-ratio tussen 0,5 en 1,6. Gezichtsherkenning is een foveale visuele taak waarbij dus alleen het centrale deel van het visuele veld betrokken is en het mesopische effect geen rol blijkt te spelen.

## Summary

### Purpose

The Ministry of Infrastructure and Environment (I & M), has followed the advice of the - by her in 2007 established - Lighting Taskforce, and started an investigation to determine to what extent energy can be saved in public lighting by using light sources that are optimized for mesopic vision. The trigger for this investigation is a recent CIE publication on mesopic vision and the emergence of led lighting, whose light spectra are relatively easy to optimize.

The light spectrum optimized for mesopic vision contains a relatively high amount of bluish light (high S/P-ratio) and is therefore effective for peripheral visual tasks at mesopic light levels. Since the current scientific knowledge concerning mesopic vision is insufficient for changing standards for public lighting, we investigated a number of issues concerning mesopic vision and public lighting are investigated. We performed a literature review on light adaptation, effect of age, atmospheric scatter and face recognition and a face recognition experiment at various light spectra.

### Methods

In the literature review we focused on the modelling of adaptation luminance, effect of observers age on S/P-ratio, atmospheric scatter and face recognition for light sources optimized for mesopic vision.

In the face recognition experiment in a simulated residential area we measured the face recognition distance of target persons for various positions and light levels. Six different light sources were used for illumination: a warm white fluorescent lamp (S/P=1.26), a high pressure sodium (HPS; S/P=0.52), two white led lamps (3000 K, S/P=1.16 and 4500 K, S/P=1.61), and two led lamps with a high S/P-ratios of 2.73 and 3.16.

Two groups (young, mean: 16.5 years; old, mean: 60.2 years) of in total 45 subjects assessed the recognition of the faces of the target persons. We measured the vertical illuminance and semi-cylindrical illuminances at the faces of the target persons. The mesopic illuminances were calculated with the CIE-model.

### Results

#### Literature review

- The visual adaptation system is complex, but there are models available for the calculation of the time course of the adaptation process, which can last for 3 minutes for luminance levels in public lighting ( $<2 \text{ cd/m}^2$ ). The adaptation is affected by eye movements and disability glare and is never optimal in practical situations. There is no reliable model that takes into account eye movements and luminance distributions in real traffic situations.
- A light source with a S/P-ratio of 3 scatters only 10% more light in a standard atmosphere than a warm white light source (S/P-ratio = 1.23). For conditions with a lower meteorological visibility (haze, fog) there is no difference in scatter between these light sources.
- The effective S/P-ratio of light sources declines with the age of the observer due to the yellowing of the eye media. For an observer at an age of 80 years the S/P-ratio of light sources for public lighting is 10% to 25% lower than for a young observer of 30 years old.
- Some studies on face recognition indicate that a higher colour rendering index results in larger face recognition distances. Other studies state that colour does not

play an important role; only in situations of degraded pictures and at threshold levels the colour may have an effect.

#### Experiment

In the experiment no effect was found of the spectrum of the six light sources on the face recognition distance. The face recognition distance strongly depends on the vertical illuminance at the face of the target persons and can be described with a square root function in the form  $y = a \cdot x^{0.5}$ . The mesopic and semi-cylindrical illuminance do not give a better prediction of the face recognition distance than the common vertical photopic illuminance. On average, the young observers show a factor 1.7 larger recognition distance than the old observers.

#### Conclusions

From the literature review we can conclude that there are useful adaptation models, which should be refined in order to take eye movements and luminance distributions in real traffic situations into account. For the time being, it is advised to use the sum of the average scene luminance and the veiling luminance due to disability glare as adaptation luminance. It also appears that the increase of light pollution due to light sources with S/P-ratios up to 3 can be neglected, but we have to account for effect of the age on the S/P-ratio when light for mesopic vision is applied. It is still under debate whether the colour of the lighting plays an important role in face recognition.

From the face recognition experiment we can conclude that the spectra of the lamps do not play a role in face recognition. Thus, light sources with a high S/P-ratio do not perform worse or better than the conventional light sources (fluorescent, HPS) and white led lamps with S/P-ratios between 0.5 and 1.6. Face recognition is a foveal visual task where only the central part of the visual field is involved and where the mesopic effect does not play a role.

# Contents

|          |  |           |
|----------|--|-----------|
|          | <b>Samenvatting.....</b>                           | <b>3</b>  |
|          | <b>Summary .....</b>                               | <b>5</b>  |
| <b>1</b> | <b>Introduction.....</b>                           | <b>9</b>  |
| 1.1      | Research questions.....                            | 9         |
| <b>2</b> | <b>Literature review: Adaptation.....</b>          | <b>13</b> |
| 2.1      | General.....                                       | 13        |
| 2.2      | Temporal adaptation .....                          | 14        |
| 2.3      | Spatial contribution.....                          | 17        |
| 2.4      | Disability glare.....                              | 18        |
| 2.5      | Discussion.....                                    | 19        |
| 2.6      | Conclusion .....                                   | 20        |
| <b>3</b> | <b>Literature review: Effect of age.....</b>       | <b>21</b> |
| 3.1      | Introduction.....                                  | 21        |
| 3.2      | Literature.....                                    | 21        |
| 3.3      | Calculations .....                                 | 22        |
| 3.4      | Conclusions.....                                   | 24        |
| <b>4</b> | <b>Literature review: Atmospheric scatter.....</b> | <b>25</b> |
| 4.1      | Theory.....  | 25        |
| 4.2      | Theory of scattering .....                         | 25        |
| 4.3      | Scattering in the atmosphere.....                  | 28        |
| 4.4      | Extinction by the atmosphere.....                  | 31        |
| 4.5      | Quantitative scattering and extinction .....       | 31        |
| 4.6      | Light scatter of lamp spectra.....                 | 34        |
| 4.7      | Discussion.....                                    | 37        |
| 4.8      | Conclusions.....                                   | 38        |
| <b>5</b> | <b>Literature review: Face recognition.....</b>    | <b>39</b> |
| 5.1      | Introduction.....                                  | 39        |
| 5.2      | Literature.....                                    | 39        |
| 5.3      | Conclusion .....                                   | 42        |
| <b>6</b> | <b>Experiment: Face recognition.....</b>           | <b>43</b> |
| 6.1      | Introduction.....                                  | 43        |
| 6.2      | Methods .....                                      | 43        |
| 6.3      | Results.....                                       | 50        |
| 6.4      | Discussion.....                                    | 63        |
| 6.5      | Conclusions experiment face recognition.....       | 67        |
| <b>7</b> | <b>General discussion .....</b>                    | <b>69</b> |
| <b>8</b> | <b>Conclusions and recommendations .....</b>       | <b>71</b> |
| 8.1      | Conclusions literature review .....                | 71        |
| 8.2      | Conclusions face recognition experiment.....       | 71        |
| 8.3      | Recommendations.....                               | 72        |

|           |                               |           |
|-----------|-------------------------------|-----------|
| <b>9</b>  | <b>Acknowledgements .....</b> | <b>73</b> |
| <b>10</b> | <b>References.....</b>        | <b>75</b> |
| <b>11</b> | <b>Signature.....</b>         | <b>79</b> |

#### **Appendices**

A Subject Information

B Subject instruction and scoring form

C Mesopic model

# 1 Introduction

The Dutch Ministry of Infrastructure and Environment (I & M), has following the advice of the - by her in 2007 established - Lighting Taskforce, and started an investigation to determine to what extent energy can be saved in public lighting by using light sources that are optimized for mesopic vision. The Lighting Taskforce, in which the market stakeholders are represented, works together with the NL Agency on various measures that have to lead to a broad introduction of means and alternatives for achieving substantial energy savings in the lighting. For public lighting eleven actions have been identified to achieve this. The current investigation on the applicability of mesopic vision in practice follows closely the actions to increase knowledge on energy efficient lighting in the market, and eventually adapting quality guidelines to the latest findings.

The trigger for this investigation is the recently published CIE publication (CIE, 2010) on vision at relatively low light levels, which are applicable to public lighting and where the light spectrum plays an important role. The emergence of led lighting, whose light spectra are relatively easy to optimize, makes the question of the practical value of mesopic vision more urgent.

The research described in this report is advised by committee of experts, established by the Ministry of I & M. The committee has performed an additional survey on mesopic vision among experts of the international lighting community. The conclusions and recommendations of this report and the results of the survey will be presented to the Dutch Institution of Illuminating Engineering (NSVV) for revision of guidelines for public lighting.

## 1.1 Research questions

At several locations in the Netherlands various types of LED-lamps are tested for public lighting. In addition, lighting is developed that is optimized for low, so-called mesopic light levels, which in this report shall be denoted as *mesopic vision lighting* (MVL). Suppliers of MVL claim additional energy efficiency gains. At various locations in the Netherlands this type of lighting is installed, mostly at foot and bicycle paths (Figure 1).

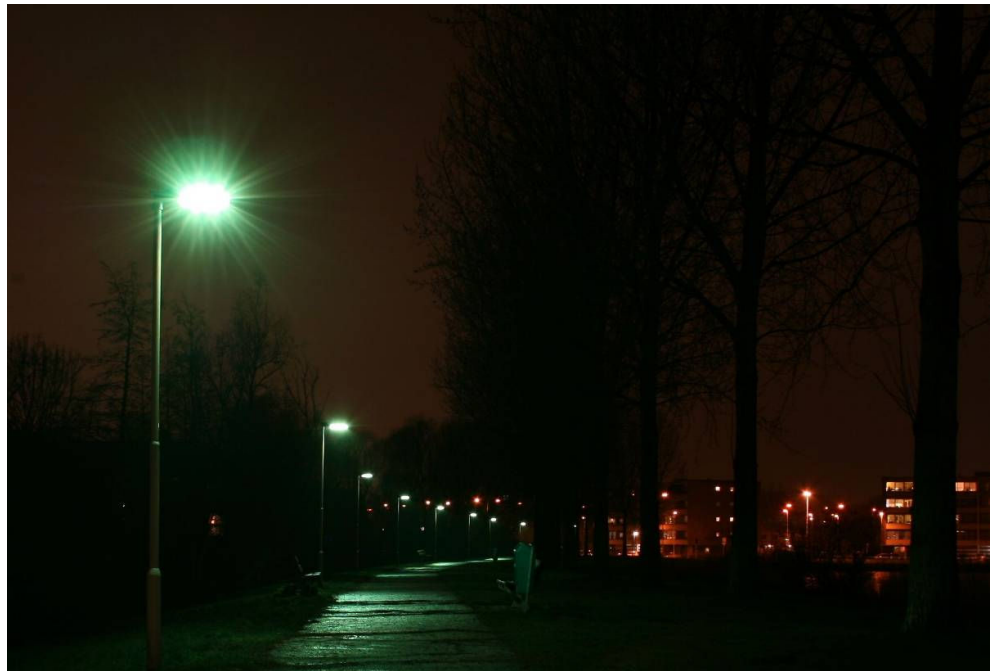


Figure 1 Public lighting designed for mesopic light levels at a bicycle path in Rotterdam (left) and conventional public lighting (right at background).

The impulse for the development of light sources for mesopic light levels was the research of recent years in the field of visual perception and public lighting. This research resulted in mesopic vision models that predict the effective light level better than the conventional light meters do (CIE, 2010). These mesopic models show that the actual effective light level is higher than normal, for mesopic light levels in the transition zone between night and day, when the light source contains more blue and green light, and peripheral perception is assumed.

Human perception at mesopic light levels is very complex; Stockman & Sharpe (2006) stated that this is “not an area for the fainthearted.” The spectral sensitivity of the eye depends on the light level, the location of the light stimulus on the retina, and the visual task of the observer. The current mesopic models are only an approximation of human vision in the mesopic range. There is still not enough knowledge of mesopic vision in practice to establish quality criteria for public lighting (Fors, 2010).

Van Bommel (2009) gives a condensed overview of mesopic vision and the problems associated with mesopic vision in public lighting. Under normal circumstances the light level is such that the human spectral sensitivity can be described by the spectral sensitivity of the cones in the eye. This condition is called photopic vision and starts from adaptation luminances of about 3 to 10  $\text{cd/m}^2$ . Under these circumstances, the spectral sensitivity of the eye is described by the standardized CIE (Commission Internationale de l'Éclairage) photopic  $V(\lambda)$  function which peaks at 555 nm (CIE, 2004a). Cones are concentrated on the fovea of the retina and the density rapidly decreases away from the fovea. When the light levels are low (for adaptation luminances lower than about 0.01 to 0.003  $\text{cd/m}^2$ ) the more sensitive rods take over and govern the human spectral sensitivity. Under these circumstances the spectral sensitivity of the eye can be described by the standardized CIE scotopic  $V'(\lambda)$  function, which peaks at a shorter (more bluish) wavelength of 505 nm (CIE, 2004a). Rods are present outside of the fovea with a maximum concentration of rods occurring at about 15 degrees in the

periphery. As a measure of how much more effective a light source is under scotopic conditions the *S/P*-ratio is used which is the ratio of the scotopic luminance (in which the spectrum of the light is weighted using the  $V'(\lambda)$ -curve) and the photopic luminance (in which the spectrum is weighted according to the standard  $V(\lambda)$ -curve).

When the adaptation state lies between that of photopic and scotopic vision this is referred to as mesopic vision. This occurs for adaptation light levels between approximately 10 and 0.003  $\text{cd/m}^2$ . Both rods and cones contribute to vision and colour vision is still present. Within this range the rods become gradually more important with a lowering in light adaptation state, and spectral sensitivity shifts towards shorter wavelengths (the “Purkinje effect”).



Figure 2 Simulated appearance of a red geranium and foliage in normal bright-light (photopic) vision (left), dusk (mesopic) vision (middle), and night (scotopic) vision (right). From: [http://en.wikipedia.org/wiki/Purkinje\\_effect](http://en.wikipedia.org/wiki/Purkinje_effect).

This suggests that under mesopic light conditions bluish light is more effective than white light. However, as pointed out by van Bommel (2009) there are various reasons that MVL may be less effective than expected based on just the spectral sensitivity curves of the rods and cones. Firstly, since the rods are present outside of the fovea, the mesopic effect only presents itself in off-axis tasks (outside of the fovea). Recent studies have found a positive effect of mesopic vision in the periphery on human performance with respect to reaction time of motorists (Rea & Bullough, 2007) and the detection of motorists, detection time, and recognition, as investigated in the MOVE-project (Alferdinck, 2006; Eloholma et al, 2005; Freiding et al, 2007; Walkey et al, 2007; Várady et al, 2007). MOVE has developed a quantitative model to deduce the effective luminance from the *S/P*-ratio and the adaptation luminance (Goodman et al., 2007; Alferdinck, 2008). Still, as pointed out by Knight et al (2007), peripheral (off-axis) vision is important for a number of tasks, e.g. it enables pedestrians to detect a stranger approaching from the side, before the stranger can be seen or recognized in the direct (on-axis) field of view. Also, off-axis vision enables drivers who are looking straight ahead to detect persons or objects before they unexpectedly move onto the driving lane. A second issue reason raised by van Bommel (2009) why MVL may be less effective in practice is that the crystalline lens in the eye turns yellowish with age. This effectively removes the bluish component from the mesopic light, and therefore makes the mesopic (more bluish) light less effective for elderly people (both for central vision as for peripheral vision). Thirdly, the adaptation state may be higher than expected based on the average road surface luminance. Often many other, often high value, luminance spots are present in the scene. Also, the scene is dynamic, so every once in a while spots with higher luminance appear. This shifts the adaptation state more into the direction of photopic lighting. Van Bommel (2009) points out that these dynamic variations may be especially important for pedestrians and less so for motorists for which the viewing direction and lighting variations are more constrained.

In order to tackle the questions raised by Van Bommel (2009) and to find out if and how MVL should be implemented in the standards for public lighting, a supervisory committee consisting of Dutch experts in the field of vision and public lighting listed a number of potential research items on mesopic vision. A part this item list is addressed in the current study, which consists of two major parts, a literature review and a face recognition experiment. The literature review is divided in the four parts. The purpose of the parts of the literature review and the face recognition experiment are addressed below.

#### *Literature review*

- *Adaptation.* The adaptation luminance is an important input for the mesopic models (CIE, 2010). The question is how the adaptation luminance can be defined and measured in practice, in a street scene with complex and dynamic non-uniform luminance distributions.
- *Effect of age.* When people get older the eye lens becomes more yellow and therefore transmits less light of short wavelengths. Since the mesopic effect only works when the short wavelengths can reach the retina the question is: How can we incorporate this age effect in mesopic models?
- *Atmospheric scatter.* Light pollution is caused by scattered light in the atmosphere. The question is: Will the colour (spectrum) of MVL scatter more or less in the atmosphere than conventional lamps for public lighting do?
- *Face recognition.* In residential areas the light levels of public lighting should be at such a level that the faces of pedestrians can be recognised at sufficient distance. The specific question is: What is the effect of the spectra of conventional public lighting and MVL on face recognition?

#### *Face recognition experiment*

The purpose of the face recognition experiment was to compare conventional lighting with lighting with a high S/P-ratio, especially designed for mesopic light levels. When lighting with high S/P-ratios is advised for public lighting it should at least not perform poorer than the existing lighting systems. Therefore the main question in this experiment is: Is there a difference in face recognition distance for light sources with a high S/P-ratio and conventional light sources?

This report first gives an overview of the literature studies. After that the face recognition experiment is addressed. Finally the results will be discussed and we will draw conclusions and will give recommendations.

## 2 Literature review: Adaptation

### 2.1 General

The human visual system can adjust to ambient light levels over a range of  $10^8$  or more. Over much of this range, we remain exquisitely sensitive to small differences in ambient light and the response to any given stimulus contrast remains approximately constant (Weber's law). Both neural and photochemical adaptation mechanisms are responsible for altering the sensitivity of the rod and cone systems and shifting the response profiles across the luminance range. Neural adaptation is a fast and symmetric process that can alter sensitivity within milliseconds, but the magnitude of its effect is limited. Photo pigment bleaching and regeneration, on the other hand, can have a much greater impact on sensitivity, but it is an asymmetric process, with potentially rapid bleaching followed by relatively slow regeneration and recovery of sensitivity. Adaptation processes have been extensively studied both physiologically and psychophysically (see for reviews Hood & Finkelstein, 1986; Shapley & Enroth-Cugell, 1984).

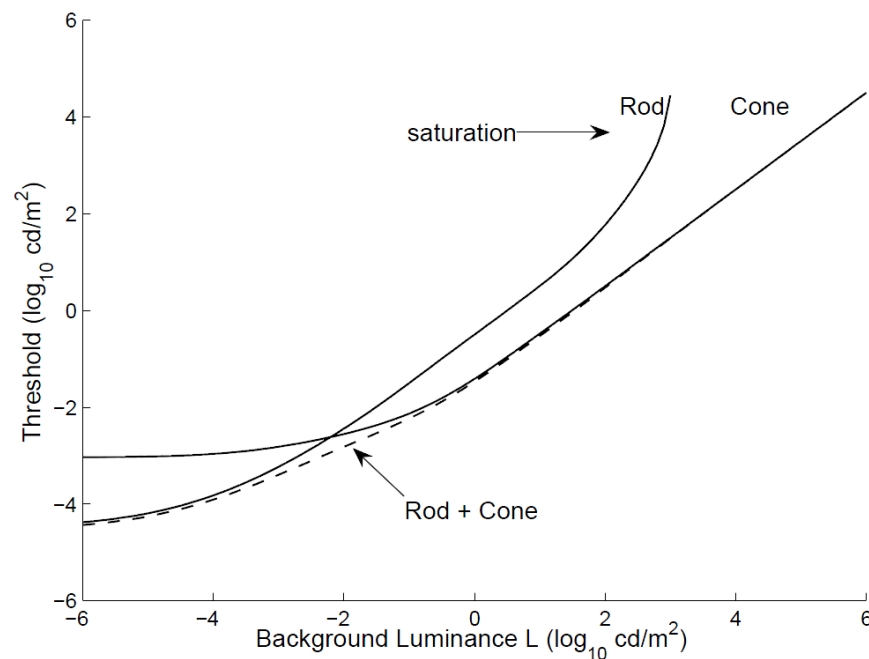


Figure 3 Threshold-versus-intensity functions. Derived by Irawan et al. (2005) from data by Blackwell (1946).

Adaptation is often described with the threshold versus intensity (TVI) functions, which give the threshold  $\Delta L$ , required to create a visible contrast at various background levels  $L$ . Figure 3 shows representative TVI functions for the rod and cone systems. Both curves are flat at extremely low luminance levels and become linear over the range where the visual system adapts well. The rod curve bends upward for high luminance due to saturation, because the rod system has a limited ability to adapt to brighter conditions.

Classically, the TVI functions are measured using spot on-background patterns. An observer is adapted to a circular background field of a particular luminance ( $L$ ) and then tested to see how much more intense ( $\Delta L$ ) a central spot has to be to be visible. In these experiments the observers are fully adapted to the backgrounds, so the TVI functions describe the optimal sensitivity of the visual system at the tested luminance levels. Under natural conditions, the visual system will only rarely achieve this sensitivity and will generally be maladapted to some degree. This has important consequences for visibility and other measures of visual performance. The effects of maladaptation on visual thresholds have been characterized with probe-on-flash experiments (Walraven et al., 1990), in which the observer adapts to a steady background, and is tested for visibility of a spot against another background. The stimulus is flashed to assure that the stimulus does not affect the adaptation state. Note that because of the active nature of the eye, maladaptation like this is a constant condition of human vision and has a significant impact on visibility under real-world conditions and should therefore be accounted for.

Irawan et al. (2005) developed a model to visualize scene visibility (a tone mapping operator) under time-varying, high dynamic range conditions. Their operator is based on a new generalized threshold model that extends the conventional threshold-versus-intensity (TVI) function to account for the viewer's adaptation state and a new temporal adaptation model that includes fast and slow neural mechanisms as well as photo-pigment bleaching.

## 2.2 Temporal adaptation

Irawan et al. (2005) recognise in total three mechanisms that control the dynamics of the adaptation state of the human eye. They ignore the effect of pupil size because of its relatively small effect. In their model they implement 1) the adaptation due to pigment bleaching, 2) slow neural adaptation and 3) fast neural adaptation. These three mechanisms differ for cones (photopic vision) and rods (scotopic vision). So, the model contains six adaptation curves in total, all with their own individual parameters, such as time constants and the light level range they are in charge.

In Figure 3 examples are shown of the three adaptation curves starting at respectively 15000, 1500, and 12.5 cd/m<sup>2</sup> and adapting to complete darkness. Immediately after the light is turned off the thresholds of the cones and the rods lowers quickly due to the fast neural system. Then the slow neural system takes over and finally the slow pigment bleaching of the rods completes the adaptation. Note that full adaptation from a high illuminance level takes about 20 minutes (1200 seconds).

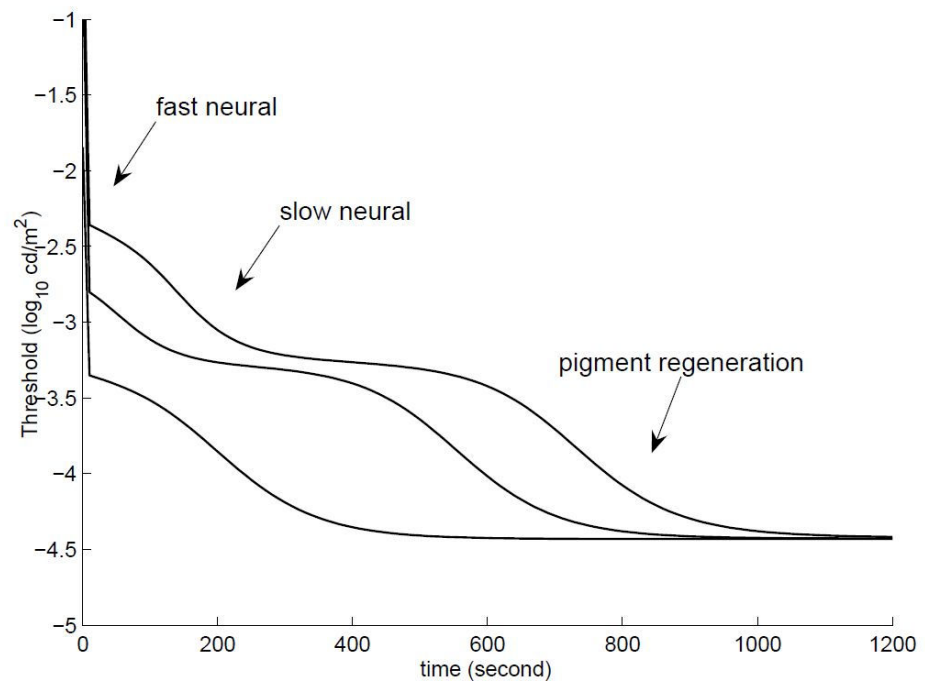


Figure 4 Modelling dark adaptation. The top curve starts with the eye adapted to 15000  $\text{cd/m}^2$ ; middle curve 1500  $\text{cd/m}^2$ ; bottom curve 12.5  $\text{cd/m}^2$ . Three parts of adaptation can be seen: fast neural adaptation, followed by the slow neural adaptation, and trailed by the pigment regeneration process (Figure 11 from Irawan et al., 2005).

For the application of MVL it is important to know the time course of adaptation in the range of light levels that are typical for the public lighting. We think that the most adaptation luminances in public lighting will not be higher than about 10  $\text{cd/m}^2$ . An exception must be made for illuminated billboards and buildings, which can have luminances of more than 100  $\text{cd/m}^2$ . But in general, this means that the adaptation process for these situations, after a fast neural adaptation, almost entirely is governed by the slow adaptation of the rods.

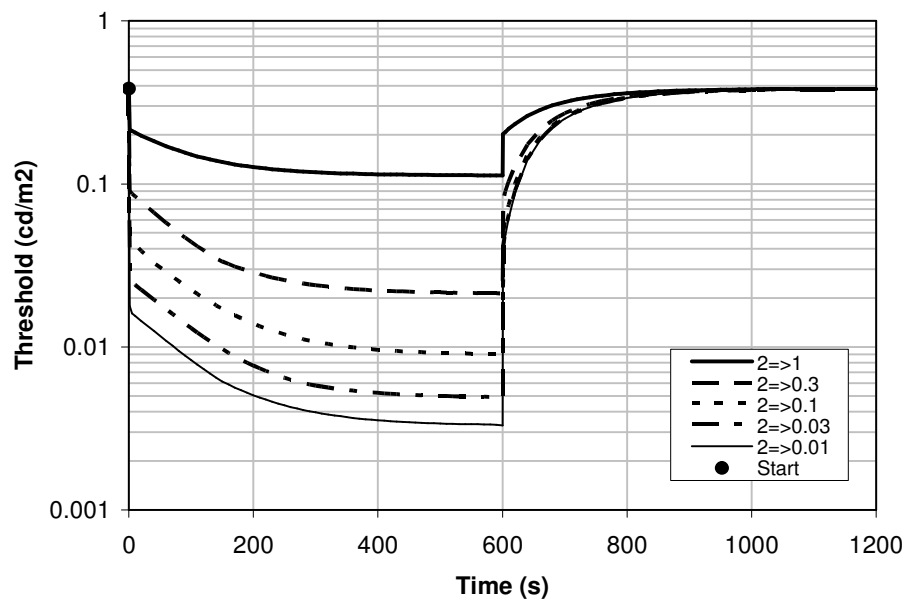


Figure 5 Time courses of the thresholds after lowering the background luminance from 2 cd/m<sup>2</sup> to various luminances in the mesopic range. After 600 seconds the background luminance is set to the starting luminance, using the model of Irawan et al. (2005).

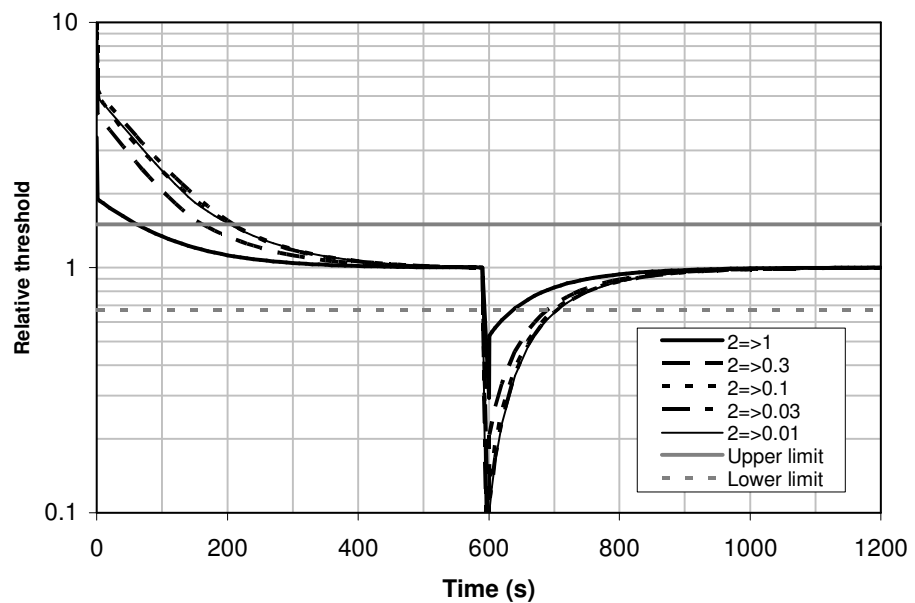


Figure 6 Time courses of the *relative* thresholds after lowering the background luminance from 2 cd/m<sup>2</sup> to various luminances in the mesopic range. After 600 seconds the background luminance is set to the starting luminance, using the model of Irawan et al. (2005). The limits are set at a factor 1.5 maladaptation.

When the observer is not fully adapted to the background luminance the visual perception will not be optimal. Therefore we calculated the time course of the threshold when the background luminance is switched from the 2 cd/m<sup>2</sup>, which is the luminance of a well-lit road, to various luminance levels in the mesopic range. In Figure 5 the

threshold as a function of the time after lowering the level is plotted. After 600 seconds the background level is switched on to the starting luminance. At the start, when background luminance is switched to a lower level, the adaptation is fast due to the fast neural adaptation mechanism. Then the adaptation is slow mainly due to the slow rod adaptation. When the background luminance is put back to its starting value the threshold increases to the starting value with an approximately twice as fast time course. In order to illustrate more clearly the time periods that the visual system is not fully adapted we plotted the relative threshold in Figure 6 based on the data of Figure 5. The maladaptation can be quantified by the relative threshold which is the ratio between the current threshold and the threshold at a moment the system is fully adapted. The relative threshold is 1 in case of full adaptation. The limits for the maladaptation in Figure 6 are arbitrary set at the factor 1.5. The crossings of these limits with the time courses show that 200 seconds after the background luminance is dropped the maladaptation is less than a relative threshold of 1.5 for end luminances lower than  $0.1 \text{ cd/m}^2$ ; for an end luminance of  $0.3$  and  $1 \text{ cd/m}^2$  this is reached after 150 and 60 seconds after the start. When switching from a low background luminances to  $2 \text{ cd/m}^2$  the adaptation is faster and the 1.5 maladaptation (relative threshold =  $1/1.5 = 0.67$ ) for all time courses passed 100 seconds. The calculation example shows that the time courses of a given start and end luminance can be calculated. The question is what criterion should be taken for the decision whether the maladaptation is acceptable or not. Based on a maximum maladaptation of a factor 1.5 the adaptation to low background luminances of  $0.01 \text{ cd/m}^2$  will take about 200 seconds, or more that 3 minutes. It is clear that the travelling speed is an important parameter for assessing the average adaptation luminance when a road users passes a road section with a lower road luminance.

## 2.3 Spatial contribution

The questions concerning spatial contribution are:

- How do the various object and lights in the visual scene contribute to the adaptation state?
- Is it possible to define an “equivalent” adaptation luminance that can be calculated from a complex luminance image?

### 2.3.1 Irawan et al. (2005)

In the method of Irawan et al. (2005) the adaptation luminance is simply set by the arithmetic mean of the luminance of the foveal part of the scene. The fovea is the circular central part of the retina and has a diameter of 2 degrees, which is in the application of Irawan in the centre of the image. Since they apply these method on (high dynamic range) image streams, in general, the adaptation luminance will change as a function of time.

Irawan et al. (2005) recognised the influence of eye fixations on the adaptation state. They state that the thresholds will be severely overestimated when a static eye position would be assumed. In reality a viewer looking at an image exhibits saccadic eye movements, fixating approximately 0.2 to 0.3 seconds at one area before jumping to another. As a result of these fixations the visual system adapts significantly. Because the image is constantly changing, the visual system will never be fully adapted. To account for the partial adaptation the authors track the average (global) adaptation for each luminance level as if the observer started in the average state and than adapted for a fixation time ( $t_f$ ) to a (local) luminance  $L$ . When the parameter  $t_f$  is infinite the adaptation state is equal to the local adaptation state; when the  $t_f$  is zero the adaptation

state is equal to the global adaptation state. Irawan et al. (2005) set the parameter  $t_f$  to 1/3 second. So, when there are brighter objects surrounding the lower luminance fixation spot the adaptation is always not complete and the visibility will not be optimal.

It should be noted that the eye movements of pedestrians are probably different from those of car drivers. It has been shown that the faster road users drive, the narrower the distribution of the fixations point is, also called “tunnel vision” (Rogé et al., 2004). Therefore we should account for the differences in eye movement behaviour of the various types of road users when these data will be used to determine the adaptation luminance.

### 2.3.2 Global and local adaptation luminance

The concepts of global and local adaptation luminance are used by Irawan et al. (2005). The global adaptation luminance is the average luminance of the whole scene that is perceived by the observer. The local luminance is the average luminance of a 2 degree spot in the centre of the scene, corresponding to the size of the fovea.

The simplest model for the measurement and the description of spatial contribution to the global adaptation luminance is  $L = E/\pi$ , where  $E$  is the illuminance (lx) measured on the eyes of the observer (in the viewing direction). Thus, the contribution of a light source in the visual field is weighted with the cosine of the angle between the viewing direction and the direction of the light source. Note that the for a homogeneous scene (equal luminance in all viewing directions) the formula  $L = E/\pi$  applies.

The local adaptation luminance in general is determined by the viewing direction of the road user. For a car drivers the viewing direction shall be mainly forward. For road users with a lower travelling speed, such as pedestrians, the eyes probably will move more to the side.

## 2.4 Disability glare

The adaptation luminance in the centre of the visual field is influenced by the effect of disability glare. Disability glare occurs when an observer looks at a relative dark part of the scene that is radiated by bright glare sources elsewhere in scene. Due to scattering of the light of these glare sources in the eye media of the observer, a so-called veiling luminance will arise that will decrease the contrast in the scene. This stray light will hinder the visual perception of objects in a scene. There are many models for the calculation of the veiling luminance. The simplest equation for the calculation of the veiling luminance,  $L_v$  (cd/m<sup>2</sup>), is the Stiles-Holladay equation (CIE, 2002).

$$L_v = E \frac{10}{\theta^2} \quad (1)$$

The illuminance at the eye due to the glare source is  $E$  (in lx) and  $\theta$  is the glare angle (in degrees) between the glare source and the viewing direction. The CIE (2002) has proposed a model based on various authors that takes account of the age and the eye colour of the observer.

$$L_v = E \left[ \frac{10}{\theta^3} + \left[ \frac{5}{\theta^2} + \frac{0.1p}{\theta} \right] \left[ 1 + \frac{A^4}{62.5} \right] + 0.0025p \right] \quad (2)$$

In this CIE general disability glare equation A represents the age of the observer in years and p the pigmentation factor of the observer's eyes, ranges from 0 for black eyes, via 0.5 for brown eyes to 1 for light eyes and 1.2 for light blue eyes.

It is obvious that in very dark scenes at mesopic light levels the adaptation luminance can be significantly influenced by bright light sources elsewhere in the scene. This glare effect will result in an adaptation luminance which has the veiling luminance as lower limit. Assume a public lighting situation in a residential area with a light pole that illuminates the observer's eyes with 3 lx and the angle between the light source and the viewing direction is 18 degrees. The veiling luminance according the Stiles-Holladay equation is  $L_v = 3.10/18^2 = 0.09 \text{ cd/m}^2$ . For a typical residential area illuminance of road surface due to public lighting varies between 0.2 lx and 3 lx (CEN, 2003a). The luminance of the road will therefore vary between 0.006 and 0.1  $\text{cd/m}^2$ . The adaptation luminance is the sum of the luminance due to the lamp and the veiling luminance. The adaptation luminance in the dark spots  $0.006 + 0.09 = 0.096 \text{ cd/m}^2$  and in the light spots  $0.09 + 0.1 = 0.19 \text{ cd/m}^2$ . It is obvious that in this example the adaptation luminance in darkest spots is completely determined by the veiling luminance. The conclusion therefore is that the veiling luminance due to disability glare determines the lower limit of the adaptation luminance. Due to the disability glare of road lighting luminaires the adaptation luminance is always higher than the road surface luminance. This glare effect will limit the mesopic effect.

## 2.5 Discussion

The adaptation of the visual system is very complex. The time courses are influenced by three different mechanisms for both cones and rod. This results in total six different adaptation processes different time constants, which come in charge at different light level ranges.

The local adaptation luminance can be defined as the luminance of a 2 degree spot in the viewing direction. The visual system will adapt to the luminance of the scene in this spot. In a static situation the local adaptation luminance will finally be equal to the local scene luminance. In practice the viewing directions will change with the eye movements. This will result in the constantly restarting the adaptation process with a new adaptation luminance. This means that the visual system never will be fully adapted. In the adaptation model of Irawan et al. (2005) is taken account for this maladaptation by combining the local and global adaptation luminance, assuming a certain eye movement behaviour. In practice on the road the eye movement behaviour is different for the various road users. It is not clear yet how to implement this eye movement behaviour in a reliable and useful model for the determination of the adaptation luminance on the road. It is possible to measure the eye movements of road users while driving. The result will be useful for the improvement of the adaptation models.

The local adaptation luminance will be influenced by brighter objects in the periphery. The lower limit of the local adaptation luminance will be determined by the veiling luminance caused by the disability glare. This veiling luminance can be calculated with well-founded formulas. The question is however what the veiling luminance will be in practice on the road, where the veiling luminance will be determined by the luminances, dimensions, and locations of the object in the visual field of the road user. It is

recommended to inventory luminance distributions and the veiling luminance of the various road types, in order to determine the applicability of MVL.

In the design phase the influence of the disability glare due from the road lighting luminaires can be derived from the TI-value and the road luminance, which can be calculated with lighting calculation software (e.g. Dialux, Calculux).

In absence of proper adaptation models for the time being it advised to use the average scene luminance as adaptation luminance. To take account for disability glare the adaptation luminance should be increased with the veiling luminance.

## 2.6 Conclusion

- The adaptation of the visual system is rather complex. The time courses are influenced by three different mechanisms for both cones and rod. This results in total six different adaptation processes different time constants, which come in charge at different light level ranges. There are models for the calculation of the time courses of the adaptation process.
- The time course of the adaptation process for luminance levels in public lighting is mainly determined by the slow neural adaptation mechanism of the rods. The adaptation from a background luminance of  $2 \text{ cd/m}^2$  to a low background luminance of  $0.01 \text{ cd/m}^2$  will take about 200 seconds, or more that 3 minutes.
- The adaptation is affected by eye movements and therefore is in practical situations never optimal. There is a model that takes account for this effect, but we are not sure that this is applicable in traffic situations.
- The veiling luminance due to light scatter in the eye media, known as disability glare, can have much influence on the adaptation state. This is especially the case when the observer is locally adapted to a relative dark area with brighter objects in the periphery of the visual field. The minimum adaptation luminance is limited by the veiling luminance. This will in turn limit the mesopic effect.
- We recommend to inventory the luminance distributions of various roads and residential areas in order to determine the veiling luminance and the adaptation state in real traffic situations.
- In absence of proper adaptation models at this moment, it advised to use the average scene luminance as adaptation luminance. To take account for disability glare the adaptation luminance should be increased with the veiling luminance.

### 3 Literature review: Effect of age

#### 3.1 Introduction

When people get older the eye lens becomes more yellow and therefore transmits less light of short wavelengths. Since the mesopic effect only works when the short wavelengths can reach the retina the question is: How can we incorporate this effect in mesopic models? In this section we will show the results of a calculation of this effect based on a model for transmission of the eye media.

#### 3.2 Literature

At birth the crystalline lens is perfectly transparent and nearly colourless. At an old age a (healthy) lens is yellowish brown. Van Kraats & van Norren (2007) analyzed the literature on the absorption in the young and aging human eye media and derived five templates to provide an adequate description of the spectra from 300 to 700 nm for the lens, cornea, aqueous, and vitreous. Moreover, they deduced aging-trend functions which can be used to correct for media losses in the light entering the eye. Figure 7 shows the transmission of the human eye media as a function of age, according to the data of van der Kraats & van Norren (2007). The transmission decreases with age and is the most for the blue and green with wavelengths between 400 nm and 550 nm.

The question now is what influence this age effect has on the mesopic effect. The spectral sensitivity of the eye therefore should be weighted with this loss in transmission with increasing age.

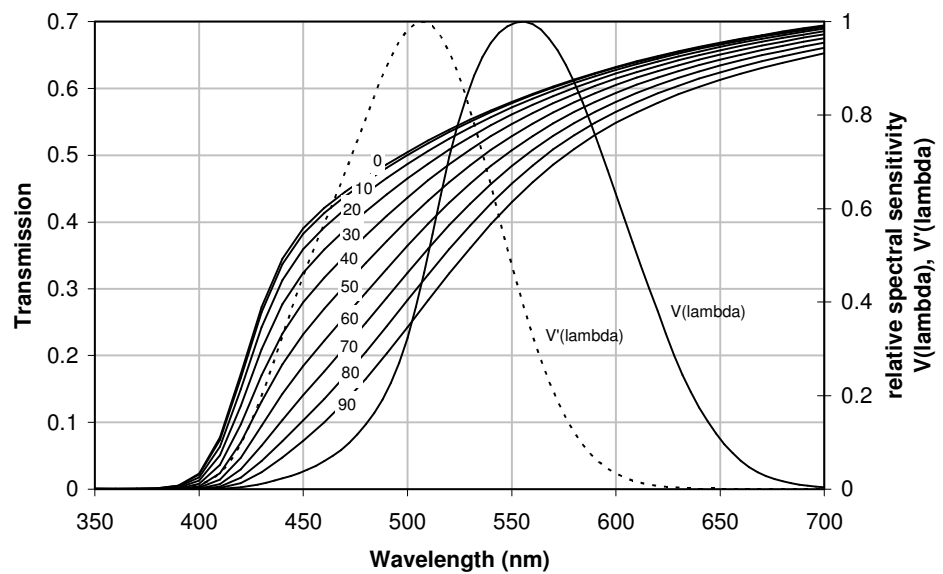


Figure 7 Transmission of the human eye media as a function of age (van der Kraats & van Norren, 2007) compared to the standard CIE spectral sensitivity functions of the eye,  $V(\lambda)$  for photopic vision and  $V'(\lambda)$  for scotopic vision.

### 3.3 Calculations

In order to calculate the effect of age on the mesopic effect it is necessary to know the average age of the subjects that originally were used for the determination of the standard CIE spectral sensitivity functions of the eye. The scotopic sensitivity function  $V'(\lambda)$  is based on 50 observers under 30 years of age (CIE, 1983). At this time we could not find the average age of the observers where the photopic sensitivity function  $V(\lambda)$  is based on, but we assume it is the same as for scotopic sensitivity function. Therefore we assume that the spectral sensitivities are determined at an age of 30 years. When the observers are older than this reference age the relative transmission of the eye can be calculated by dividing the spectral transmission at the current age by the transmission at the reference age. The relative transmission is plotted in Figure 8. The product of this relative spectral sensitivity and the standard sensitivity of the eye is the real spectral sensitivity of the eye at the current age. This current spectral sensitivity is used to calculate S/P-ratio at different ages.

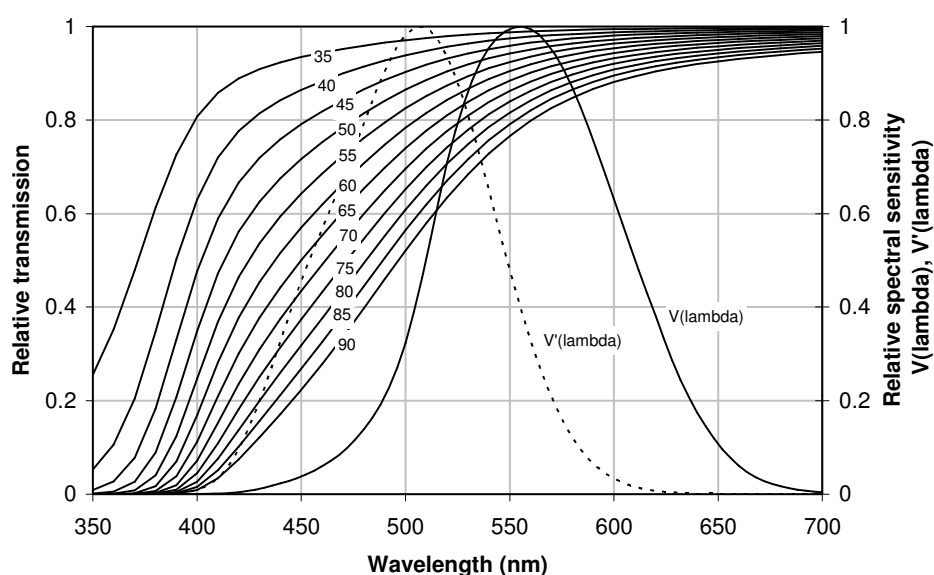


Figure 8 Relative transmission of the human eye media as a function of age (van der Kraats & van Norren, 2007) compared to the standard CIE spectral sensitivity functions of the eye,  $V(\lambda)$  for photopic vision and  $V'(\lambda)$  for scotopic vision. The reference age (on which age the  $V(\lambda)$  and  $V'(\lambda)$  are based) is 30 years with a relative transmission of 1 for all wavelengths.

Table 3-1 Light sources used for calculation age effect.

| Nr | Light source type    | Brand             | Type annotation      | Colour temperature $T_c$ (K) | S/P-ratio | Colour rendering index $R_a$ |
|----|----------------------|-------------------|----------------------|------------------------------|-----------|------------------------------|
| 1  | fluorescent          | Philips           | TLD36W/83            | 2981                         | 1.23      | 81                           |
| 2  | fluorescent          | Philips           | TLD36W/84            | 4008                         | 1.56      | 80                           |
| 3  | high pressure sodium | Philips           | SON-T                | 1965                         | 0.63      | 28                           |
| 4  | white led            | Philips, Lumileds | K2, cool-white       | 6073                         | 1.85      | 67                           |
| 5  | white led            | Philips, Lumileds | K2, warm-white       | 3175                         | 1.21      | 73                           |
| 6  | not white led        | Innolumis         | Ecowhite             | 3758                         | 2.36      | 27                           |
| 7  | not white led        | Innolumis         | Green                | 5539                         | 2.81      | 43                           |
| 8  | A                    | CIE standard      | incandescent, 2856 K | 2856                         | 1.41      | 100                          |
| 9  | D65                  | CIE standard      | daylight, 6500 K     | 6502                         | 2.46      | 100                          |
| 10 | equal energy         | -                 | -                    | 5454                         | 2.26      | 95                           |

In order to determine the effect of age on the S/P-ratio of the light sources we calculate the S/P-ratio of the set spectra of common light sources. These light sources are listed in Table 3-1 with the type, brand, type annotation and the photometric properties as colour temperature, colour rendering index (CRI), calculated with the standard colorimetric methods. In addition to the existing light sources (numbers 1 to 7) we added three standard illuminants (numbers 8 to 10) which are often used in colorimetric calculations.

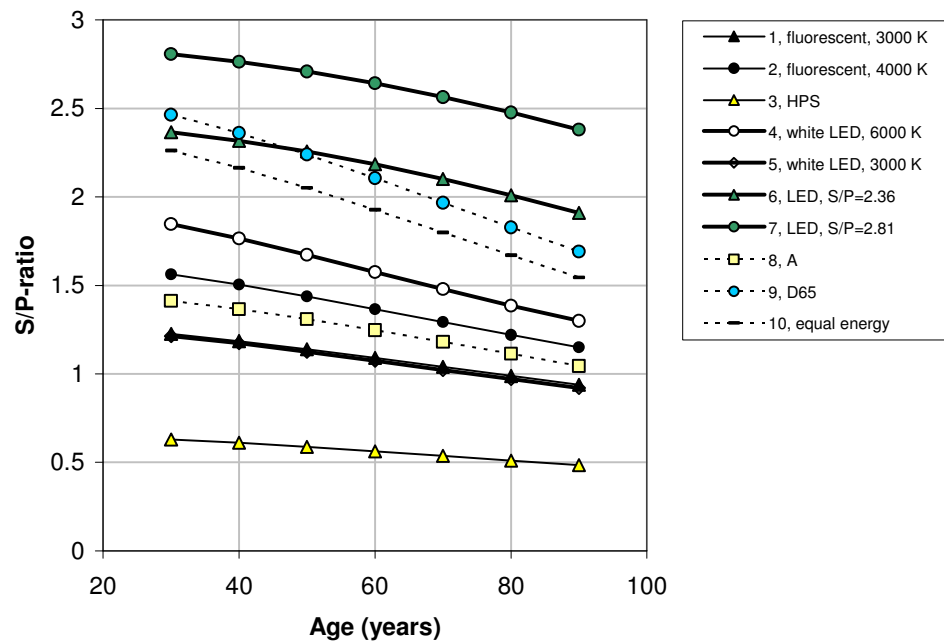


Figure 9 S/P-ratio as a function of age for different light sources for public lighting and standard illuminants (A, D65, equal energy).

Figure 9 shows the S/P-ratio as a function of the age of the observer for the light sources and the standard illuminants. Note that 30 years is set as the age of the standard young observer; the S/P-ratios at this age are equal to the S/P-ratios in Table 3-1 for standard conditions with young observers. From the figure it is clear that the S/P-ratio declines with increasing age for all light sources. For various light sources for public lighting this effect is 10% to 25% for an observer of 80 years.

### 3.4 Conclusions

- The effective S/P-ratio decreases slightly with increasing age of the observer. For various light sources for public lighting this effect is 10% to 25% for an observer of 80 years.
- When the mean age of a population is growing one has to take into account for a decrease of the mesopic effect.

## 4 Literature review: Atmospheric scatter

### 4.1 Theory

When electromagnetic radiation propagates through a medium, the intensity of radiant beam decreases with the distance travelled due to absorption and scattering of radiation by the medium. Absorption and scattering both remove photons from the beam. However, the absorption process removes the incident photon from the beam, whereas in a scattering process the incident photon changes propagation direction. This may cause stray radiation, i.e., a certain amount of radiant intensity is found in directions other than the main propagation direction of the beam. This latter process is relevant for the question that prompted the present study, i.e., to obtain a measure for the amount of stray light of street lighting.

In particular, there is interest in the amount of light that is scattered sideways or upward, since this creates ‘light pollution’, especially when the scattered light reflects once more off (low-level) clouds.

There are currently a number of light sources available for street lighting, which all have different spectra (light intensity versus wavelength). In an aim to minimize light pollution, there is thus an interest to know if the scattering process is wavelength dependent. If so, this may favour the selection of a particular light source for street lighting. The study reported here investigates the wavelength dependence of the scattering process. In the remainder of this text, a theoretical introduction of the scattering process is presented, based on standards reference books on this subject (Middleton, 1952; van der Hulst, 1981; Wolfe & Zissis, 1978). This is followed by the results of calculations for ‘typical’ atmospheric conditions as may be expected in Dutch cities (Kneizys, 1996).

### 4.2 Theory of scattering

In the Earth’s atmosphere, absorption and scattering is caused by molecules and aerosols (particles such as fine dust or water droplets). The combined effect of absorption and scattering is called extinction, and this quantity is generally expressed in [km<sup>-1</sup>]. Thus, the extinction  $\epsilon$  provides information on how much radiation is left after a certain propagation distance. This amount is often expressed as a transmission factor  $T$ , (in the limit of not too high values of  $\epsilon$ ) defined by:

$$T = \frac{I}{I_0} = \exp(-\epsilon R) \quad (3)$$

where  $R$  is the length of the propagation path (distance) in [km]. Although transmission is often used in engineering applications, it should be kept in mind that its value depends on  $R$ , whereas extinction is a property of the atmosphere itself.

The theory of scattering encompasses three domains that are distinguished on the basis of the dimensionless size parameter  $\alpha$ :

$$\alpha = \frac{\pi D}{\lambda} = \frac{2\pi r}{\lambda} = k r \quad (4)$$

where  $D$  and  $r$  are the diameter and radius of the scatterer, respectively,  $\lambda$  is the wavelength, and  $k$  is the wavenumber. If  $\alpha \ll 1$ , Rayleigh scattering applies; for  $\alpha \gg 1$  geometrical optics apply, and for the domain  $\alpha \approx 1$ , Mie scattering applies. Since we are interested in light pollution by street lights,  $\lambda$  is on the order of  $0.5 \mu\text{m}$ . This then suggests that scattering by molecules is described by Rayleigh scattering, scattering by aerosols by Mie scattering, and scattering by rain droplets and snow flakes by geometrical optics (cf. the rainbow). The three scattering theories are related: Rayleigh scattering and geometrical optics are limiting cases of the more complex Mie theory.

Within the framework of the present project, we will neglect geometrical optics since this only becomes relevant during rain. Rain causes a strong extinction of visible light, which leads to a total loss of all light within a few hundred meters. Consequently, the risk of light pollution is small.

Turning to the other limiting case, it suffices to state that the directionality and the wavelength dependence of the Rayleigh scattering  $I_R(\theta)$  are given by:

$$I_R(\theta) \propto \lambda^{-4} (1 + \cos^2 \theta) \quad (5)$$

where  $\theta$  is the angle between the incident beam and the direction of the scattered light. From this, it follows that blue light is more efficiently scattered than red light. Furthermore, it follows that 50% of the scattered light departs in a backwards direction (90-180 degrees) with respect to the propagation direction of the beam. The directional dependence of Rayleigh scattering is shown in the left panel of Figure 10.

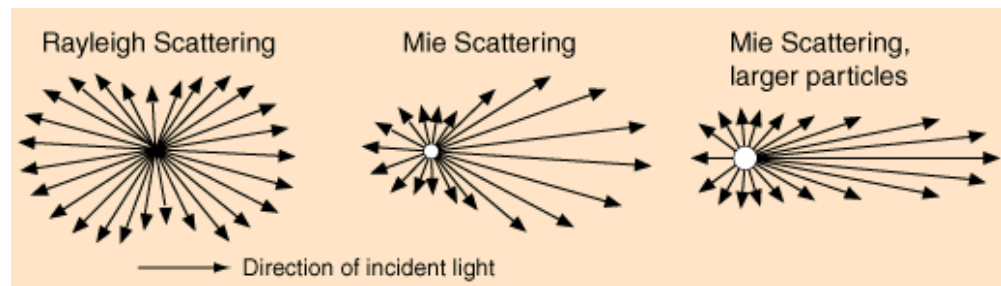


Figure 10 Directionality of scattering in the atmosphere.

The panel shows that the pattern is symmetrical, with stronger scattering in the forward and backward directions. In the case of street lighting, one might thus state that 50% of the Rayleigh scattering potentially contributes to light pollution.

Unfortunately, the directionality and the wavelength dependence of the Mie scattering are not easily expressed in a proportionality relation. The fundamental equations of Mie theory are the intensity distribution functions  $i_1$  and  $i_2$ . They denote the intensity of light, observed under an angle  $\theta$  and scattered from a spherical particle with dimensionless size  $\alpha$  and complex refractive index  $n$ , in the parallel and perpendicular polarization with respect to the plane of observation:

$$i_1(\alpha, n, \theta) = \left| \sum_{n=1}^{\infty} \frac{2n+1}{n(n+1)} (a_n \pi_n(\cos \theta) + b_n \tau_n(\cos \theta)) \right|^2 \quad (6)$$

$$i_2(\alpha, n, \theta) = \left| \sum_{n=1}^{\infty} \frac{2n+1}{n(n+1)} (a_n \tau_n(\cos \theta) + b_n \pi_n(\cos \theta)) \right|^2$$

where  $\pi_n$  and  $\tau_n$  are Legendre polynomials. If the incident light is unpolarized (and the scatterer is spherical), the total light intensity  $I_{sca}(\theta)$  that is scattered in direction  $\theta$  is given by:

$$I_{sca}(\theta) = E \frac{\lambda^2}{4\pi^2} \left( \frac{i_1 + i_2}{2} \right) \quad [\text{W} \cdot \text{sr}^{-1}] \quad (7)$$

where  $E$  is the radiance in  $[\text{W}/\text{m}^2]$  of the incident light. The requirement of unpolarized light is not necessarily fulfilled for street lights: a refinement of equation (6) is possible to account for polarized light. The assumption that the scatterer is spherical is generally only fulfilled for hygroscopic particles in the atmosphere (water droplets). Dust, black carbon and sand tend to be irregularly shaped. Exact solutions of the Mie theory for non-spherical scatterers are rare and computationally demanding; since the exact shapes and orientations of the non-spherical scatterers in the atmosphere are not known, it is customary to assume an ensemble of spherical scatterers.

The so-called angular cross section  $\sigma_{sca}(\theta)$  is the normalized intensity of scattered light in direction  $\theta$ :

$$\sigma_{sca}^2(\theta) = \frac{I(\theta)}{E} = \frac{\lambda^2}{4\pi^2} \left( \frac{i_1 + i_2}{2} \right) \quad [\text{m}^2 \cdot \text{sr}^{-1}] \quad (8)$$

The integral of  $\sigma_{sca}(\theta)$  over the total scattering sphere yields the total amount of light scattered, which is referred to as the total scattering cross section  $\sigma_{sca}$ . Although the precise directionality of the scattering is complex, a general rule of thumb is that Mie scattering favours the forward directions and more so when the dimensionless size parameter  $\alpha$  increases. This is indicated in the middle and right panels of Figure 10.

The scattering by an ensemble of particles is described by the volume coefficients  $\beta$ . Since scattering of each particle is incoherent with scattering by another particle, the coefficients  $\beta$  can be calculated as a simple multiplication of the individual cross sections and the number of particles. For the volume angular scattering coefficient  $\beta_{sca}(\theta)$  we find:

$$\beta_{sca}(\theta) = N \sigma_{sca}(\theta) \quad [\text{m}^{-1} \cdot \text{sr}^{-1}] \quad (9)$$

The number of particles  $N$  is given by the particle size distribution (PSD) that describes the number of particles as function of size:

$$N = \int n(r) dr \quad [\text{m}^{-3}] \quad (10)$$

Combining equations (8), (9) and (10), we find:

$$\beta_{sca}(\theta) = \frac{\lambda^2}{4\pi^2} \int 0.5 \cdot [i_1(\theta) + i_2(\theta)] n(r) dr \quad [\text{m}^{-1} \cdot \text{sr}^{-1}] \quad (11)$$

The directionality of the scattering is generally expressed in the normalized phase function  $P(\theta)$ . This quantity gives the ratio of the energy scattered per unit solid angle in a given direction to the average energy scattered per unit solid angle in all directions:

$$P(\theta) = \frac{4\pi \beta_{sca}(\theta)}{\beta_{sca}} \quad (12)$$

As mentioned above, equation 11 applies to an ensemble of aerosol particles. The evaluation of equation 11 thus requires knowledge about the number of aerosol particles of a particular size (to evaluate the dimensionless size parameter) and composition (to evaluate the refractive index).

### 4.3 Scattering in the atmosphere

The molecular composition of the atmosphere is fairly constant. Neglecting locally generated pollution (such as gases emitted by car exhausts), the atmospheric concentration of molecular species is basically a function of pressure and temperature. The water vapour concentration is generally considered as a variable, depending on the humidity. Engineering codes are available that evaluate the absorption and scattering of molecules in the atmosphere; at TNO, the MODTRAN code is used for this purpose (Kneizys et al., 1996). Figure 11 provides the scattering cross section of Rayleigh scattering at street level for a “typical” atmosphere in The Netherlands. The cross section shown in figure 2 does not vary significantly for the dynamic ranges of pressure, temperature and humidity encountered in The Netherlands.

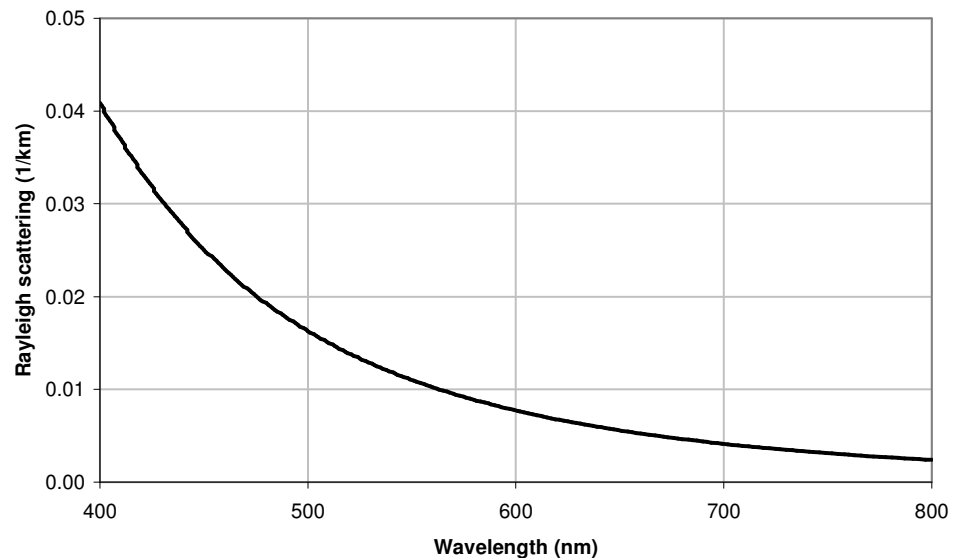


Figure 11 Cross section for molecular (Rayleigh) scattering for typical Dutch conditions at street level.

The Mie scattering due to aerosols in the Earth's atmosphere is more difficult to assess than molecular scattering. As shown by equation 11, the evaluation of the Mie integral requires knowledge about the size and chemical composition of the individual aerosol

particles present in the atmosphere. These two quantities vary greatly in space and time. In part, this is due to the irregular distribution of aerosol sources over the Earth. Natural aerosol sources, such as the oceans (sea spray), may cover large areas and are always present. Anthropogenic sources, such as industrial stack plumes or car exhausts, may be much more localized in space and time. Aerosols come in many sizes: the smallest are on the order of nanometres, whereas the larger ones reach several tens of microns. It is possible to define ‘typical’ sizes for various types of aerosols (such as sea-spray, volcanic ash, black carbon, etc), but there is a considerable spread around these typical values and size ranges of aerosol types strongly overlap. The inertia of the aerosols causes them to be less efficiently dispersed through the atmosphere; furthermore gravitation and scavenging (rain) acts to remove the aerosols from the atmosphere. These dynamic processes are size-dependent and result in significant gradients in the concentration (horizontal and vertical) of the aerosols.

The above introduction on aerosols serves as a caution that it is not straightforward to define the proper aerosol mixture (in size and composition) that is input to the Mie calculation. Nevertheless, we have constructed two ‘typical’ mixtures that could be encountered in Dutch cities. One mixture is labelled ‘marine-continental’ and represents a relatively clean atmosphere in a coastal city such as The Hague. It consists of 5% organic components, 5% water-soluble anthropogenic aerosols and 40% sea salt aerosols. The other is labelled ‘industrial aerosol’ and represents a more polluted atmosphere with 30% organic components, 30% water-soluble anthropogenic aerosols and 40% sea salt aerosols. For demonstration purposes, we have also added an (artificial) distribution that has a very high content of organic and anthropogenic aerosols, and negligible contributions of sea salt.

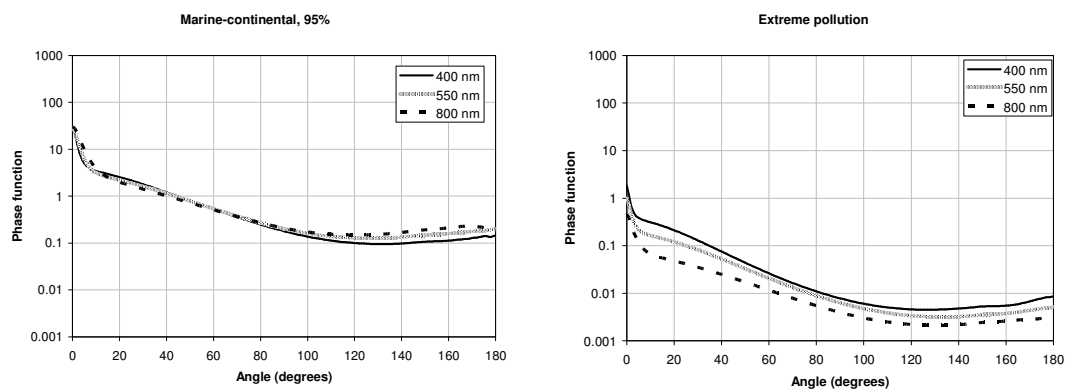


Figure 12 Wavelength dependence of phase functions. Wavelengths: 400 nm, 550 nm, 800 nm. Left panel: marine-continental aerosol mixture (humidity = 95%). Right panel: artificial ‘extreme pollution’ mixture. The angle at the x-axis is the angle between the incident beam and the direction of the scattered light.

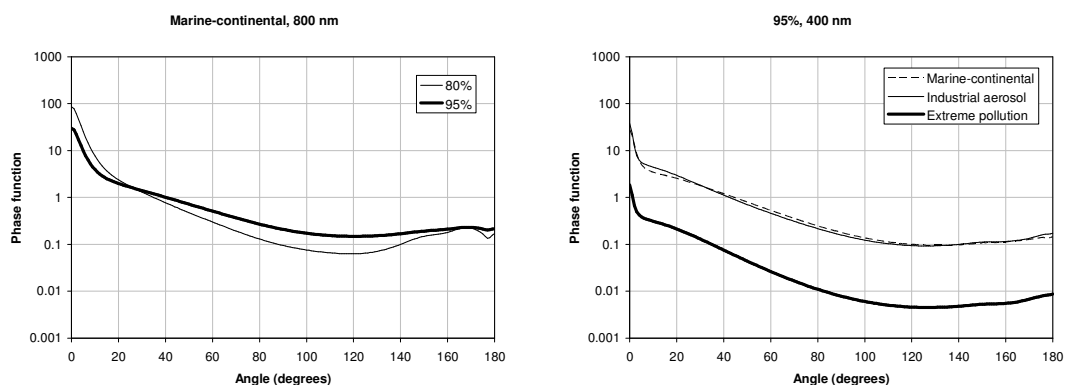


Figure 13 Left panel: phase functions for a wavelength of 800 nm and a marine-continental aerosol mixture at two humidities (80%, 95%). Right panel: phase functions for a wavelength of 400 nm and 95% humidity and three aerosol mixtures (marine-continental, industrial aerosol, (artificial) extreme pollution). The angle at the x-axis is the angle between the incident beam and the direction of the scattered light.

The plots shown in Figure 12 and Figure 13 represent the most prominent differences in the (non-normalized) phase functions. Most importantly, Figure 12 shows that the wavelength dependence of the phase functions is weak. The right panel of Figure 12 shows that the artificial aerosol distribution (extreme pollution) has the most prominent wavelength dependence. However, the shape of the phase function remains rather constant. This implies that there is less absolute scattering in a backward direction at 800 nm than at 400 nm, but that the relative amount of scattering in a backward direction is rather constant. The left panel of Figure 13 demonstrates that the ambient relative humidity has a modest effect on the phase functions: the panel shows the most prominent effect, which was found for the marine-continental distribution at 800 nm. This effect is caused by the changes in size of the hygroscopic water droplets, and is thus most prominent for the aerosol distribution with a relatively large percentage of sea salt and water-soluble anthropogenic aerosols. The right panel of Figure 13 shows that the absolute scattering efficiency drops significantly when the sea salt is removed from the distribution. The panel shows the effect at 400 nm, which is the wavelength at which the effect is most prominent. The sea salt aerosols have sizes of the order of a micron, corresponding to a dimensionless size parameter close to unity for the wavelengths under consideration. Consequently, their scattering efficiency is greater than that of the relatively small (sub-micron) organic components.

Figure 12 and Figure 13 demonstrate that it is reasonable to assume a generic (normalized) phase function for the atmospheric aerosols in the wavelength domain of interest. However, this only tells us that the percentage of light scattered in a given direction is constant. It does not tell us how much light is scattered. Figure 13 shows that the absolute amount of scattered light depends on the specific aerosols that are present in the atmosphere. Furthermore, it follows from Mie theory that the amount of scattered light depends on the number of aerosols that are present in the atmosphere, and that the absolute amount of scattering is wavelength dependent. As we will see in the next section, a typical aerosol loading of the atmosphere in a Dutch coastal city causes more intense scattering at 400 nm than at 800 nm, indicating that street lights having a spectrum that peaks at shorter wavelengths will be more intensely scattered and hence, contribute relatively more to light pollution.

## 4.4 Extinction by the atmosphere

As mentioned in the introduction, transmission losses in the atmosphere result from scattering and absorption. In the case of light pollution, scattering by molecules and aerosols redirects a percentage of the street lights towards the sky. This percentage can be evaluated from the phase functions and Rayleigh scattering efficiency presented in the previous sections. However, the effect of light pollution is not a local phenomenon: the scattered light (the “pollution”) will generally travel a certain distance through the Earth’s atmosphere, e.g., to the base of the clouds which are then illuminated. While propagating through the atmosphere, a certain percentage of the light is lost due to extinction effects, i.e., absorption and scattering by molecules and aerosols.

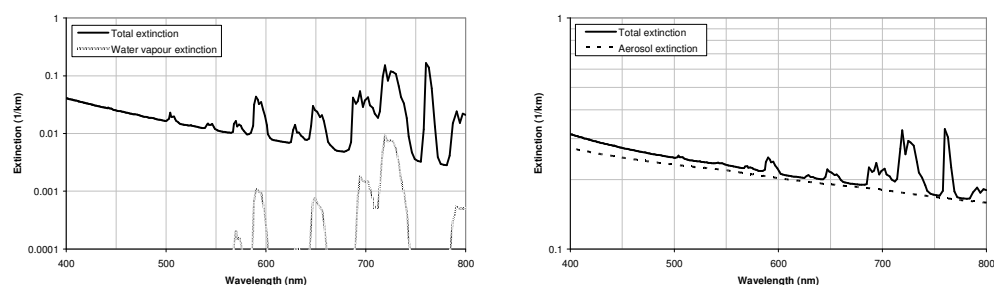


Figure 14 Extinction of the Earth’s atmosphere. Left panel: molecular effects. Right panel: molecular + aerosol effects. Black line: total extinction; Grey line: water vapour extinction; dashed line: aerosol extinction.

Figure 14 shows plots of the extinction of the Earth’s atmosphere, for a typical atmosphere over The Netherlands. The left panel shows the transmission due to molecules only. The smooth increase in extinction from longer to shorter wavelengths represents the increasing efficiency of the Rayleigh scattering. The “peaks” at longer wavelength represent molecular absorptions by water vapour and CO<sub>2</sub>. The absorption bands at 580, 650, 690 and 730 nm are due to water vapour and will become more pronounced when the relative humidity in the atmosphere increases. The right panel of Figure 14 shows the extinction due to molecules and aerosols. The aerosols (dashed line) do not give rise to absorption peaks, but cause a smooth increase of the extinction towards shorter wavelengths. All factors combined (black line in the right panel), the “minimal” extinction of the Earth’s atmosphere is found for the mid-interval, 500 – 700 nm (visual light). This implies that the light pollution due to street lamps emitting in this mid-interval will relatively efficiently propagate towards cloud bases. Note that the extinction in the mid-interval is about 0.25 km<sup>-1</sup>. This extinction corresponds to a meteorological visibility of about 12 km<sup>1</sup>.

## 4.5 Quantitative scattering and extinction

The previous sections have identified all the factors that contribute to light pollution. The primary process is the scattering of street light upwards (or away from the street), for which molecules (Rayleigh) and aerosols (Mie) are responsible. The secondary process is the propagation of the light pollution through the Earth’s atmosphere, where molecular and aerosol extinction cause transmission losses. In this section, some quantitative numbers will be assigned to these processes.

<sup>1</sup> Based on the definition that the meteorological visibility  $V$  equals to  $3/\epsilon$ , with  $\epsilon$  = extinction.

First, the primary process will be quantified. Figure 11 shows the absolute values of Rayleigh scattering for a typical atmosphere:  $0.04 \text{ km}^{-1}$  for 400 nm, decreasing to virtually zero at 800 nm. For simplicity, we will assume that all light that is scattered between 90 and 180 degrees contributes to light pollution. Because Rayleigh scattering is symmetrical, the absolute values in Figure 11 need to be divided by two.

For aerosol scattering, we will also assume that all light that is scattered between 90 and 180 degrees contributes to light pollution. To quantify this, we will integrate the phase functions between 90 and 180 degrees, and between 0 and 180 degrees. The ratio of these two integrals, multiplied by the total scattering cross section then provides the absolute value of “pollution”:

$$\beta_{\text{pollution}} = \frac{\int_{90}^{180} \beta_{\text{sca}}(\theta) d\theta}{\int_{0}^{180} \beta_{\text{sca}}(\theta) d\theta} \cdot \beta_{\text{sca}} \quad (13)$$

The ratio of the integrals is typically  $0.01 - 0.05$ , which indicates that just a few percent of the street light is scattered in a backwards direction. As mentioned before, the value of  $\beta_{\text{sca}}$  is a function of aerosol concentration, aerosol composition and wavelength. For the “typical” conditions under consideration in this study, we calculated that  $\beta_{\text{sca}}$  varies between  $0.05$  and  $0.5 \text{ km}^{-1}$ . Consequently,  $\beta_{\text{pollution}}$  is of the order of  $10^{-4} - 10^{-2} \text{ km}^{-1}$ . This order of magnitude calculation shows that aerosol scattering is at best of equal intensity as Rayleigh scattering, except when the atmosphere is extremely polluted.

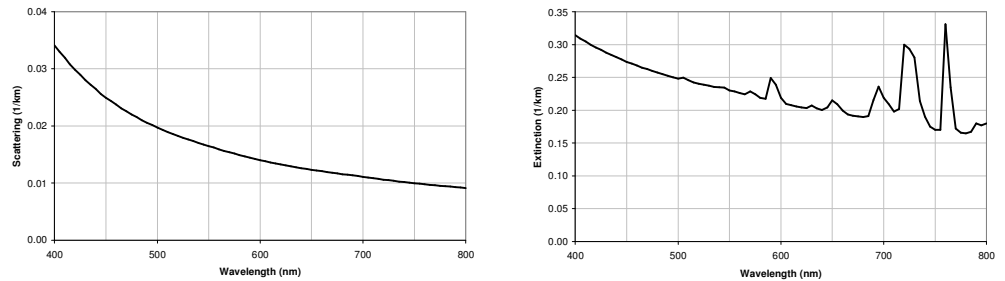


Figure 15 Quantitative functions  $f_s$  (left panel) and  $f_t$  (right panel) for scattering of street light and propagation through the atmosphere, respectively.

Addition of the Rayleigh scattering and the aerosol scattering provides the final cross section for the primary process: backward scattering of street light. This curve is shown in the left panel of Figure 15, and can be multiplied with the spectra of the street lamps and weighted with the spectral sensitivity of the eye on other to quantify the human visibility.

For the quantification we assume that a certain part the light of public lighting  $I_0$  leaks to the sky. This is typically a few percents of the whole luminous flux of the lamp. This light travellers upwards through the atmosphere. If there is a cloud the light will be reflected back to the observer at ground level. On the way to the cloud and back a part of the light will be scattered in the atmosphere. The scatter and the transmission is wavelength dependent. The scattered radiation  $I_{s1}$  in the atmosphere between lamp and

cloud can be expressed in the equation, where the path length  $R$  between ground and cloud and the scatter function of left panel of Figure 15 ( $f_s$ ) needs to be included:

$$I_{s1}(\lambda) = I_0(\lambda) \cdot (1 - e^{-f_s(\lambda) \cdot R}) \quad (14)$$

The radiation from the lamp that reached the cloud reflected at the cloud can be calculated with the transmission formula:

$$I_{cloud}(\lambda) = I_0(\lambda) \cdot e^{-f_t(\lambda) \cdot R} \cdot \rho \quad (15)$$

where  $f_t$  is the transmission function of right panel of Figure 15, and  $\rho$  is the reflection of the cloud, which we assume to be independent of wavelength (neutral colour).

The radiation that reached an observer on the ground  $I_{ground}$  has travelled twice through the distance ground-cloud and will be attenuated according the equation:

$$I_{ground}(\lambda) = I_0(\lambda) \cdot e^{-2f_t(\lambda) \cdot R} \cdot \rho \quad (16)$$

The reflected radiation of the cloud  $I_{cloud}$  is scattered on the way from the cloud back to the ground:

$$I_{s2}(\lambda) = I_{cloud}(\lambda) \cdot (1 - e^{-f_s(\lambda) \cdot R}) \quad (17)$$

The total scattered radiation is the summation of Equation 14 and Equation 17:

$$I_{scatter}(\lambda) = I_0(\lambda) \cdot (1 + \rho \cdot e^{-f_t(\lambda) \cdot R}) \cdot (1 - e^{-f_s(\lambda) \cdot R}) \quad (18)$$

So, the spectral effect of the atmosphere on the transmission is described by Equation 16 and the effect of scatter by Equation 18. It should be noted these formulae are a simplified model. In reality, for instance, the light is scattered more ones at various angles. However, these formulae will supply a first order approximation and will give a quite a good estimation of the differences between the various lamp spectra.

The scattered light produces light pollution. To calculate the effect on human observers the calculated spectral distribution of the scattered and transmitted light must be weighted by the spectral sensitivity of the human eye according:

$$I_{scatter,v} = k \int_{400nm}^{740nm} I_{scatter}(\lambda) \cdot V(\lambda) d\lambda \quad (19)$$

where  $I_{scatter,v}$  is the visible scattered light,  $V(\lambda)$  is the standard spectral sensitivity of the human eye (CIE, 2004a) and  $k$  is a constant. The integrations limits are the boundaries of the visible range of electromagnetic radiation. In our calculations we applied 400 nm to 740 nm. The visible transmitted light  $I_{transmission,v}$  and the light of the lamp, without influence of the atmosphere  $I_{0,v}$  are determined in same way. The fraction of the light that is scattered on the total path from the ground to the cloud and back can be calculated by:

$$F_{scatter,v} = \frac{I_{scatter,v}}{I_{0,v}} \quad (20)$$

The fraction of the light that is transmitted on this path is:

$$F_{\text{transmission},v} = \frac{I_{\text{transmission},v}}{I_{0,v}} \quad (21)$$

These functions can be determined for various spectra and path lengths (cloud heights). It should be noted that we have determined the light pollution for a human observer. For other species, such as animals and plants, the spectral sensitivity may be different.

#### 4.6 Light scatter of lamp spectra

In this paragraph we have quantify the scatter by and transmission through the atmosphere for the various lamp spectra and standard illuminants. We took the same spectra as were have used in the age study (Table 3-1), seven spectra of various light sources and three standard illuminants for comparison. In Figure 16 the scatter and transmission fractions are plotted in one graph. The high pressure sodium lamp (HPS) shows the lowest scatter fraction and the LED lamp with a S/P-ratio of 2.81 has the highest scatter fraction. The HPS lamp has the highest transmission and the LED lamp with a S/P-ratio of 2.81 has the lowest transmission. The shape of the transmission fraction curve is the mirror image of the scatter fraction. This makes sense because the part of the light that scatters does not propagate straight forward.

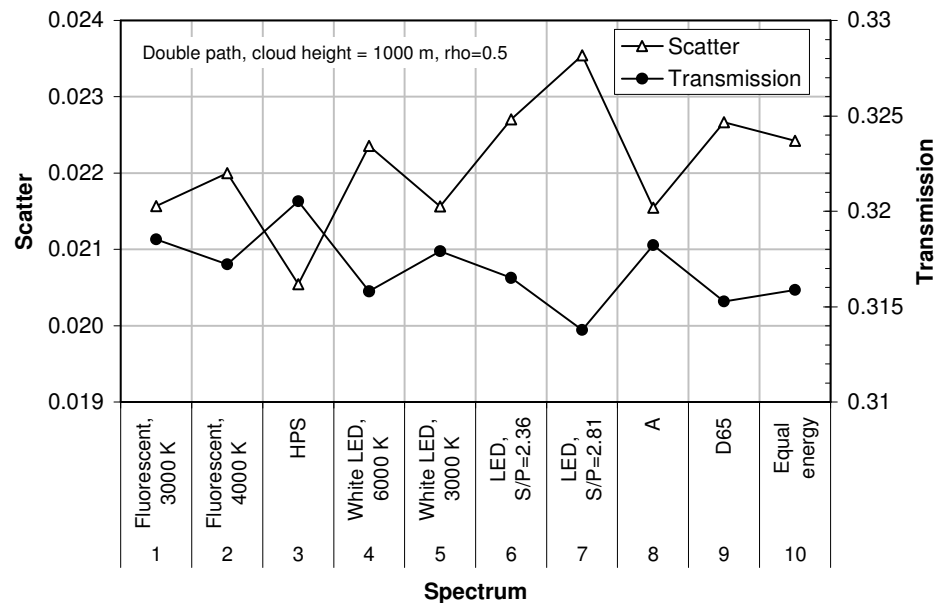


Figure 16 The scatter and transmission fractions of various spectra (7 light sources for public lighting and 3 standard illuminants) for the path from ground to cloud and back. rho is the (neutral) reflection of the cloud.

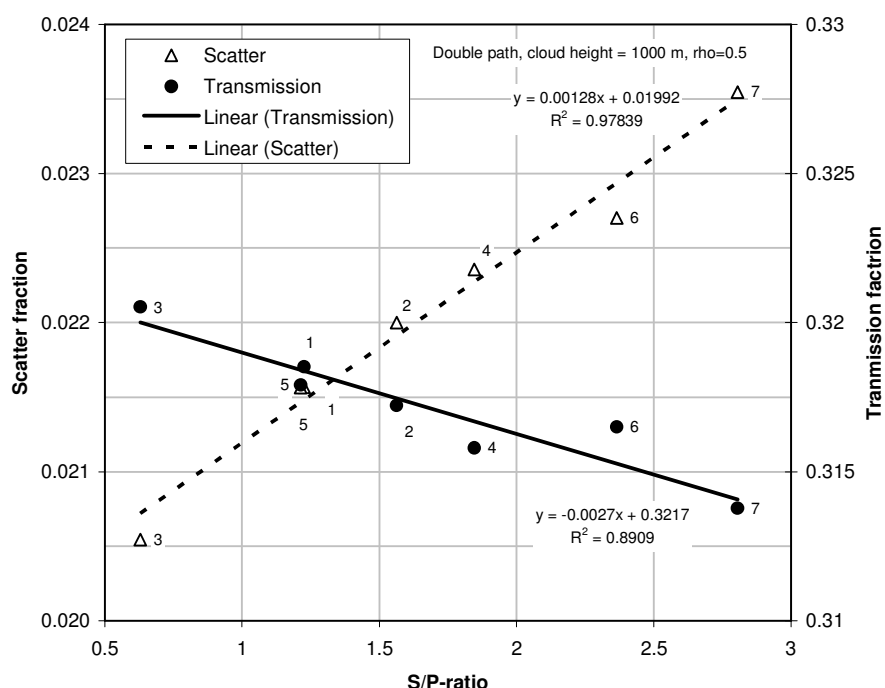


Figure 17 Scatter and transmission fraction as a function of the S/P-ratio for seven light sources with the regression lines ( $y=f(x)$ ). R = regression coefficient. The figures at the data points refer to the spectra of the light sources (Table 4-1).

It appears that the scatter fraction has a strong correlation with the S/P-ratio. This is illustrated in Figure 17. In this graph the scatter and transmission is plotted against the S/P-ratio for the seven public lighting light sources. The higher the S/P-ratio is, the more the light is scattered. The scatter of the LED lamp with a S/P-ratio of 2.81 has almost 10% more scatter than the warm white fluorescent lamp with a S/P-ratio of 1.23. The transmission of this LED lamp is about 3% less than of the warm white fluorescent lamp. The relative scatter and transmission values are calculated for cloud heights of 100 m and 2000 m. These values are listed in Table 4-1. The values are normalised at unity for spectrum 1, the warm white fluorescent lamp with a colour temperature of 3000 K, which is currently a very common light source in public lighting.

Table 4-1 Relative scatter and transmission of spectra of light sources for public lighting (1 to 7) and standard illuminants (8 to 10) for cloud heights of 100 m and 200 m. The values are normalised at 1 for spectrum 1.

| Nr | Spectrum type       | S/P-ratio | Relative scatter |       |         | Relative transmission |       |         |
|----|---------------------|-----------|------------------|-------|---------|-----------------------|-------|---------|
|    |                     |           | 100              | 2000  | average | 100                   | 2000  | average |
| 1  | Fluorescent, 3000 K | 1.23      | 1.000            | 1.000 | 1.000   | 1.000                 | 1.000 | 1.000   |
| 2  | Fluorescent, 4000 K | 1.56      | 1.021            | 1.019 | 1.020   | 1.000                 | 0.992 | 0.996   |
| 3  | HPS                 | 0.63      | 0.951            | 0.954 | 0.952   | 1.001                 | 1.012 | 1.006   |
| 4  | White LED, 6000 K   | 1.85      | 1.038            | 1.035 | 1.037   | 0.999                 | 0.983 | 0.992   |
| 5  | White LED, 3000 K   | 1.21      | 1.000            | 1.000 | 1.000   | 1.000                 | 0.996 | 0.998   |
| 6  | LED, S/P=2.36       | 2.36      | 1.054            | 1.051 | 1.053   | 0.999                 | 0.988 | 0.994   |
| 7  | LED, S/P=2.81       | 2.81      | 1.095            | 1.089 | 1.092   | 0.998                 | 0.971 | 0.987   |
| 8  | A                   | 1.41      | 0.999            | 0.999 | 0.999   | 1.000                 | 0.998 | 0.999   |
| 9  | D65                 | 2.46      | 1.053            | 1.049 | 1.051   | 0.999                 | 0.980 | 0.991   |
| 10 | Equal energy        | 2.26      | 1.041            | 1.038 | 1.040   | 0.999                 | 0.984 | 0.993   |

It appears that the *relative* scatter is quite insensitive for the cloud height, i.e., the length of the propagation path through the atmosphere. For the spectrum with the highest S/P-ratio the relative scatter varies only between 1.095 and 1.089 for cloud heights between 100 m and 2000 m. The relative transmission varies only between 0.998 and 0.971 for these cloud heights. Therefore we will consider only the average values of these two cloud heights. These values are plotted in Figure 18 with the same scales for scatter and transmission with regression lines. The graph shows that the scatter is more sensitive for the S/P-ratio than the transmission. Compared to warm white light sources (number 1 and 5) the scatter of the spectrum with the highest S/P-ratio, the non-white LED lamp, is 9% higher and the transmission is 1.3% lower. For an spectrum with a S/P-ratio of 3 the scatter will be 10% more than for a warm white light source. The transmission in this case will be only 1.4% lower in this case.

The equations of the regression lines in Figure 18 describe the of percentages more or less scatter or transmission in relation to the reference spectrum of the warm white fluorescent lamp. The percentage scatter relative to the reference spectrum can be calculated with: 5.9 times the S/P-ratio minus 7.7. The percentage transmission relative to the reference spectrum can be calculated with: -0.74 times the S/P-ratio plus 0.89.

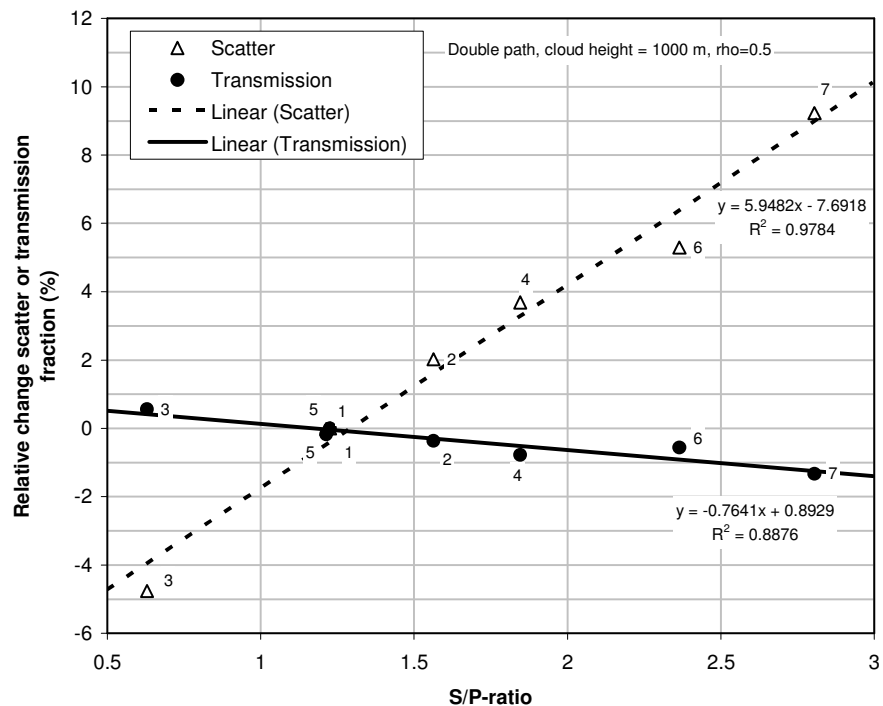


Figure 18 Relative change of the scatter and transmission fraction as a function of the S/P-ratio for seven light sources with the regression lines ( $y=f(x)$ ).  $R$  = regression coefficient. The figures at the data points refer to the spectra of the light sources (Table 4-1).

#### 4.7 Discussion

In this study we found that the light with short wavelengths scatters more than in a standard atmosphere than light with long wavelengths. We found a relationship between the S/P-ratio and the amount of light scatter. Compared to a warm white fluorescent lamp with the scattering of a light source with a S/P-ratio of 3 is 10% more. In terms of visibility and light hindrance this percentage is quite low. We expect that changes in the amount of scattered light of more than at least 50% will lead to significant more light hindrance. Therefore we can conclude that light sources up with S/P-ratios up to a values of 3 will not substantially contribute to more light hindrance than common conventional warm white fluorescent light sources with a colour temperature of 3000 K and a S/P-ratio of about 1.25. It should be noted that comparing to another common light source, for instance the fluorescent lamp with a colour temperature of 4000 K, will lower the scatter percentages with about 2%.

The transmission of the atmosphere is important when the stray light from the lamps reaches the clouds, reflects back and therefore becomes visible for the observer on the ground. For lamp with high S/P-ratios of about 3 this light will become only a few percents lower, and practically does not change at all, as seen through the eyes of the observer on the ground. Therefore the spectral influence for transmission can be neglected.

The calculations of the influence of the light spectrum on scatter and transmission are based on a standard atmosphere. The meteorological visibility in this standard atmosphere is about 12 km. This is a rather good visibility and is close to the median of the visibility in the Netherlands. The visibility becomes poorer when the humidity increases. In that case the number of water droplets and their sizes increase. The consequence of this is that the scatter becomes more independent of wavelength. In foggy conditions the size water drops so large that the scatter and transmission is independent of wavelength, i.e., the scatter and transmission has a neutral colour.

A report of the IDA (2010) gives an overview of the influence of the spectrum of public lighting on the sky glow. The authors of the report note that there is increased use of white lighting, which is more bluish (blue-rich) compared to the HPS technology currently used for the most for area lighting in the USA. They state that this blue-rich lighting causes an increase of the light pollution and they underpin this by comparing the scatter index of various light sources. They based their calculation on the model for Rayleigh, where the scatter is proportional with the inverse fourth power of the wavelength ( $1/\lambda^4$ ) (see Equation 5). According this model they calculated that led lamps with a S/P-factor of 3 scatter a factor two more than HPS lamps. In our calculations we found a factor 1.15 between scatter of these two light sources (Table 4-1). However, we used not only the Rayleigh scattering due to small molecules, but assumed an average atmosphere with a mixture of molecules and aerosols. This atmosphere has a less strong dependence of wavelength; the scatter is proportional with approximately the inverse 2.1 power of the wavelength ( $1/\lambda^{2.1}$ ) (Figure 15). IDA (2010) recognize that the Rayleigh model is the worst case situation and that the real atmosphere generally is a mixture of molecules (Rayleigh) and aerosols and that this mixture has a less strong wavelength dependency. The scatter due to aerosols is proportional with the inverse of the wavelength ( $1/\lambda$ ) (Garstang, 1986). The wavelength dependency of our mixed atmosphere model with a power of 2.1 is right between that of molecules and aerosols, with powers of 4 and 1.

The scatter calculations in this study were performed for a pathway from the ground to a cloud and back. For longer pathways, more parallel to the ground (from luminaires leaking light almost horizontally), over longer distances may have an other outcome. Along horizontal directions the wavelength dependency is more influenced by haze ( $1/\lambda$ ) and in vertical directions more by molecules (Rayleigh,  $1/\lambda^4$ ). The blue part of the spectrum scatters the most and will therefore be absent at large distance. Therefore the light pollution near the light source will be more bluish than the light pollution at long distance (IDA, 2010).

#### 4.8 Conclusions

- Light with short wavelengths (bluish) is more scattered than light with large wavelengths (yellowish) for a standard atmosphere with a mixture of molecules and aerosols.
- There is a correlation between the amount of scattered light and the S/P-ratio of the light source.
- For a standard atmosphere, with a meteorological visibility of about 12 km, a non-white light source with a S/P-ratio of 3 scatters 10% more light than a warm white light source with a colour temperature of 3000 K and an S/P-ratio of 1.23.
- For conditions with a lower meteorological conditions the scattering becomes independent from wavelength and the atmosphere can be considered as a neutral medium for scattering and transmission.

## 5 Literature review: Face recognition

### 5.1 Introduction

In residential areas the light levels of public lighting should be at such a level that the faces of pedestrians can be recognised at a sufficient large distance. The question is : What is the effect of the spectra of mesopic public lighting on face recognition compared to the spectra of the currently widely used light sources? This question will be addressed in this part of the literature review.

### 5.2 Literature

An important role of lighting is to facilitate good face recognition. Face recognition is thought to play a crucial role in the people's perception of safety. This is why facial recognition distance is often used as a measure of lighting performance. This concept was developed by van Bommel & Caminada (1997) based on the work of Hall (1966). Hall found that people only like other people to approach close to them if they have been recognised. He established a series of 'zones of proximity' and characterized them by the interpersonal reactions within them (see Figure 19).

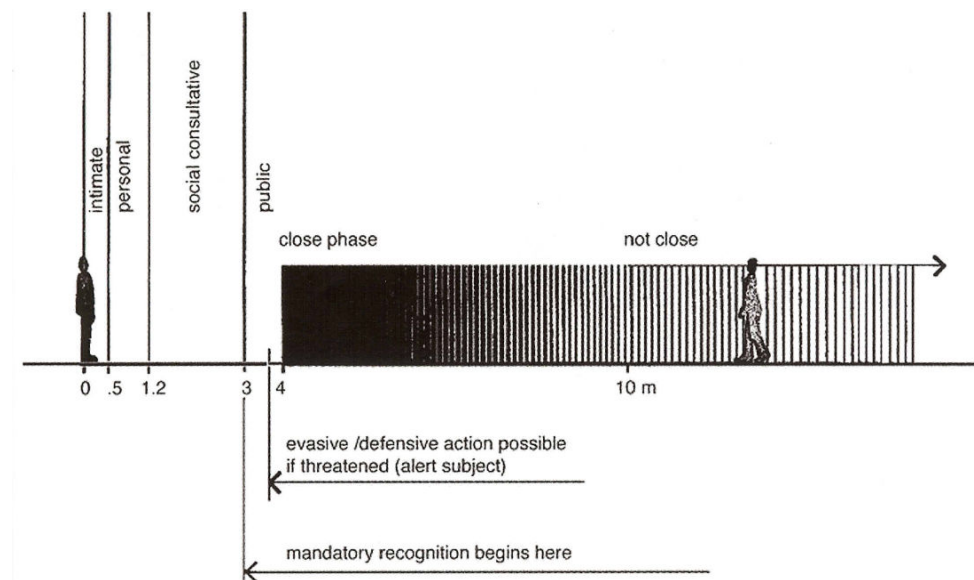


Figure 19 Hall's zones of proximity (from Caminada & Van Bommel, 1980).

Caminada & van Bommel (1980) measured the face recognition distances (using  $n = 20$  observers) for various illumination levels and various directional face illumination conditions. They correlated the face recognition distances with the vertical illuminance ( $E_{vert}$ ), semi-cylindrical illuminance ( $E_{semicyl}$ ) and hemispherical illuminance ( $E_{hemisph}$ ). They found  $E_{semicyl}$  to give the best correlation with face recognition distance, reasonable correlation with  $E_{hemisph}$  and no reliable correlation with  $E_{vert}$  and concluded that the semi-cylindrical illuminance was best suited for specifying the required recognition distance. They also found that visual comfort was largely determined by glare and they established the luminance and light areas corresponding to the just

admissible glare (at which point the relationship between the luminance  $L$  and space angle  $\omega$  is described by  $L\omega^{0.23} = 270$ ). The effect of spectrum was not studied by Caminada & van Bommel (1980); they only used a single light spectrum of a high pressure mercury lamp with a colour temperature of 4000 K and a colour rendering index of 45)<sup>2</sup>.

Boyce & Rea (1990) established minimum light levels for detecting and recognizing intruders (by guards). They found that to detect an intruder walking along a known path a vertical illumination of 0.4 lx was required for a detection probability of 50% and 2 lx for 90% detection probability. When the intruder was walking along an unknown path these values were elevated (to 1 lx for 50% probability, 10 lx for 90% probability). The faces of the intruders were recognized with 75% probability at a distance of 17 m and a vertical illuminance of 12 lx. With a 50% probability the recognition distance was 21 m with a vertical illuminance of 7 lx. Boyce & Rea (1990) used two different light sources, a low pressure sodium lamp (LPS) and a high pressure sodium lamp (HPS). There have found no difference in detection and recognition distance between the two lamp types.

Various studies indicate that human face recognition improves with better colour rendering. As a measure of how well colours are represented (and can be discriminated) the colour rendering index ( $R_a$ ) is used (CIE, 1995). Under mesopic conditions, identification of human faces with white light with better colour rendering was found to be much easier than with lower  $R_a$  (Raynham & Saksvikrønning, 2003; Knight et al, 2007; Yoa et al. 2009). On the other hand, Boyce & Rea (1990) concluded that the spectrum of the two tested lights (low-pressure vs. high pressure sodium discharge lamps) had no impact on the recognition of faces.

Raynham & Saksvikrønning (2003) compared the impact of light source spectrum under mesopic conditions of three light sources on face recognition. The light sources (high pressure sodium HPS, fluorescent CFL2700, fluorescent CFL4000) differed in their colour rendering index ( $R_a = 25, 82$  and  $82$ ) and colour temperature (2000, 2700 and 4000 K). In an experiment (with a limited number of 6 to 8 observers) face recognition distances were established. They found that the HPS light source required much larger illumination corresponding to recognition distance of 4 meters than the other two fluorescent light sources (by about a factor of 3). This indicates the importance of the colour rendering index on face recognition. They found no difference in recognition distance between the two lights with the same colour rendering index ( $R_a$  of 82) but different colour temperature (2700 vs. 4000 K). Moreover, they found no evidence for a mesopic effect, which supports the conclusion that face recognition is a foveal task and that the photometry can be performed with a photopic spectral sensitivity,  $V(\lambda)$ .

Also Knight et al. (2007) performed a study in which the effect of light spectrum on face recognition was determined. In this study they compared the light in a residential area before and after it was switched from high pressure sodium (HPS) to ceramic metal halide (CMH) lighting. This study involved the comparison of lights with different colour rendering index, different colour temperatures and  $S/P$ -ratios: HPS light (2000 K,  $R_a = 25$ ,  $S/P = 0.54$ ), CMH-light (2800 K,  $R_a = 83$ ,  $S/P = 1.35$ ). In their experiment (with  $n = 55$  subjects) they determined face recognition distances for faces using coloured prints of

<sup>2</sup> Personal communication with Wout van Bommel (2010).

faces as targets. They found that the gender of the person on the picture could be identified from a large distance of about 13 m and the person could be identified at about 6 m. The study showed that residents were able to identify the face on the pictures from further away under the CMH illumination despite the fact that the average vertical illuminance on the pictures at the chosen positions was considerably lower than with the HPS-lighting. Also, it was found that the performance of older people (55+) improved considerably under CMH light and became comparable to the performance of younger people (<55). It was also established that naming of colours improved with the application of CMH-light. A different experiment showed a significant (but small) effect of the change to CMH-light on eccentric detection of objects during driving. From these experiments it is not clear whether (or to what extent) the improvement is due to better colour rendering or a higher *S/P*-ratio. Given the results of Raynham & Saksvikrønning (2003) it is likely that the improvement in face recognition is primarily due to better colour rendering.

Yoa et al. (2009) performed a study which was similar to the study of Knight et al. (2007). They performed two experiments involving facial recognition and colour identification using two light sources, high pressure sodium (HPS, colour temperature 2000 K, colour rendering index is 30 to 40) and ceramic metal halide (CMH, colour temperature is 2800 K, colour rendering index is 65). In the facial recognition experiment they used 8 cards with coloured images of well-known persons. The 48 subject approached the cards under illumination of the two light sources and recorded the distances at which they could recognise the faces for three criteria (gender identification, guess identity, sure identification). The vertical illumination of the faces in the two light source conditions were at the same illuminance level 5.5 lx. They found that the recognition distances for the CHM light source were between 31% and 48% higher than for the HPS light source. In the colour identification experiment it was found that the identification of yellow, green and blue under CHM light better than under HPS light.

Whether colour plays an important role in face recognition is still under debate. Only a few studies (mostly performed using images) has examined the contribution of colour in face recognition. Kemp et al (1996) found that observers were able to process quite normally even those faces that had been subjected to hue-reversals (tasks included recognizing familiar faces or spotting differences between faces). Colour appeared to confer no significant recognition advantage beyond the luminance information. Bruce & Young (1998) who tried to explain this have suggested that the lack of a contribution of colour cues to face recognition is because they do not affect shape from shading processes, which are believed to be largely 'colour-blind' (Cavanagh & Leclerc, 1989). Yip & Sinha (2001) found that colour cues do play a role in face recognition when the shape cues (from luminance) are degraded. This may explain why Knight et al (2007) and Raynham & Saksvikrønning (2003) found an effect of colour rendering index on face recognition distance, since this is established at a threshold distance at which the features can barely be discriminated.

In the face recognition experiment of Yoa et al. (2009) images of well-known persons were used. They found the largest recognition distances for the light source with the largest colour rendering index. In Figure 20 the experimental set-up is shown of Yoa et al. (2009). The inset of the figure shows the pictures of the well-knows persons they used in the experiment. The pictures are not very similar. They contain different background colours and the person in one of the picture has another hair colour. Therefore it is possible that subject may have recognized other features of the picture,

rather than purely the face. For instance, depending on the colour of the illumination the contour (transition between the head and the background) will be more or less visible.

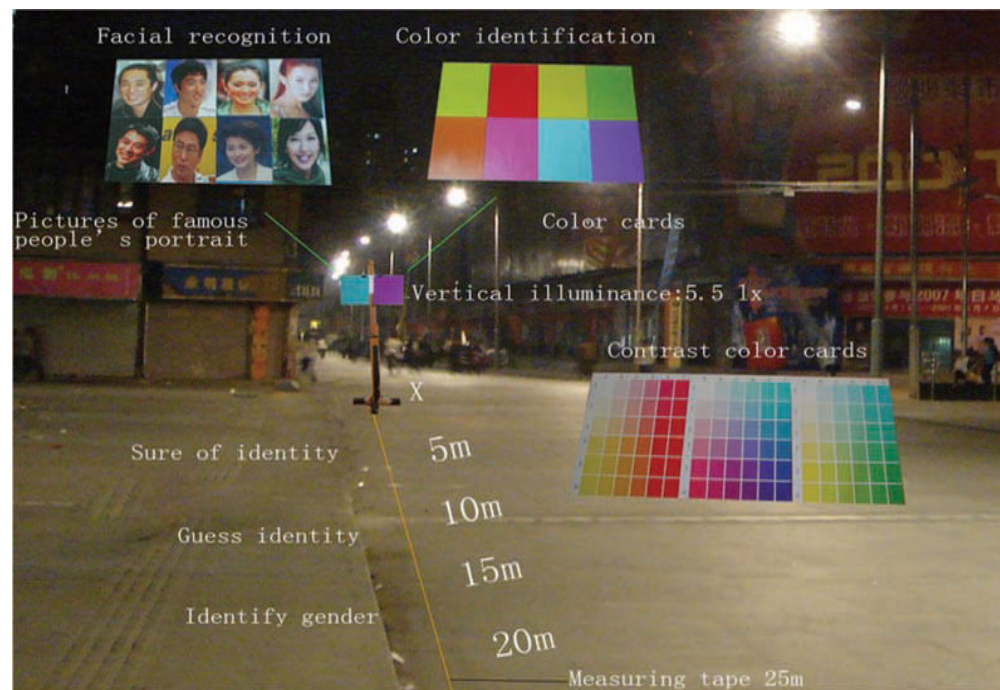


Figure 20 Experimental set up in the field of Yoa et al. (2009).

### 5.3 Conclusion

- We found three studies that indicate that the spectrum of the light plays a role in face recognition. They concluded that a larger colour rendering index results in a larger recognition distance. In one of these studies real faces were used in the recognition experiment; in the other two studies printed faces of well-known person were applied.
- Other laboratory studies on face recognition found no important role of colour in the recognition of faces. Only in situations of degraded pictures the colour may have an effect, which is the case when faces are recognised at threshold levels.
- We conclude that whether colour plays role in face recognition is still under debate.

## 6 Experiment: Face recognition

### 6.1 Introduction

The purpose of the experiment was to compare conventional lighting with lighting specially designed for mesopic light levels in a face recognition experiment. In standards for public lighting it is recommended to apply lighting with a sufficiently high colour rendering index in order to recognize persons in public areas. MVL generally is not very white and has a bad colour rendering index. When MVL is advised for public lighting it should at least perform equal in terms of recognition distance of human faces. We tested in an experiment whether this is achievable. We asked subjects to judge the recognition of the faces of so-called target persons under the light of conventional lighting and MVL at various distances and light levels. This resulted in the face recognition distances for various light levels and spectra.

### 6.2 Methods

#### 6.2.1 *Experimental setup*

The photograph in Figure 21 shows the experimental set-up with the light poles, three locations of the target persons (sitting on a platform), and the subjects (standing) assessing recognition of the target person faces. The experiment was conducted indoor in an hall (40 x 200 x 8 m). The skylights in the middle of the hall were shielded from daylight with black plastic sheeting. Although the weather during the experimental period was warm and sunny, the shielding was sufficient to perform perception experiments at very low light levels. At the site of the experiment an illumination of 0.01 lx was measured, while outside the sun illumination was 30,000 lx.

Figure 22 shows a top view of the experimental setup. Four light poles were drawn in a row with a spacing of 25 m. The row of light poles was positioned 13 m from the side wall of the hall and the last light pole 4 was 27 m from the back wall of the hall. Between the first two light poles three positions were target persons were located during the experiment. The subjects assessed the recognition of the faces of the target persons. The three target person locations between the light poles (A, B, C) were chosen in such a way that the illuminances at the faces of the target persons were representative for the various positions of pedestrians under light poles in practice. For comfort reasons the target persons were seated on the chair on a platform. Their faces were at normal standing height.



Figure 21 Overview of the experimental set-up, with the light poles, three locations of the target persons (sitting on a platform) and the subjects (standing) assessing recognition of the target person faces.

The task of the subjects was to assess the recognisability of the face of the target person on a scale of 0-100%, at eleven different distances (32, 23, 16, 11, 8, 6, 4, 3, 2, 1.5, 1 m) from the face of the target person, beginning with the largest distance. At the distance of 4 m from the target person, the subjects had to assess the discomfort glare of the lighting situation on a 9-point scale which is widely used scale in the for car and road lighting (De Boer, 1967). The values and the designations of this scale are shown in Table 6-1. The subjects could also give scores with figures after the decimal point. Note that a high score on the scale means little discomfort glare. The subjects noted their scores on a scoring form (see Appendix B.2.).

Table 6-1 Scale for evaluation of discomfort glare according to De Boer (1967). See Appendix B.2 for the scale in Dutch as shown to the subjects.

| Score | Designation    |
|-------|----------------|
| 9     | Inappreciable  |
| 8     | -              |
| 7     | Acceptable     |
| 6     | -              |
| 5     | Just allowable |
| 4     | -              |
| 3     | Disturbing     |
| 2     | -              |
| 1     | Unbearable     |

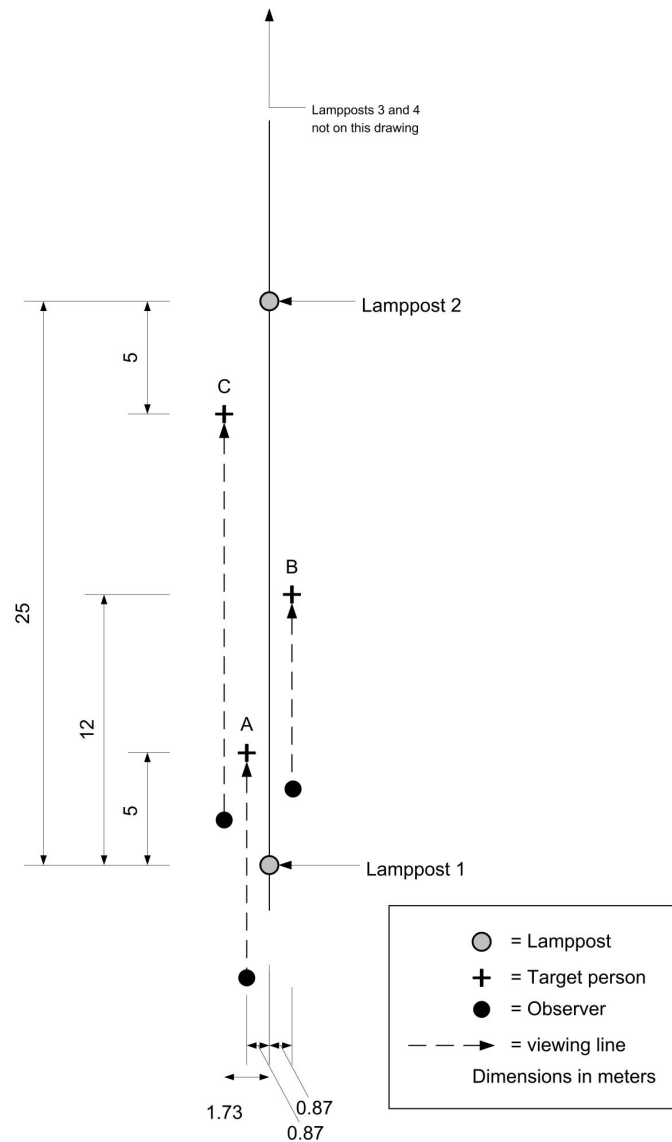


Figure 22 Experimental setup (top view). The three observers are at arbitrary viewing distances from target persons. Lampposts 3 and 4 (not in this drawing) are in line with lampposts 1 and 2. Distance between lampposts is 25 m.

### 6.2.2 Lamps

We have prepared four light poles with the same cone shaped luminaire (Lighttronics, GFK, ice motif) (Figure 23). The diameter of the cone was 70 cm and the height of the translucent area was 30 cm. The lower side of the luminaire was 3.4 m above the ground. The centre of the light source was about 3.6 m above the ground. The luminaires were prepared in such a way that six different light sources could be installed and could be interchanged relatively fast during the experiment. The lamps are listed in Table 6-2.



Figure 23 Luminaire.

Table 6-2 Lamps.

| Lamp | Light source type    | Brand     | Brand / type nr        |
|------|----------------------|-----------|------------------------|
| 1    | Fluorescent          | Phillips  | 830                    |
| 2    | High pressure sodium | Phillips  | SON-T, 50 W            |
| 3    | white LED            | Philips   | LLM, 1800 lm, 3000 K   |
| 4    | white LED            | Philips   | LLM, 1800 lm, 5000 K)* |
| 5    | Not white LED        | Innolumis | Ecowhite               |
| 6    | Not white LED        | Innolumis | Moonlight              |

)\* Appeared to have a colour temperature of 4500 K after measurement (Table 6-9).

Lamp 1 is a conventional fluorescent light source which is applied widely in the Netherlands. The second lamp source is a high pressure sodium light source which is also very common. These two light sources are added to serve as a reference for the other less common light sources. Lamp 3 and 4 are white led lamps with different light colours, i.e., with colour temperatures of 3000 K and 5000 K. The last two light sources are led lamps with different light colours and are specially designed for mesopic light levels.

### 6.2.3 Light levels

Our goal was to simulate a part of a light installation for a road non-motorised traffic in two light levels, normal (high) and dimmed (low). We chose lighting class S5 of the standard EN 13201-2:2003 (CEN, 2003a), which is intended for pedestrians and pedal cyclists on footways, cycleway, and in residential areas. The average illuminance for this class should be at least 3 lx and the minimum illuminance should be at least 0.6 lx (Table 6-3). This was the high light level. The low light level was intended to be one third of the high lighting level. This level is not a standard lighting level but is chosen since this light level is generally used in the Netherlands as a dimmed version the high light level. Note that the uniformity, which is defined as the minimum illuminance divided by the average illuminance, equals 0,2.

Table 6-3 Light levels.

| Lighting level | Horizontal illuminance |                         | Lighting class CEN (2003a) |
|----------------|------------------------|-------------------------|----------------------------|
|                | Average $\bar{E}$ (lx) | Minimum $E_{\min}$ (lx) |                            |
| Low (dimmed)   | 1                      | 0.2                     | -                          |
| High (normal)  | 3                      | 0.6                     | S5                         |

With a lighting design software the horizontal illuminances were calculated at a grid of positions on the ground between two light poles with six different lamps. The distance between the light poles was 25 m and the calculation area was 25 m x 8 m. The lamps were positioned on a line 2 m from the long side of this area. The calculated average, minimum, and maximum illuminances are listed in Table 6-4. The desired average illuminance of 3 lx and is met for all lamps. Also the minimum illuminances comply with the requirement of 0.6 lx. The only outlier is lamp 2 with an average illuminance of 8.66 lx. Lamp 2 is a high pressure sodium lamp and is not dimmable in an easy way without influencing the spectrum. Therefore we installed a gauze filter in the luminaire of lamp 2 which provided a neutral reduction of the light level of a factor 0.43 and resulted in a further approximation of the desired illuminance.

Table 6-4 Design illuminances of the lamps. The values between brackets correspond to a lamp without a neutral gauze filter.

| Lamp    | Horizontal illuminance (lx), high light level |             |             |                     |         | Dimming factor |
|---------|---|-------------|-------------|---------------------|---------|----------------|
|         | High  |             |             |                     | Low     |                |
|         | Average                                       | Minimum     | Maximum     | Minimum/<br>maximum | Average |                |
| 1       | 3.83  | 0.90        | 9.86        | 0.23                | 1.29    | 0.34           |
| 2       | 3.72 (8.66)                                   | 0.54 (1.26) | 13.3 (31.0) | 0.15                | 1.99    | 0.54           |
| 3       | 3.73  | 0.84        | 9.10        | 0.23                | 1.32    | 0.35           |
| 4       | 3.73  | 0.84        | 9.10        | 0.23                | 1.32    | 0.35           |
| 5       | 3.57  | 0.70        | 11.00       | 0.20                | 1.27    | 0.36           |
| 6       | 3.15  | 0.62        | 10.00       | 0.20                | 1.00    | 0.32           |
| Average | 3.62  | 0.74        | 10.40       | 0.20                | 1.37    | 0.38           |

For the low light levels our goal was to dim all lamps to one-third of the high light level. To do this we built in another gauze filter in lamp 4, the high pressure sodium lamp. For the led lamps 3 and 4 a neutral density sheet filter was applied, which did not significantly influence the spectral output of the lamps. The lamps 1, 5, and 6 were dimmed by lowering the supply of control voltage on the lamps.

#### 6.2.4 Subjects

A total of 57 paid subjects were involved in the experiment, 45 observers and 12 target persons. The group observers consisted of 24 young and 21 young observers. The age of the young observers ranged from 16 to 18 years, with an average of 16.5 years. The age of the old observers ranged from 49 to 73 years, with an average of 60.2 years. All subject had normal visual acuity. The average visual acuity, measured with the Landolt-C TNO acuity test, was 2.02 for the young observers and 1.65 for the old observers. One young subject had a mild green-red colour vision deficiency, tested with the Ishihara test for colour blindness. Further details are listed in Annex A.

#### 6.2.5 Photometric measurements

For each lamp and light level the vertical illuminance was measured at the faces of the target persons at the locations A, B, and C with an illuminance meter (Lichtmesstechnik, pocketlux). Also the vertical semi-cylindrical illuminance was determined at the same spots using the illuminance meter with a semi-cylindrical detector. The spectrum of the lamps was measured with a spectroradiometer (Photo Research, PR 650) at a white standard which was put at 2 m from de lamppost in the line of lampposts. The relative spectral output of the lamps was used to calculate the CIE xy colour coordinates, colour rendering index (CRI) and the S/P-ratio (CIE, 1995, 2010). For lamp 5 and 6 the spectral output was also measured in the direction of the faces of the target persons.

With a luminance camera (LMK 98-4 color) we took luminance images from the scene with the four lamps. The luminance camera was located at 9 m in front of lamp 1 and 1 m left of the line through the lampposts, at a height of 1,5 m. Using image analysing software we extracted the desired photometric parameters from the luminance images (Figure 24). We marked the areas of the street and the lamps, and determined the average luminance of the street and the luminous intensity of each of the four lamps.

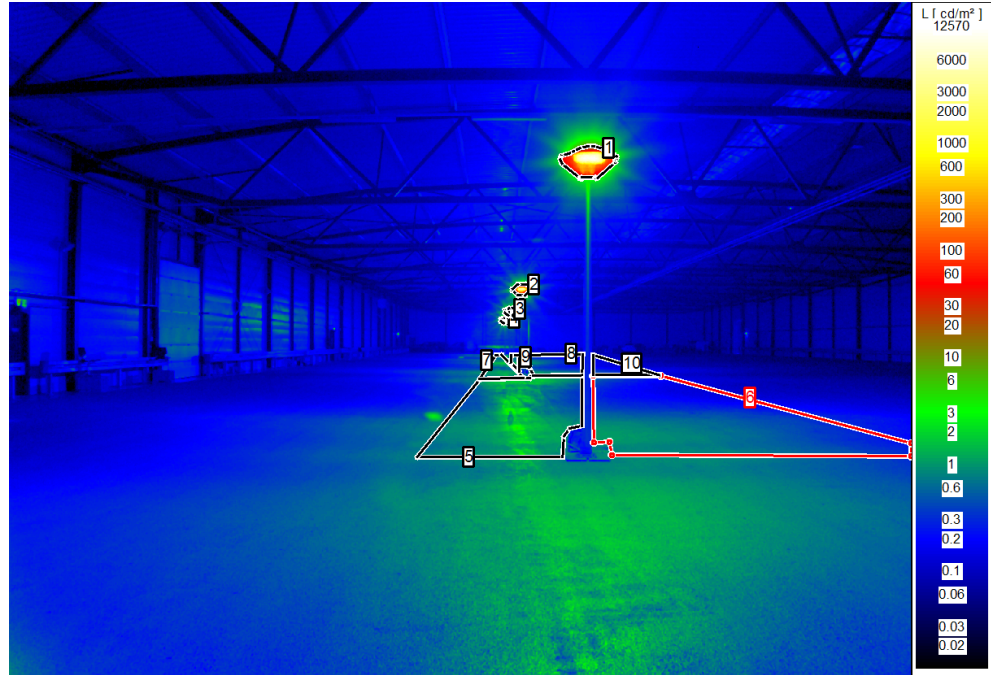


Figure 24 Luminance image with marked areas for the calculation of the average road luminance and the luminous intensity of the lamps.

This data was used to calculate the glare parameter, threshold increment (TI), as it is defined in the standard for public lighting EN 13201-3 (CEN, 2003b). This formula for the TI is:

$$TI = \frac{65}{L_{road}^{0.8}} L_v \quad [\%] \quad (22)$$

where  $L_v$  is the veiling luminance (in  $\text{cd/m}^2$ ),  $L_{road}$  is the average luminance of the road (in  $\text{cd/m}^2$ ). For the calculation of the average road luminance the “road” to the area between lamppost 1 and lamppost 4, and the 2 m on the left side (side walk side) and 6 m on the right side (road side).

The veiling luminance  $L_v$  is the sum of the contributions of all four lampposts and is calculated with:

$$L_v = 10 \sum_{k=1}^{k=4} \frac{E_k}{\theta_k^2} \quad [\text{cd/m}^2] \quad (23)$$

where  $E_k$  is the illuminance in lux due to lamppost  $k$  at the measuring point and  $\theta_k$  is the glare angle of lamppost  $k$  in degrees, which is the angle between the viewing direction and the light source of lamppost  $k$ .  $L_v$  is the veiling luminance, a measure for disability glare. The viewing direction in our calculation was parallel to the “road” and the line

through the lampposts. The location of the luminance camera (1 m left of the lamppost line) was chosen to imitate the walking route of the pedestrian on the middle of the sidewalk, looking straight forward. The height of the viewing point is dictated the public lighting standard EN 13201-3 (CEN, 2003b). The glare angle  $\theta_k$  was calculated on basis of these geometrical data.

#### 6.2.6 Procedure

Due to logistics reasons the actual experiment was performed with four different subject groups at four different day parts. The first two groups were old and the second two groups were young.

Before the start of the experiment we ask the subjects to read the instructions with information about the experiment (Appendix B). We stated that we do this research on new types of lighting (such as LED lighting) for the government and with energy saving as ultimate goal. We declared that we want to answer a question concerning social security: "Is it possible to recognize people under the light of the new lamps at the same distance as under the light of the current conventional light?" Then we explained the experimental procedure: The target persons are seated at three locations between light pole 1 and 2. The subjects were instructed to approach the target persons at a large distance or 32 m and to stop at the pylons to make an assessment of the recognition of the face of the target person on a scale between 0% (absolutely not recognizable) and 100% (very good). The three target persons were recruited from each group and were in most cases unknown to the other subjects. We instructed the subjects to imagine that they encounter this target person in the street at night and asked the subject to assess only the recognition of the face and ignore the clothing, hairstyle, length, and posture of the target persons.

To learn the procedure the subjects started with a practice session where they had to approach to all three target persons and so filling in one sheet of the scoring form (See Appendix B).

After the practicing session the real sessions started. In each session the recognition distances were measured for one lamp at one light level. In order to avoid order effect we presented the lamps a different sequence for each subject group (Table 6-5). Also the order of the light levels (high and low) were varied over the subject groups; half of the groups started with the high light level and half of the groups started with the low light level.

Table 6-5 Order of the presentation of the lamps and the light levels to the four groups.

| Group     | Lamp order |   |   |   |   |   | Light level order |
|-----------|------------|---|---|---|---|---|-------------------|
| 1 (old)   | 1          | 6 | 2 | 3 | 4 | 5 | high, low         |
| 2 (old)   | 5          | 4 | 3 | 6 | 2 | 1 | low, high         |
| 3 (young) | 2          | 1 | 5 | 4 | 3 | 6 | high, low         |
| 4 (young) | 6          | 3 | 1 | 2 | 5 | 4 | low, high         |

After installing the proper lamps, setting the desired light level, and the positioning the target persons, the whole group of subject started at the same time the assessment session. The subject started with an arbitrary target person depending on the queue length, due to other subjects. We instructed the subjects to make their judgements at the straight line in front of the target person, then step aside to make room for other observing subjects behind, and note their score on the scoring form. In total each subject had to complete 12

sessions  
(6 lamps x 2 light levels). Each session lasted about 15 minutes.

### 6.3 Results

#### 6.3.1 Statistical analysis

The differences between the average values of the various conditions were tested with an analysis of variance (ANOVA). The ANOVA calculates the probability  $p$  that a difference between two conditions is due to coincidence. When this probability is low enough ( $p < 0.05$ ) the difference is considered as a real effect caused by the conditions and the effect is called statistically significant. The post-hoc test (Tukey or Newman-Keuls) was applied to test the differences when a condition has more than two levels. The statistical analysis of the recognition distance was performed on the logarithm of the recognition distance.

#### 6.3.2 Recognition distance

##### 6.3.2.1 Deriving the recognition distance

The recognition of the face of the target persons was expressed in a percentage between 0% and 100% at eleven distances between subject and target person. Thus, each approach eleven percentage were noted by the subject. For each approach one recognition distance was derived. This was done by fitting a s-curve through the measured recognition percentages  $R$ . The s-curve formula is shown in Equation 24.

$$R = 100 \frac{C^n}{C^n + d^n} \quad [\%] \quad (24)$$

The parameter  $C$  determines the position of the s-curve at the x-axis and the exponent  $n$  determines the steepness of the s-curve. Both parameters were found by minimizing the square of the differences between the measured percentages and the s-curve. In Figure 25 shows examples of measured recognition percentage as a function of the distance. The recognition distance is the distance the curve crossed the line of 50% recognition. Note at this criterion the recognition distance has the same value as the parameter  $C$ . The s-curve is symmetrical around the 50% point when the x-axis is a log scale.

Generally, the perception of objects obeys the Weber's law, i.e., the threshold for seeing the difference between two objects is proportionally with the observed size. Therefore the distances at which the recognition judgements took place were chosen in such a way that the perceived difference in recognition between the subsequent distances is more or less the same. As a consequence the distances are distributed quite evenly along a log distance scale (See Figure 25).

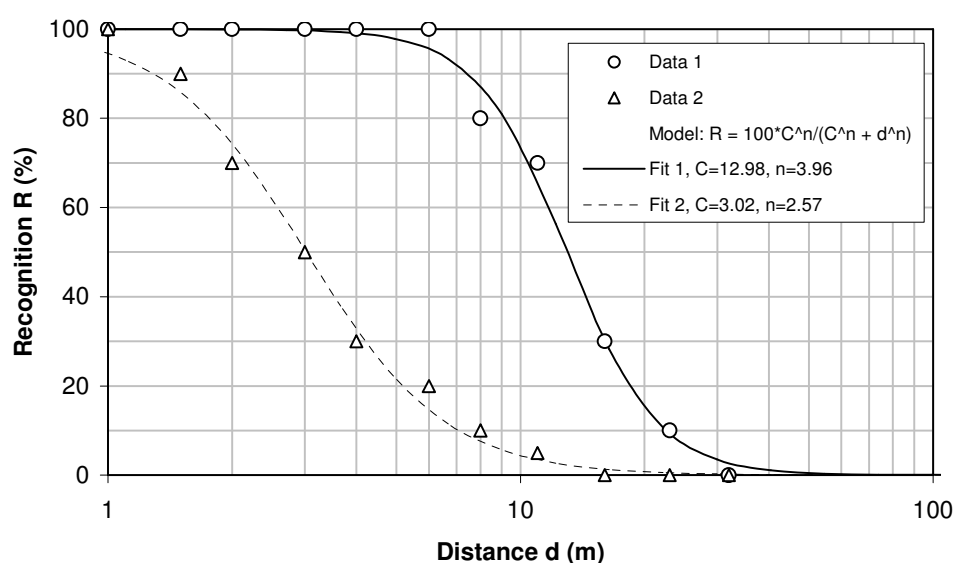


Figure 25 Examples of measured recognition percentages (Data 1, Data 2) and the fits with the s-curve model (Fit 1, Fit 2). The recognition distance depends on the criterion. For a criterion of 50% the recognition distance is the same as C.

The exponent  $n$  in the equation of the s-curve depends on the target location. This is shown in Table 6-6. The exponent varies from 0.62 to 150. The maximum of 150 is the limit of the fitting algorithm and is reached when the subjects scored 100% just after a 0% when approaching the target person. The average and the median of the exponent are the largest for target location A, with the highest face illumination and recognition distances and the lowest for target location C with the lowest face illumination and shortest recognition distances. Since the distribution of the exponents contains outliers with large values the median is a better descriptor than the mean.

Table 6-6 Statistical parameters of exponent  $n$  of the s-curve the target locations. The maximum of 150 is the limit of the fitting algorithm.

| Target location | Exponent $n$ |        |                    |         |         |
|-----------------|--------------|--------|--------------------|---------|---------|
|                 | Average      | Median | Standard deviation | Minimum | Maximum |
| A               | 3.83         | 3.47   | 2.18               | 0.90    | 40.7    |
| B               | 3.77         | 3.09   | 2.70               | 0.68    | 150     |
| C               | 3.33         | 2.60   | 4.47               | 0.62    | 150     |
| Average         | 3.64         | 3.01   | 2.58               | 0.62    | 150     |

### 6.3.2.2 Effect of presentation order

The ANOVA on the recognition distance revealed that the recognition distance depends on the presentation order of the lamps ( $F(5,725)=10,47$ ,  $p<0.000001$ ), i.e., the average recognition distance in the beginning of the experiment is larger than later in the experiment. The effect is illustrated in Figure 26 where the recognition distance is plotted as a function of the presentation order and the four subject groups.

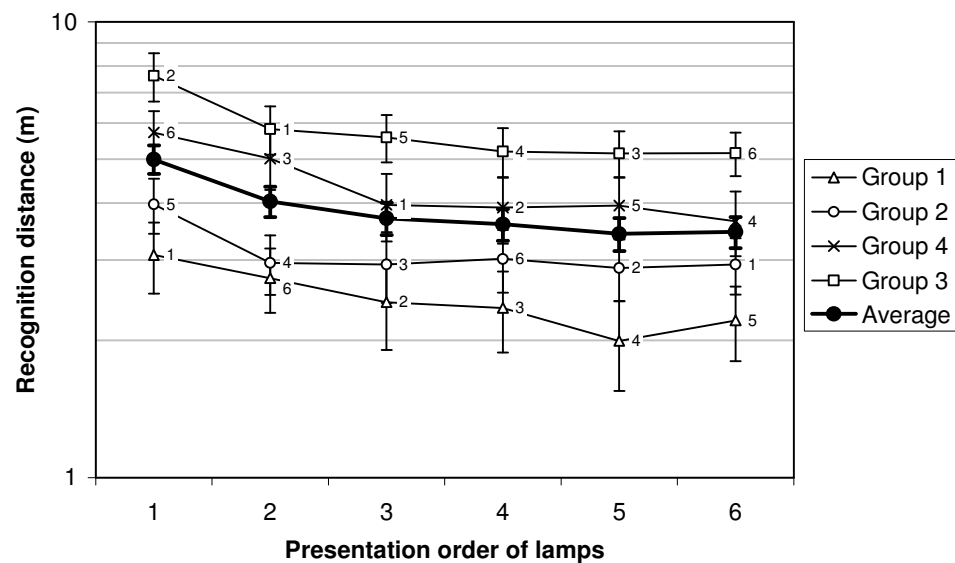


Figure 26 Recognition distance as a function of the (chronological) presentation order, lamps and group. The error bars indicate the standard error of the mean (SEM). The figures at the data points are the lamp numbers.

The post-hoc Tukey test showed that only the first presentation differs from all other presentations ( $p=0.009$ ), and there are no differences between the other presentations, 2 to 6 ( $p>0.09$ ). Further analysis shows also that the decrease in recognition distance does not differ between the four groups. In statistical terms, there is no significant interaction between groups and the presentation order ( $F(15,725) = 0.39$ ,  $p = 0.98$ ). This means that for all four groups, the shape of the decline curve is equal to the average curve. Note that the various lamps (see figures at data points) for the different groups are presented in a different order, at different moments during the experiment. Therefore it is possible that due to the effect of presentation order the differences between lamps for the different groups are erroneous. The effect of presentation order thus provides an additional noise and thus additional inaccuracy in the measurements. Since the effect of presentation order is the same for all groups, the data were corrected by multiplying all measured recognition distances by a correction factor which depends on the presentation order. The correction factors are determined by dividing the average detection by the recognition distance for each presentation order. The correction factors are 0.768, 0.950, 1.034, 1.067, 1.119, and 1.109 for the presentation orders 1 to 6.

### 6.3.2.3 Recognition distance

The (corrected) recognition distance averaged over all subjects (young and old) is plotted as a function of the vertical face illuminance in Figure 27 for the six lamps. The three locations of the target persons and the two light levels result in six different illuminance levels for each lamp. Each data point is an average of maximal 45 measured recognition distances. The error bars indicate the standard error of the mean (SEM<sup>3</sup>). The graph shows a clear effect of the illuminance on the recognition distance: the recognition distance increases with increasing illuminance. Note the data is plotted on a log-log graph and the data points in this plot are on a straight line. The regression line can be described by the function:  $d = 4.1E_v^{0.54}$ . The data of the six different lamps

<sup>3</sup> The standard error of the mean (SEM) equals to the standard deviation divided by the square root of the number of measurements.

all lay quite close to the line. Note that there are six data points for each lamp, corresponding to three target person positions times two light levels.

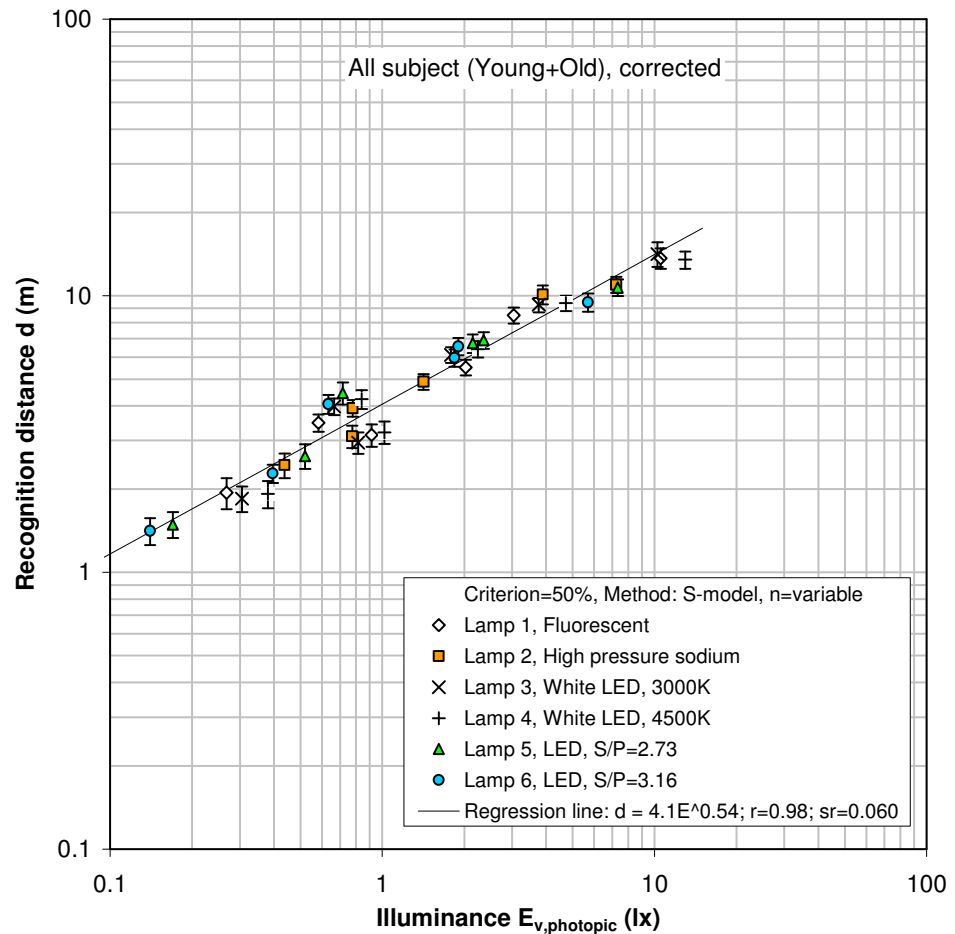


Figure 27 Recognition distance as a function of the (photopic) vertical illuminance at the face of the target persons for six different lamps. The error bars indicate the standard error of the mean (SEM).

The differences between the conditions were tested with an ANOVA. Since the illuminances in the experiment were not equal for all lamps (see Table 6-8), we calculated the a new set of recognition distances at three fixed values for the vertical illuminances, 4, 1, and 0.4 lx, by interpolating between low and high light level of respectively the target person positions A, B, and C. For semi-cylindrical illuminances the fixed values for the ANOVA were 1.6, 0.4, and 0.16 lx. The ANOVA was applied to this new data set with the conditions lamp, age and target person position as independent variables and the logarithm of the recognition distance as the dependent variable. This ANOVA revealed that there is a statistical significant effect of age ( $F(1,761) = 269$ ,  $p=0$ ) and target person position ( $F(2,761)=584$ ,  $p=0$ ) and no difference between the lamps ( $F(5,761)=0.63$ ,  $p=0.68$ ). No statistical significant interactions between the conditions lamp, age, and target person position were found.

In Figure 28 the recognition distances are plotted as a function of the face illuminance for the two age groups. The average data points of both the young and old subjects lay on a straight line in the log-log graph. The recognition distances for the young subjects are a factor  $5/2.9 = 1.72$  larger than for the old subjects.

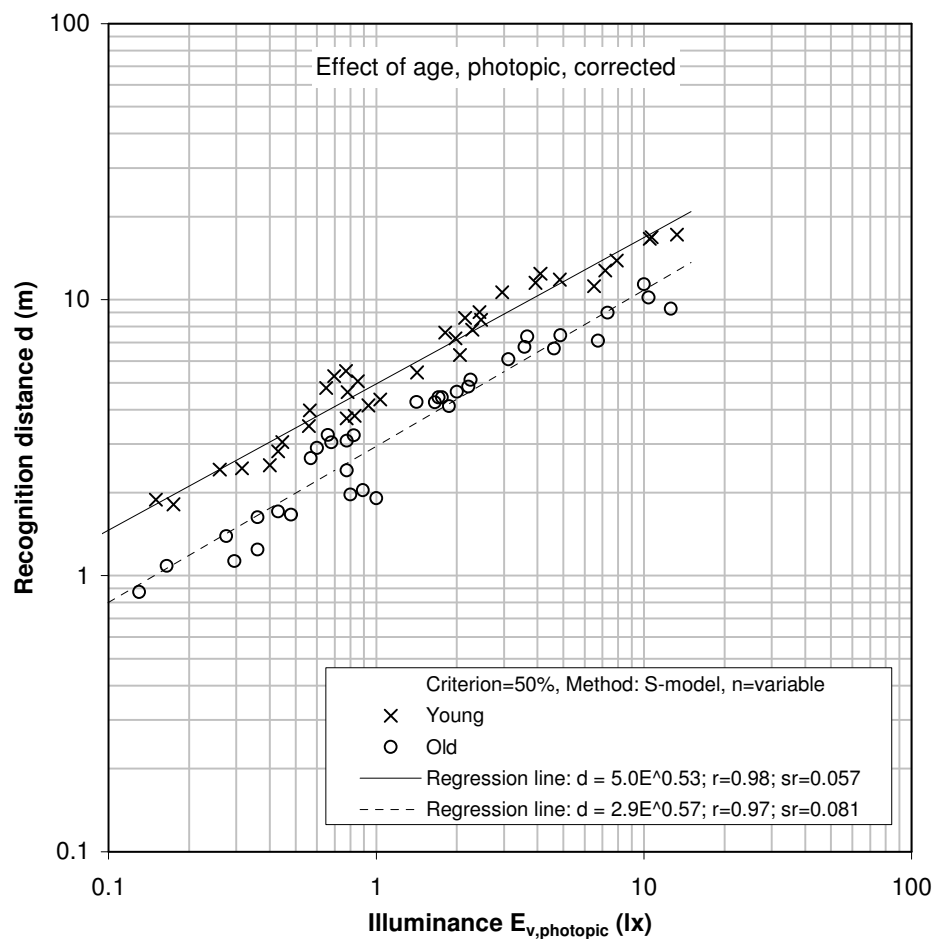


Figure 28 Recognition distance as a function of the (photopic) vertical illuminance at the face of the target persons for two age groups (young, old).

#### 6.3.2.4 Mesopic analysis

We also studied the recognition distances as a function of the *mesopic* illuminance at the face. For the calculation of the mesopic illuminance scale we applied the model MES 2 that is recommended by the CIE (2010). This model is derived from existing mesopic models; It is an intermediate between the “unified system of photometry” of Rea et al. (2004) and the MOVE-model of Goodman et al. (2007). The input for this model is the background luminance, the photopic illuminance, and the S/P-ratio. As background illuminance we applied the face luminance, using an estimated reflection of 20%. As S/P-ratio we applied the values we measured for each lamp at the experimental site (Table 6-9).

In Figure 29 the recognition distances averaged across all subjects and all lamps are plotted as a function of the *mesopic* vertical face illuminance. This graph should be compared with the Figure 27 where the same data is plotted against the *photopic* vertical face illuminance. It is clear that the data in mesopic plot in Figure 29 show more scattered around the regression line than the data of the photopic plot in Figure 27. This is also quantified by the lower regression coefficient for the mesopic plot ( $r=0.96$ ) than in the photopic plot ( $r=0.97$ ). Also the residual standard deviation (sr) has become higher when the data was plotted along a mesopic scale, and increased from 0.060 for photopic to 0.084 for mesopic. When the mesopic model gives a better prediction of the

results than the regression coefficient should increase and the residual standard deviation should drop compared to the photopic scale. Therefore we can conclude that the mesopic model is not a good predictor for face recognition. The explanation for this is that face recognition is a foveal task and the mesopic model only applies to peripheral tasks at about 10 degrees from the fovea. For foveal tasks the conventional photopic scale should be used. Our results confirm this.

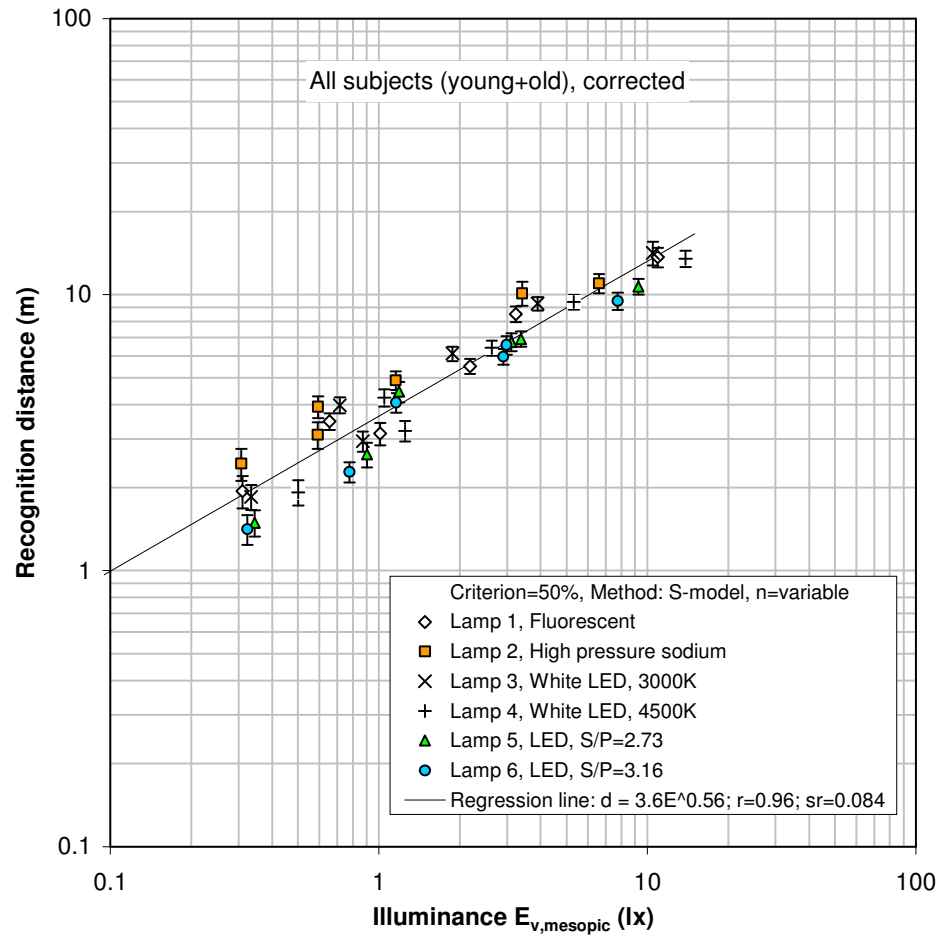


Figure 29 Recognition distance as a function of the *mesopic* vertical illuminance at the face of the target persons for six different lamps. The error bars indicate the standard error of the mean (SEM).

#### 6.3.2.5 Fitting parameters

The measured recognition distance  $R$  can be described by the general equation:

$$R = aE^b \quad [m] \quad (25)$$

where  $E$  is the illuminance at the face of the target person. This equation appears as a straight line in a log-log-plot, where  $b$  is the slope and  $a$  is the crossing at the y-axis at an illuminance of 1 lx. The function is only valid between the illuminance limits of 0.1 lx and 10 lx, i.e., approximately the illuminance range the experiment. Table 6-7 gives an overview of the parameters of the function that is fitted through the recognition distances as a function of different face illuminance conditions (photopic, mesopic; vertical, semi-cylindrical), age and criterion level. The correlation coefficient  $r$  and the

standard deviation of the residual (of the log data) is a measure for the goodness of the fit. For an ideal fit the correlation coefficient is 1 and the standard deviation of the residual is zero. Note that the derived functions for the calculations of the recognition distances are only valid for illuminances between 0.1 lx and 10 lx.

Table 6-7 Parameters of the fitting function  $R=a.E^b$  for different age groups (old, young, all), criteria, and type of face illuminance E (phot = photopic, mes = mesopic, v = vertical, sc = semi-cylindrical). r = correlation coefficient, sr = standard deviation of the residual.

| Age   | Parameter | Criterion = 25% |               |             |              | Criterion = 50% |               |             |              | Criterion = 75% |               |             |              |
|-------|-----------|-----------------|---------------|-------------|--------------|-----------------|---------------|-------------|--------------|-----------------|---------------|-------------|--------------|
|       |           | $E_{v,phot}$    | $E_{sc,phot}$ | $E_{v,mes}$ | $E_{sc,mes}$ | $E_{v,phot}$    | $E_{sc,phot}$ | $E_{v,mes}$ | $E_{sc,mes}$ | $E_{v,phot}$    | $E_{sc,phot}$ | $E_{v,mes}$ | $E_{sc,mes}$ |
| Young | a =       | 7.7             | 11.5          | 7.0         | 10.5         | 5.0             | 7.8           | 4.5         | 7.1          | 3.3             | 5.4           | 3.0         | 4.9          |
|       | b =       | 0.47            | 0.51          | 0.49        | 0.53         | 0.53            | 0.56          | 0.55        | 0.59         | 0.57            | 0.61          | 0.60        | 0.64         |
|       | r =       | 0.98            | 0.93          | 0.96        | 0.91         | 0.98            | 0.92          | 0.96        | 0.91         | 0.98            | 0.92          | 0.96        | 0.90         |
|       | sr =      | 0.049           | 0.093         | 0.074       | 0.107        | 0.057           | 0.109         | 0.078       | 0.121        | 0.066           | 0.125         | 0.083       | 0.134        |
| Old   | a =       | 5.2             | 7.2           | 4.7         | 6.5          | 2.9             | 4.3           | 2.6         | 3.8          | 1.8             | 2.7           | 1.6         | 2.4          |
|       | b =       | 0.50            | 0.53          | 0.51        | 0.52         | 0.57            | 0.60          | 0.59        | 0.60         | 0.61            | 0.65          | 0.64        | 0.67         |
|       | r =       | 0.97            | 0.90          | 0.93        | 0.85         | 0.97            | 0.89          | 0.94        | 0.86         | 0.95            | 0.87          | 0.94        | 0.85         |
|       | sr =      | 0.064           | 0.111         | 0.100       | 0.134        | 0.081           | 0.135         | 0.107       | 0.151        | 0.102           | 0.160         | 0.120       | 0.171        |
| All   | a =       | 6.5             | 9.4           | 5.9         | 8.6          | 4.1             | 6.1           | 3.6         | 5.5          | 2.6             | 4.1           | 2.3         | 3.7          |
|       | b =       | 0.48            | 0.51          | 0.50        | 0.53         | 0.54            | 0.56          | 0.56        | 0.60         | 0.59            | 0.61          | 0.61        | 0.65         |
|       | r =       | 0.98            | 0.93          | 0.95        | 0.91         | 0.98            | 0.92          | 0.96        | 0.91         | 0.97            | 0.91          | 0.96        | 0.90         |
|       | sr =      | 0.049           | 0.095         | 0.079       | 0.110        | 0.060           | 0.114         | 0.084       | 0.124        | 0.073           | 0.131         | 0.089       | 0.137        |

The best fits are achieved when the recognition distances are fitted as a function of the vertical photopic face illuminance ( $E_{v,phot}$ ). In this condition the correlation coefficients are the highest and the residual standard deviation is the lowest. The semi-cylindrical illuminance and the mesopic illuminance, and the combination of these two ( $E_{sc,phot}$ ,  $E_{v,mes}$ ,  $E_{sc,mes}$ ), give not a better description for the recognition distance than the photopic vertical illuminance ( $E_{v,phot}$ ). The standard deviations of the residual (sr) are always the lowest for the photopic vertical illuminance. The values of the parameter  $a$  show that the recognition distance depends on the criterion. If the observer wants to have more certainty about the recognition of the face he will come closer to the target person. The recognition distance decreases with the same factor 1.6 ( $=4.1/2.6$ ) or when the criterion changes from 50% to 75%. About the same factor is found between the criteria 50% and 25%. In that case recognition distance increases with the same factor 1.6 ( $=6.5/4.1$ ). Recognition distances for other criteria can be derived using the parameters of Table 6-7 and the model of Equation 24. In Figure 30 the model for recognition distance is shown as a function of the vertical photopic illuminance and the three criteria. The slopes of the lines in the log-log plot are slightly different. Further analysis shows that only the slopes of the criterion 25% and 75% are statistically significant different ( $F(34,34)=2.2$ ,  $p=0.012$ ). However, the slopes of all three criteria are not different from a slope of 0.5 ( $F(33,34)<1.38$ ,  $p>0.17$ ), which means that the face recognition model for criteria between 25% and 75% and vertical illuminances below 10 lx, can be approximated by a simple square root function.

$$R = a\sqrt{E_v} \quad (26)$$

The parameter  $a$  is 6.5, 4.1, and 2.7 for respectively the criteria 25%, 50% and 75%.

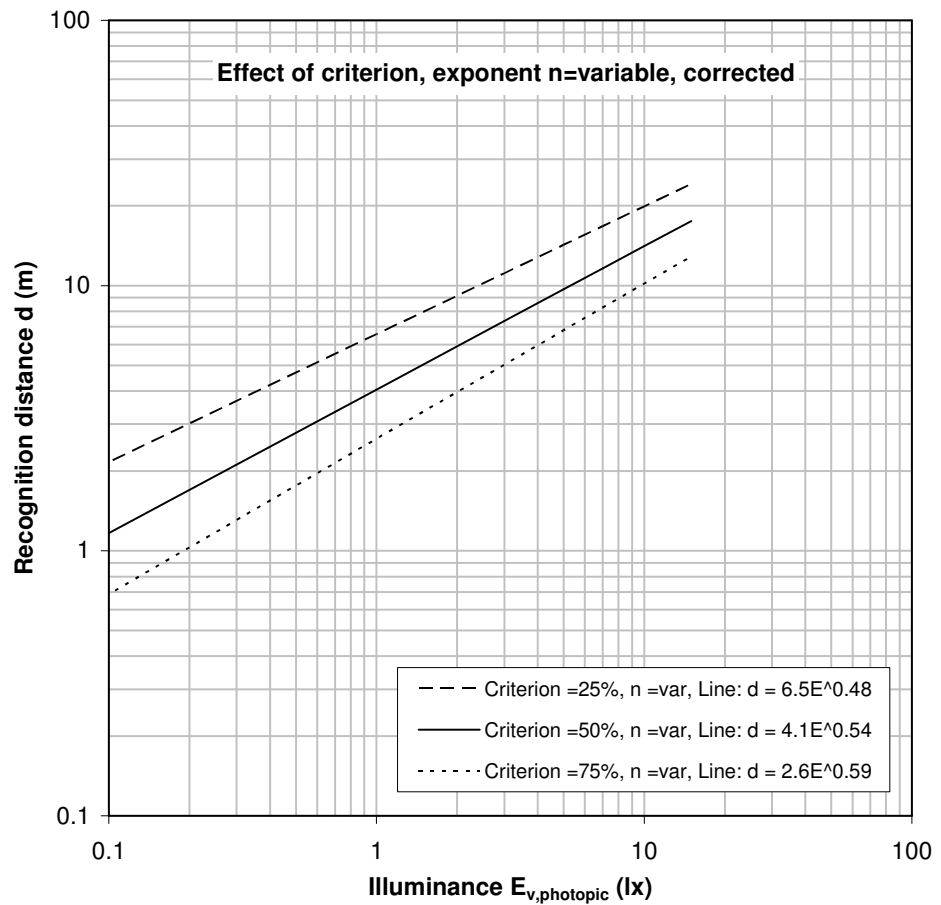


Figure 30 Model for the recognition distance as a function of vertical photopic illuminance and three criteria.

### 6.3.3 Photometric measurements

#### 6.3.3.1 Illuminances

Table 6-8 shows the measured average vertical photopic illuminances at the faces of the target persons during the experiment.

Table 6-8 The average measured vertical photopic illuminances at the faces of the target persons (A, B, C) for high and low light level and the six lamps.

| Lamp    | Average vertical illuminance at the target persons face $E_{v,face}$ (lx) |      |      |                 |      |      |
|---------|---|------|------|-----------------|------|------|
|         | High light level  |      |      | Low light level |      |      |
|         | A   | B    | C    | A               | B    | C    |
| 1       | 10.54   | 2.03 | 0.91 | 3.04            | 0.58 | 0.27 |
| 2       | 7.24  | 1.42 | 0.78 | 3.88            | 0.78 | 0.44 |
| 3       | 10.26   | 1.79 | 0.82 | 3.76            | 0.67 | 0.31 |
| 4       | 12.95   | 2.25 | 1.02 | 4.73            | 0.84 | 0.38 |
| 5       | 7.32  | 2.36 | 0.52 | 2.15            | 0.72 | 0.17 |
| 6       | 5.69  | 1.84 | 0.40 | 1.90            | 0.63 | 0.14 |
| Average | 9.00  | 1.95 | 0.74 | 3.24            | 0.70 | 0.28 |

### 6.3.3.2 Spectral measurements

The photometric parameters based on the spectral measurements of the six lamps used in the experiment are listed in Table 6-9. The (correlated) colour temperature, S/P-ratio, colour rendering index (CRI), and the colour coordinates were calculated based on the measured relative spectral power distributions of the lamps. Lamp 5 has a light source consisting of LEDs with various colours, which cause a slight variation of the spectrum as a function of the radiation direction the light. Therefore we measured the spectrum of lamp 5 at the ground right below the lamp (as we did for all the other lamps) and also in the direction of the faces of the target persons. It appears that the light in the direction of the face of the target persons has a slightly lower colour temperature and a lower S/P-ratio compared to the ground direction. Note that lamps designed for mesopic light levels have the highest S/P-ratio's and the poorest colour rendering index. The high pressure sodium lamp has the lowest S/P-ratio and also a low colour rendering index.

Table 6-9 Measured colorimetric parameters of the lamps used in the face recognition experiment. The parameters of lamp 5a are measured

| Nr   | Lamp              | Colour Temperature $T_c$ (K) | S/P-ratio | Colour rendering index |                   | Colour coordinates |        |
|------|-------------------|------------------------------|-----------|------------------------|-------------------|--------------------|--------|
|      |                   |                              |           | $R_a$                  | Qualification)*** | x                  | y      |
| 1    | Fluorescent       | 3021                         | 1.26      | 83                     | Good              | 0.4403             | 0.4138 |
| 2    | HPS               | 1870                         | 0.52      | 20                     | bad               | 0.5435             | 0.4132 |
| 3    | White LED, 3000 K | 2912                         | 1.16      | 78                     | moderate          | 0.4406             | 0.4007 |
| 4    | White LED, 4500 K | 4519                         | 1.61      | 71                     | moderate          | 0.3612             | 0.3693 |
| 5)*  | LED, Ecowhite     | 5643                         | 3.03      | 36                     | bad               | 0.3268             | 0.5185 |
| 5)** | LED, Ecowhite     | 5014                         | 2.73      | 32                     | bad               | 0.3593             | 0.5192 |
| 6    | LED, Moonlight    | 4862                         | 3.16      | 15                     | bad               | 0.3512             | 0.3736 |

)\* Measured from below (ground). )\*\* Measured from the target person's face. )\*\*\* Based on Schreuder et al. (2005).  $100 \geq R_a \geq 90$ : very good;  $90 > R_a \geq 80$ : good;  $80 > R_a \geq 50$ : moderate;  $R_a < 50$ : bad.

Figure 31 shows the colour coordinates of the six lamps in the CIE 1931 chromaticity diagram. Note that all colour coordinates of the lamps 1, 2, 3, 4, and 6 lay close to the Planckian locus of the colour coordinates for an incandescent black body. These colours therefore are perceived as natural "white" lighting colours, although the colour temperatures of these lamps vary between approximately 2000 K and 4500 K. The colour coordinates of lamp 5 lay in the green area, quite far away from the Planckian locus and are therefore perceived as an uncommon lighting colour.

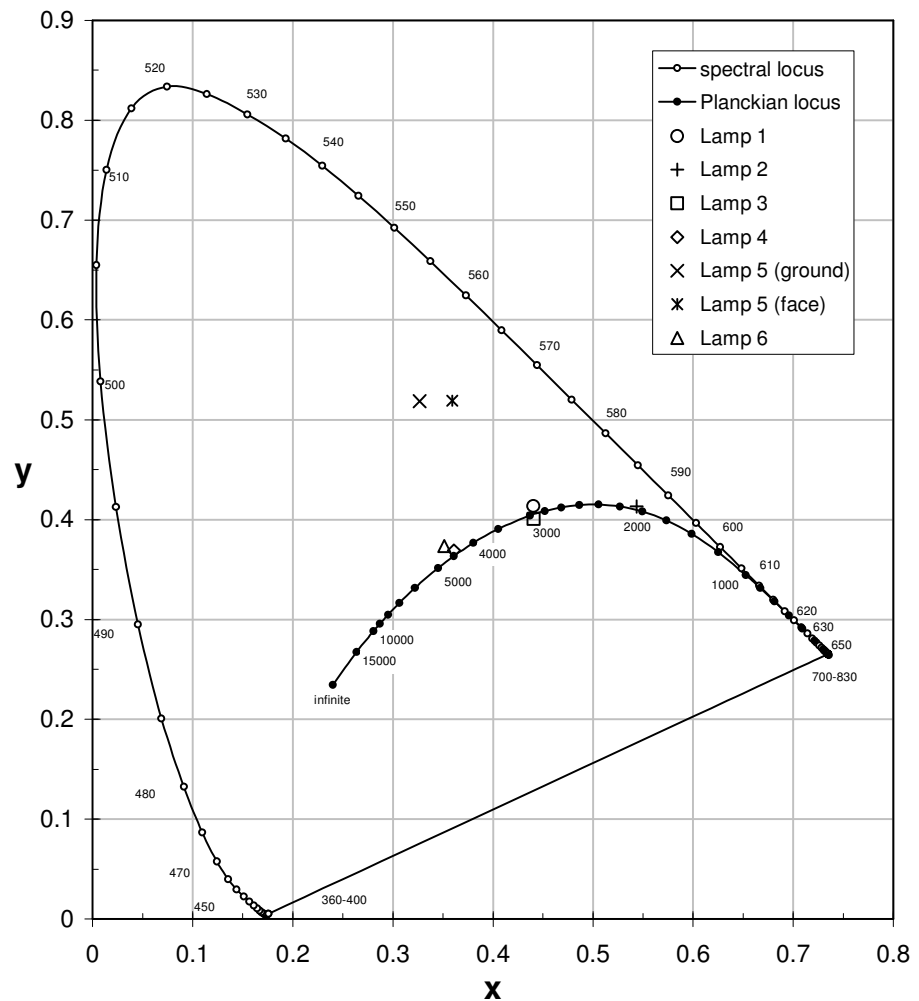


Figure 31 Colour coordinates of the lamps in the CIE 1931 chromaticity diagram. The Planckian locus indicates the colour coordinates of an incandescent black body of various temperatures (Kelvin).

### 6.3.4 Glare

#### 6.3.4.1 Discomfort glare

The discomfort glare was rated by the subjects once every approach. With the ANOVA it was tested whether the rated discomfort glare was affected by the various conditions. It appears that there was a significant effect of lamp ( $F(5,1536)=7.64$ ,  $p=0$ ), age ( $F(1,1536)=12.6$ ,  $p=0.0004$ ), light level ( $F(1,1536)=8.0$ ,  $p=0.005$ ), and target person position ( $F(2,1536)=70$ ,  $p=0$ ). There was no significant effect of presentation order of the lamps ( $F(5,1464)=5$ ,  $p=0.17$ ). Therefore it was not necessary to correct the discomfort glare data for such an effect.

The average measured discomfort glare as a function of lamp is displayed in Figure 32.

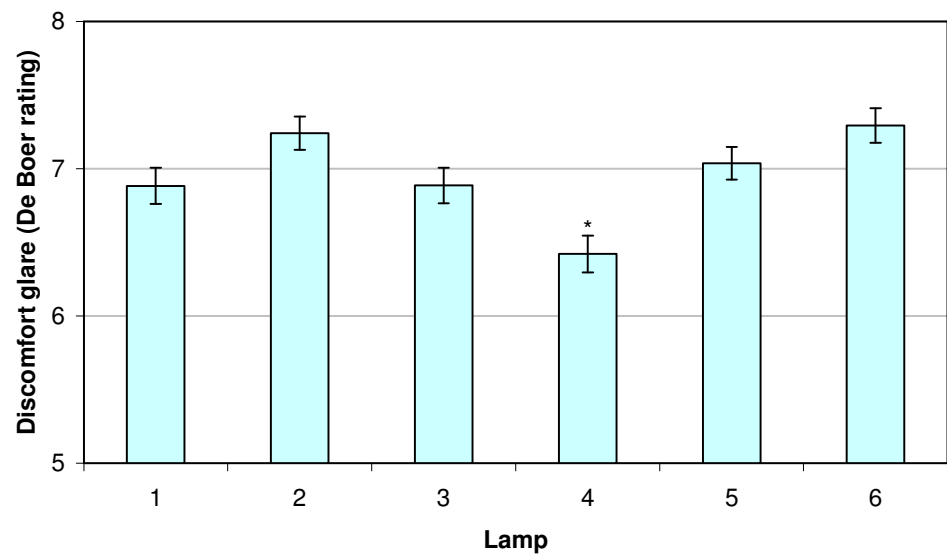


Figure 32 Average measured discomfort glare as a function of the six lamps. De lamp marked with an asterisk (\*) is statistically significant different from all other lamps. The error bars indicate the standard error of the mean (SEM).

A post hoc test revealed that only lamp 4 was different from all other lamps ( $p=0.044$ ). Lamp 4 has a lower De Boer rating which means that this lamp caused more discomfort glare than all other lamps in this experiment. However, the higher discomfort glare of lamp 4 is probably not due to a different spectrum but might be explained by the fact that the average illuminance at the eyes of the observers during the experiment was the highest for lamp 4. This is shown in Table 6-8 (assuming that the illuminances at the target person faces are proportional with the illuminances at the observers at 4 m distance). The effect of the illuminance on discomfort glare becomes clear when this is plotted in a graph (see Figure 33). The data points are pretty well predicted by models for discomfort glare of headlamps (Schmidt-Clausen, 1974; Alferdinck, 1996) and discomfort glare due to sun reflections in sound barriers (Alferdinck et al., 2008). These models show, except for Alferdinck et al. (2008), a straight line in a log-log-plot. Note that lamp 4 has the largest illuminance and the most discomfort glare (lowest rating value). We can conclude that the discomfort glare in this experiment does not depend on the spectrum of the light source.

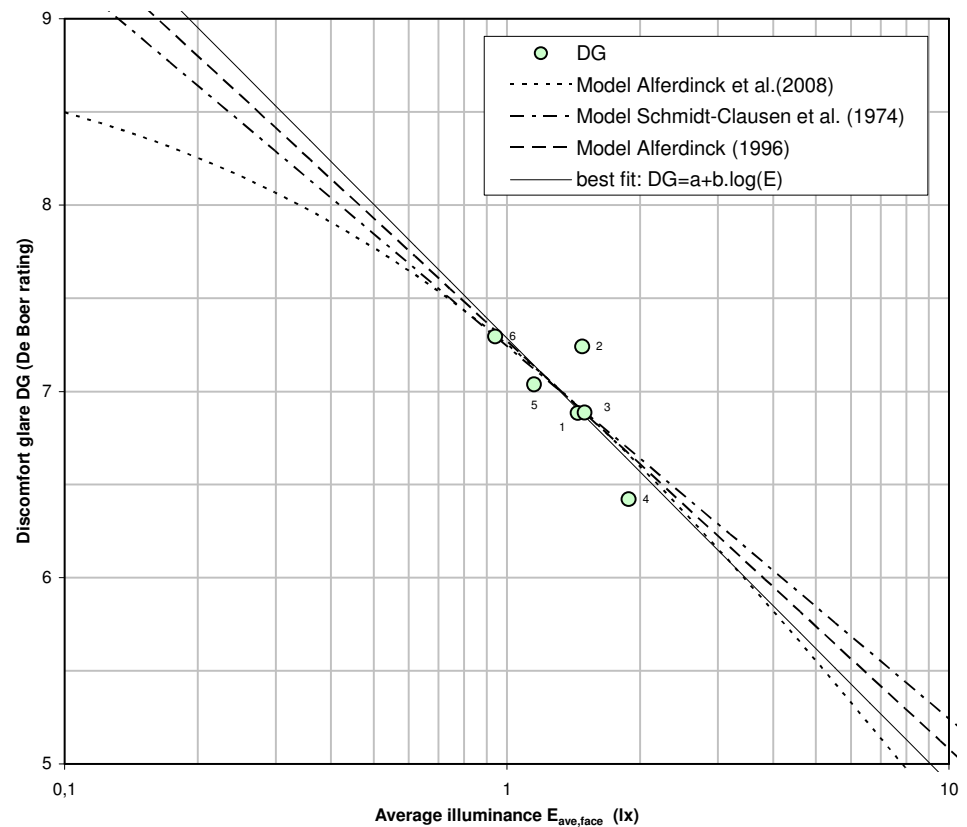


Figure 33 Discomfort glare as a function of the average vertical illuminance at the face of the target person, compared with discomfort glare models.

The discomfort glare rating was different for the two age groups ( $F(1,1536)=12.6$ ,  $p=0.0004$ ). The average discomfort rating for the young group was 7.1 and for the old group 6.8, which is a small but statistically significant difference. Thus, the old groups experienced slightly more discomfort glare than the young group. Further analysis revealed that this difference was only apparent for low light levels, which is illustrated in Figure 34. The discomfort glare rating for the young group at a low light level is different from all three other conditions ( $p=0.002$ ), which do not differ among each other.

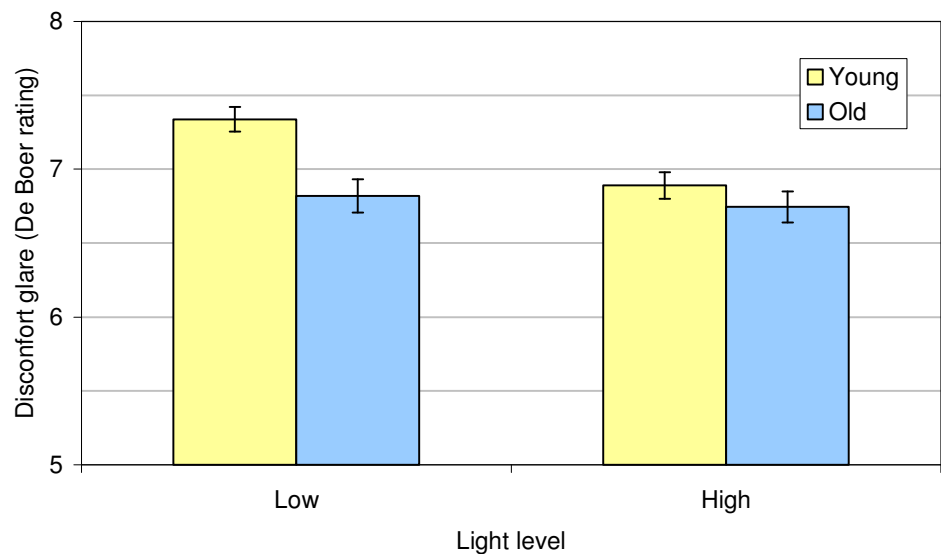


Figure 34 Discomfort glare as a function of light level and age. The error bars indicate the standard error of the mean (SEM).

#### 6.3.4.2 Disability glare and threshold increment

Table 6-10 shows the measured results that describe the glare of the lamp used in the experiment. In this table the road luminance and the veiling luminance are listed for two lighting levels (low, high). This data was used to calculate the threshold increment TI. The veiling luminance is a measure for the disability glare.

Table 6-10 The road luminance, veiling luminance (disability glare), and threshold increment for the lamps in the face recognition experiment at two light levels (low, high).

| Lamp    | Road luminance<br>$L_{road}$ (cd/m <sup>2</sup> ) |      | Veiling luminance $L_v$<br>(cd/m <sup>2</sup> ) |       | Threshold increment<br>TI (%) |      |
|---------|---|------|---|-------|-------------------------------|------|
|         | High  | Low  | High  | Low   | High                          | Low  |
| 1       | 0.72  | 0.21 | 0.30  | 0.082 | 25                            | 19   |
| 2       | 0.65  | 0.38 | 0.20  | 0.084 | 18                            | 12   |
| 3       | 0.73  | 0.26 | 0.24  | 0.086 | 20                            | 16   |
| 4       | 0.86  | 0.31 | 0.30  | 0.113 | 22                            | 19   |
| 5       | 0.75  | 0.27 | 0.31  | 0.110 | 25                            | 21   |
| 6       | 0.50  | 0.16 | 0.20  | 0.065 | 23                            | 19   |
| average | 0.70  | 0.26 | 0.26  | 0.090 | 22.3                          | 17.5 |

The glare data show that the glare depends on the light level. The disability glare (veiling luminance) is about a factor three higher for the high light levels than for the low light level. This is proportional to the difference between low and high light level, which also is about the same factor (see Table 6-4 and Table 6-8). The threshold increment TI for high light levels is about 5% higher than for low light levels.

In the standard for public light there are only requirements for the threshold increment for roads for motorized vehicles driving at medium to high speeds (CEN, 2003a). Depending on the lighting class the threshold increment TI should be restricted to 10% or 15%. There are no TI requirements for cycle paths, pedestrian zone and residential areas. The threshold increments measured for the lamps in our experiment vary from

12% to 21% for low light levels and from 18% to 25% for high light levels. These TI-values are higher than prescribed for motorways but this seems not to be a problem since our experimental set-up was designed as a residential area.

## 6.4 Discussion

### 6.4.1 *Effect of age*

The results of the experiment show an effect of age, i.e., on average the old group has a shorter recognition distance than the young group. We have not found an effect of spectrum in combination with the two age groups, i.e., in statistical terms: no interaction between age and spectrum. Since older people have a more yellow eye lens one would expect that there is a difference between spectra for the young subjects and not for the old subjects.

### 6.4.2 *Comparison with literature data on face recognition*

In the current study we found a relationship between the recognition distance of faces and the illuminance of the face. The data points can be described with a function of the form  $y = a \cdot x^b$ , which is a straight line on a log-log graph. This is already illustrated in Figure 27 for a 50% recognition criterion and a vertical face illuminance. In Figure 35 these regression lines are plotted as a function of the semi-cylindrical illuminance for three recognition criteria (25%, 50%, and 75%).

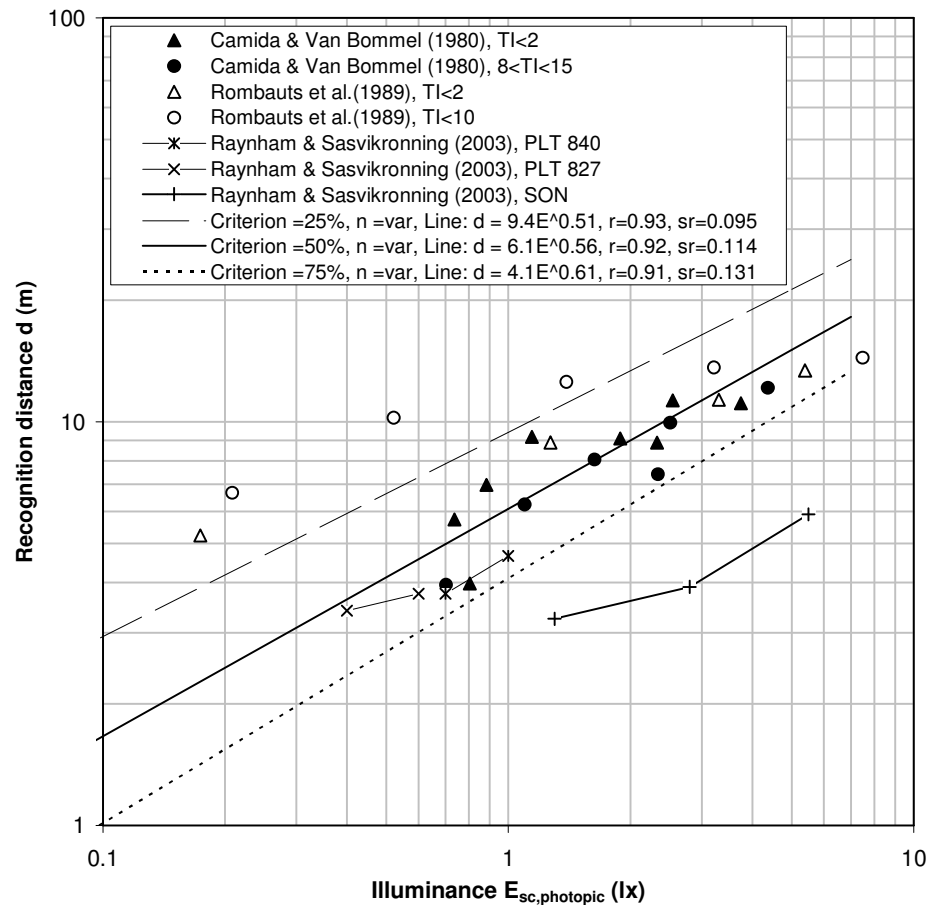


Figure 35 Comparison of the average measured recognition distances of three criteria (25%, 50%, and 75%) as a function of the semi-cylindrical face illuminance with the literature data.

These average recognition distances of the current study are compared with the data of three studies where the recognition distance is determined as a function of the semi-cylindrical illuminance.

In the first study on Caminada & Van Bommel (1980) the recognition distances were measured in a low glare condition ( $TI < 2$ ) and a high glare condition ( $8 < TI < 15$ ). In this the authors asked the subject to approach the target person until they recognized the face “without any doubt”. This means that the data should be comparable with the data of the 75% criterion in our study. In the high glare condition the recognition distances are shorter in comparison to the low glare condition. Since the TI of the current study is about 20% the current data should be compared with the high glare condition of Caminada & Van Bommel (1980). It appears that the data point of the high glare condition lay in between the lines for 50% en 75% criterion. The data points of Caminada & Van Bommel (1980) also follow the straight lines in the graph which means that the data can be described by a function of the form  $y = a \cdot x^b$  and thus match with the current study.

In second study of Rombauts et al. (1989) also recognition distances were measured as a function of the semi-cylindrical face illuminance and glare condition. These data do not match quite well with the data of Caminada & Van Bommel (1980) and the data of the current study. The data of Rombauts et al. (1989) follow a less steep slope at larger recognition distances.

The third study (Raynham & Saksvikrønning, 2003) was performed in order to determine the effect of the spectrum of the light on the facial recognition distance. In the recognition experiment three different light sources were used, one high pressure sodium lamp (SON) and two white fluorescent lamps (PLT 840, PLT 827). The data compared in Figure 35 with our data and other literature data. The data of the white light sources lie, just as the data of Caminada & Van Bommel, between the average lines for 50% en 75% criterion of our study. However, the data of the high pressure sodium lamp do not fit our data and the data of Caminada & Van Bommel (1980); the recognition distances for the high pressure sodium lamp are much shorter than of the white light sources. Note that that we found no difference between fluorescent lamps and high pressure lamps. Thus, the difference between spectra as found by Raynham & Saksvikrønning (2003) is not confirmed by our measurements.

#### 6.4.3 *Comparison with literature data on object visibility*

The measured recognition distances can be compared with the literature data of the visibility of objects. Figure 36 shows the visual acuity as a function of the illuminance of a circular target with a certain contrast with the background. The data is derived from the visibility model of Adrian (1989), based on data of Blackwell (1946) and a study of Vos et al., (1956). The visual acuity is in fact the reciprocal value of the size of the target. The visual acuity decreases when the illuminance goes down. The maximum visual acuity is reached at the maximum contrast of 1 and an illuminance of more than 2000 lx (not in graph). The lower the contrast the lower the acuity and the faster the acuity drops with the decrease of the illuminance. The recognition distance is in principal proportional with the visual acuity and also drops with decreasing light level. The data of the current experiment are fitted with a straight line on a log-log graph between the illuminance limits of 0.1 lx and 10 lx (see Figure 27). The slope of the fitted lines vary between 0.48 and 0.59 depending on the criterion (Figure 30). The curves in Figure 36 also fit between the illuminance limits of the experiment. It appears that the curve for a contrast of 0.2, with a slope of 0.52, fits the best to the measured recognition distances. This could mean that for the recognition of faces contrast of about 0.2 probably play an important role and the curve for  $C=0.2$  can be applied for fitting the measured recognition data. Applying the model of Adrian on the average maximum visual acuity of the subjects (1.85) it can be derived that in our experiment the visual acuity varies between 0.02 and 0.25 for this a contrast of 0.2 between the illuminances 0.1 lx and 10 lx. Based on the measured recognition distances it can be derived that for recognition a face with a 75% criterion, details of about 1/30 of the face height should be visible. For a 50% criterion details of about 1/18 of the face height should be visible.

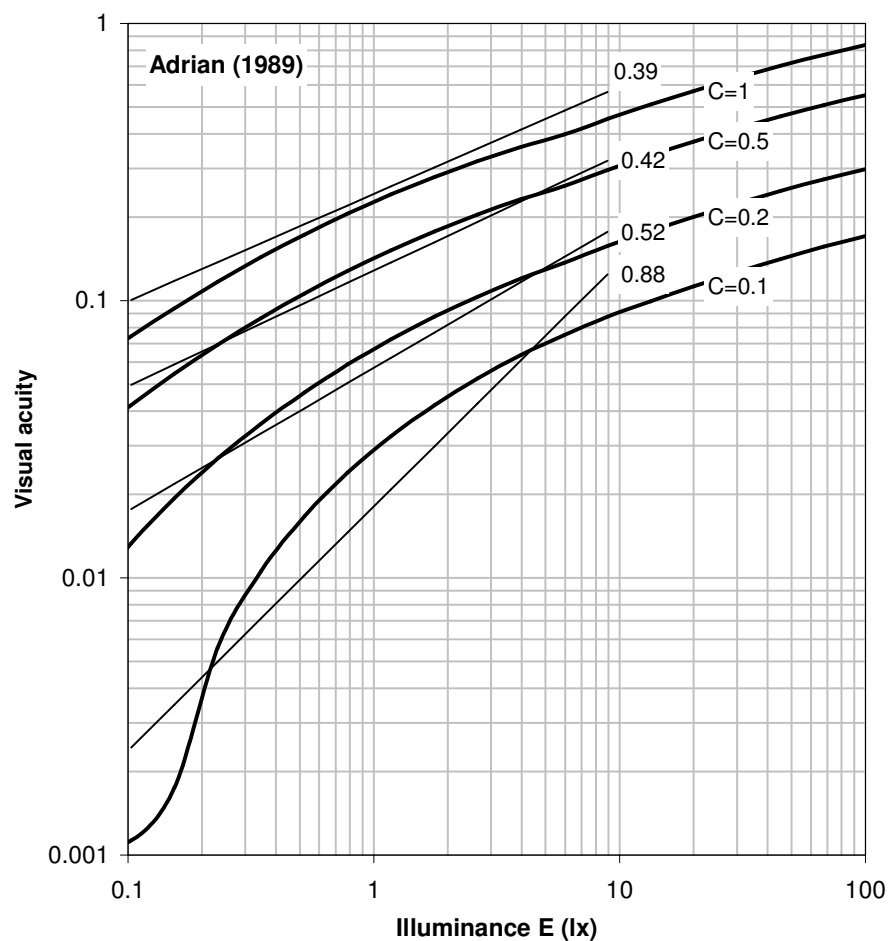


Figure 36 Visual acuity as a function of illuminance of the target  $E$  and the contrast of the target with the background  $C$ , derived from Adrian (1989). The straight lines are the fitted trough the data between 0.1 and 10 lx. The figures at the lines are the exponent  $b$  in the model: Visual acuity =  $a \cdot E^b$ .

#### 6.4.4 Effect of spectrum

In the current experiment we found no effect of the spectrum of light sources on the recognition distance of faces. The spectra of the light sources included the current widely used lamps (fluorescent, HPS), and white led lamps (3000 K, 4500 K), with S/P-ratios between 0.5 and 1.6, and also led light sources for MVL with a high S/P-ratio, of about 3. The colour rendering index  $R_a$  of the light sources ranged from 15 to 83. Based on the current experimental results we can say that the spectrum of light source is not important for face recognition. However, it should be noted that some authors found an effect of spectrum, i.e., they measured larger face recognition distances for higher colour rendering indices. The absence of the effect of spectrum in our experiment may be due to the measuring method. With the instruction of the subjects we stressed that they only should look at the face of the target persons and ignore features of posture, clothing and hair. In two of the three experiments where an effect was found of spectrum the subject had to recognise well-known persons from pictures and therefore they likely have used other features than the face only and probably even the background.

#### 6.4.5 *Mesopic illuminance*

We found that the mesopic illuminance does not give a better prediction for the face recognition distance than the common photopic illuminance. This result is not surprising since the mesopic models (CIE, 2010) only differ from the common photopic photometry for peripheral perception tasks; for foveal tasks still the photopic illuminance should be applied. We can conclude that the face recognition is a foveal task to which the mesopic model does not apply.

#### 6.4.6 *Semi-cylindrical illuminance*

In this experiment we found that the semi-cylindrical illuminance does not correlate better than the photopic illuminance with the recognition distance. In other studies was found that the semi-cylindrical illuminance was the appropriate descriptive parameter to describe the face recognition (Rombauts et al., 1989, Caminada & van Bommel, 1980). The rationale for their finding is that human faces should be illuminated from all sides for optimal recognition and therefore the detector of the illuminance meter should be sensitive to all these relevant directions at the human face. The reason we have not found this effect can be that in our experiment the faces of our target persons were mainly illuminated from the front and therefore the vertical illuminance is also a good descriptor. For the measuring the advantage of semi-cylindrical illuminance (which was not the main goal of our study) more variation in the light directions at the faces are necessary. The other cause may be the limited sensitivity of our semi-cylindrical illuminance meter which causes higher uncertainties at low light levels.

### 6.5 **Conclusions experiment face recognition**

We have measured the face recognition distance in a perception experiment with six different light sources typical for use in a residential area, a warm white fluorescent lamp (S/P=1.26), a high pressure sodium lamp (HPS, S/P=0.52), two white led lamps (3000 K, S/P=1.16 and 4500 K, S/P=1.61), and two led lamps with a high S/P-ratio of about 3. The colour rendering index ranged from  $R_a=15$  for a led lamp with a high S/P-ratio to  $R_a=83$  for the warm white fluorescent lamp. Further condition were: two age groups (young, average 16.5 years; old, average 60.2 years), two light levels (low, high), and three position of the target persons. We measured the vertical illuminance and the semi-cylindrical illuminances at the faces of the target persons. The mesopic illuminances were calculated with the CIE-model. We can draw the following conclusions:

- The spectrum of the light sources in the experiment has no effect on the recognition distance. This means that the led lamps for MVL with the high S/P-ratio do not perform worse or better than the conventional light sources (fluorescent, HPS) and white led lamps, with S/P-ratios between 0.5 and 1.6. The other consequence of this is that, unlike findings in other studies, we have found no effect of the colour rendering index on the recognition distance.
- The face recognition distance strongly depends on the vertical illuminance  $E_v$  at the face of the target persons. Between the illuminance limits of the experiment (0.1 to 10 lx) the recognition distance  $R$  can be described with a square root function in the form  $R=a \cdot E_v^{0.5}$ , which is a straight line on a log-log graph. The parameter  $a$  depends on the recognition probability.
- We found that the mesopic illuminance does not give a better prediction for the face recognition distance than the common photopic illuminance. This confirms the fact that the mesopic effect only occurs for peripheral visual tasks and that face recognition is a foveal visual task.

- In our experiment we found that the semi-cylindrical illuminance does not give a better prediction for the face recognition distance than the vertical illuminance. This is probably caused by a too low variation in lighting directions in the experiment and a limited sensitivity of the illuminance meter.
- On average the young observers show recognition distances that are a factor 1.7 larger than the old observers. One could expect also an spectrum effect because of the blue light loss of the elderly. This spectral effect however was not found in our experiment.

## 7 General discussion

The goal of this study is to find out whether lighting should be recommended that is especially designed for mesopic light levels. In this report we have denoted this lighting as mesopic vision lighting (MVL). Several studies have resulted in a model for the calculation of the mesopic light levels (CIE, 2010). For mesopic light levels in which the light contains enough short wavelengths (high S/P-ratio) and for a visual task in the periphery of the visual field, the effective light level is higher than measured with the conventional light meters. When it is proven that MVL, i.e., lighting with a high S/P-ratio, would be beneficial in terms of visual performance or energy saving, the lighting standards (for example CEN, 2004) should be revised.

In the current study we found that face recognition is a visual task that does not benefit from the mesopic effect. We also found no effect of the spectrum of the light, i.e., there was no difference in human detection performance between fluorescent lamps, high pressure sodium lamps, white led lamps and the led lamps with a high S/P-ratio. This means that high S/P-ratio led lamps do not improve face recognition and neither degrade face recognition. Thus MVL can be installed to serve other lighting purposes while in the same time it does not impair face recognition.

In the literature review of the current study we found that there are models for the determination of the (dynamic) adaptation luminance, which is an important parameter for mesopic models. This adaptation luminance however depends on eye movement behaviour and the luminance distribution in the visual field of the different road users (car drivers, cyclists, pedestrians) in the various traffic environments (motorways, secondary roads, residential area, etc.). The simplest way is to set the adaptation luminance to the global adaptation luminance, which is the average luminance of the visual field (which can be determined in practice by dividing the measured vertical face illuminance by  $\pi$ ). This is probably an overestimation of the actual adaption luminance when the observer is looking at a local spot with a low luminance, e.g., the road surface. On the other hand it can be an underestimation when the observer has just gazed at a brightly lit advertisement. It should be noted that taking the average road luminance as the adaptation luminance always will be an underestimation because of the influence of the disability glare of the luminaires and possible other bright areas in the field of view. Additional research will give more insight in luminance distributions and eye movements in real traffic situations. After that the method for the determining the adaptation luminance should be revised.

The rising average age of the road users is disadvantageous to the benefit of the mesopic effect. At an age of 80 years the S/P-ratio decreases with a maximum of about 25%. At an age of 60 years this percentage is 15%. When we know the age distribution of the road users we can calculate the overall effect of the age on the reduction of the S/P-ratio.

The question now is where and when MVL is useful and how the lighting standards can or should be revised. Knowing that the mesopic effect only works under special conditions (mesopic light levels, peripheral vision, high S/P-ratio) we think that these lighting are *not* useful for the next applications:

- Foveal vision tasks such as:
  - reading signs,
  - recognising faces,
  - centre line of the road.

Mesopic light may be useful in the following conditions:

- Lighting objects in the periphery of the visual field, such as:
  - side lines and borders of the road,
  - traffic at crossing roads (objects in the periphery will be detected faster),
  - steering tasks of road users (the optic flow in periphery is used for the steering task).
- In residential areas, parks, footpaths, and cyclist paths. Mesopic light will be perceived as brighter and the people may feel safer. It should be noted that the evidence for this effect is not yet measured in a scientific experiment.

When lighting applied with high S/P-ratios, the light level for visual task in the periphery can be lowered according to the factor determined by the mesopic model of the CIE (2010). When this is an overall light level decrease it will hamper foveal vision tasks, such as face recognition and reading signs, since the mesopic effect does not apply to foveal vision. In theory, it is possible to have an increase in peripheral visual function at the expense of decrease of the foveal visual function, with the overall traffic safety remains at the same level. The problem however is to quantify this trade-off and to make an evidence based decision on the lighting guidelines. Further research should reveal the details of this trade-off. Therefore it is advised to play safe for the time being and apply lighting with high S/P-ratios only when the foveal visual function is not hampered.

## 8 Conclusions and recommendations

This study on mesopic vision and public lighting has two major parts, a literature review and a face recognition experiment.

### 8.1 Conclusions literature review

The literature review concerns mesopic vision and the effect of light sources especially designed for mesopic vision and was focused on four issues: adaptation, atmospheric scatter, effect of age, and face recognition. From the literature review we can conclude:

- The adaptation of the visual system is very complex, but there are useful models available for the calculation of the time courses of the adaptation process. The time course of the adaptation process for luminance levels in public lighting ( $<2 \text{ cd/m}^2$ ) can last more than 3 minutes. The adaptation is affected by eye movements and therefore never optimal in practical situations. There is no reliable model that accounts for this effect. The lower limit of the adaptation luminance is determined by the veiling luminance due to disability glare. In absence of proper adaptation models at this moment, it is advised to use the average scene luminance as adaptation luminance. To take account for disability glare the adaptation luminance should be increased with the veiling luminance.
- For standard atmospheric conditions short wavelength wavelengths (bluish light) is more scattered than light with large wavelengths (yellowish, reddish light). A non-white light source with an S/P-ratio of 3 scatters only 10% more light than a warm white light source with a colour temperature of 3000 K and an S/P-ratio of 1.23. For conditions with a lower meteorological visibility (haze, fog) the scattering is independent from wavelength and there is no difference in scattering between light sources of different S/P-ratios. Therefore we can conclude that the increase of light pollution due to light sources with S/P-ratios up to 3 can be neglected.
- The effective S/P-ratio of light sources declines with the age of the observer due to the yellowing of the eye media. For an observer at an age of 80 years the S/P-ratio of light sources for public lighting is 10% to 25% lower than for a young observer of 30 years old. We have to take account for this age effect when designing MVL.
- Some studies on face recognition suggest that the spectrum of the light is an important factor of face recognition, and that a larger colour rendering index results in a larger recognition distance. However, other studies suggest that colour does not play an important role in the recognition of faces. Some of the differences in the findings may be due to the task or the stimuli used (e.g. real faces, complete persons, paper images). We conclude that it is still under debate whether colour plays an important role in face recognition.

### 8.2 Conclusions face recognition experiment

In the experiment we measured the face recognition distance of six different light sources which are typical for use in a residential area: a warm white fluorescent lamp (S/P=1.26), a high pressure sodium (HPS, S/P=0.52), two white led lamps (3000 K, S/P=1.16 and 4500 K, S/P=1.61), and two led lamps with a high S/P-ratio (2.73 and 3.16), for two age groups (young, average 16.5 years; old, average 60.2 years).

From the results we can conclude:

- The spectra of the light sources used in this experiment has no effect on the face recognition distance. This means that the led lamps with the high S/P-ratio do not perform worse or better than the conventional light sources (fluorescent, HPS) and white led lamps. The also means that, unlike findings in other studies, we found no effect of the colour rendering index on the recognition distance.
- The face recognition distance strongly depends on the vertical illuminance at the face of the target persons. Between the illuminance limits of the experiment (0.1 to 10 lx) the recognition distance R can be described with a square root function in the form  $R=a.E_v^{0.5}$ , which is a straight line on a log-log graph. The parameter a depends on the recognition probability.
- We found that mesopic illuminance does not give a better prediction for face the recognition distance than the standard photopic illuminance. This confirms earlier findings that the mesopic effect only occurs for peripheral perception tasks and not for foveal tasks, such as face recognition.
- We found no evidence for previous findings that the semi-cylindrical illuminance gives better prediction for the face recognition distance than the vertical illuminance. This is probably caused by a too low variation in lighting directions in our experiment and a limited sensitivity of the illuminance meter.
- Elderly need an importantly higher lighting level than young people. In our experiment we found the young observers have a factor 1.7 larger recognition distances than the old observers, which means that the old group needs almost a factor three more light level for the same performance. One could expect also an spectrum effect because of the blue light loss of the elderly. This spectral effect however was not found in our experiment.

### 8.3 Recommendations

- The mesopic lighting model should not be applied for situations in which foveal vision, such as face recognition and reading signs, is important. However, according the findings in our experiment, lighting with a high S/P-ratio (and low colour rendering index) will not hamper face recognition. It should be noted that on the other hand, there are studies that show an effect of spectrum on face recognition and the influence of the spectrum is still under debate. Potential applications of lighting with a high S/P-ratio are the lighting road sides, crossing roads, residential areas, and cyclist and foot paths.
- Since it has been shown that the S/P-ratio has no effect on foveal vision, light levels in the fovea cannot be lowered when using lighting with a high S/P-ratio. For peripheral visual tasks the light level can be lowered according the mesopic model of the CIE.
- It is recommended to inventory the luminance distributions of various roads and residential areas in order to determine the veiling luminance and the adaptation state in real traffic situations. Alternatively, the effect of adaptation state under these conditions can be measured on a representative task (e.g. reading, acuity).

## 9 Acknowledgements

We thank Innolumis, Lightronics, and Philips for providing the light sources, lamp posts, light control equipment, and technical advice. Thanks to the project advisory committee (Ruben van Bochove, Wout van Bommel, Ton van den Brink, Peter van der Burgt, Bouke Bussemaker, Boudewijn Huenges Wajer, Collette Knight, Han van der Steen) for the fruitful discussions on the scientific and technical aspects of this study.



## 10 References

- Adrian, W. (1989). *Visibility of targets: Model for calculation*. Lighting Research and Technology, 21, (4), 181-188.
- Alferdinck, J.W.A.M. (1996). *Traffic safety aspects of high-intensity discharge headlamps: Discomfort glare and direction indicator conspicuity*. In: A. G. Gale (Ed.), *Vision in Vehicles V* (pp. 337-344). Amsterdam: Elsevier.
- Alferdinck, J.W.A.M. (2006). *Target detection and driving behaviour measurements in a driving simulator at mesopic light levels*. Ophthalmic and Physiological Optics, 26, (3), 264-280.
- Alferdinck, J.W.A.M. (2008). *Waarnemingsexperimenten bij verschillende kleuren mesopische verlichting*. [Perception experiments with mesopic lighting of various colours] In: *Het Nationale Lichtcongres 2008*. Ede, Netherlands: Nederlandse Stichting Voor Verlichtingskunde (NSVV).
- Alferdinck, J.W.A.M., Toet, A., van der Leden, N., & Zonneveldt, L. (2008). *Glare from sound barriers. Phase 2 and 3: Experiments and modelling* (TNO-report TNO-DV 2008 C148). Soesterberg, The Netherlands: TNO Defence, Security and Safety.
- Blackwell, H.R. (1946) *Contrast thresholds of the human eye*. Journal of the Optical Society of America 36 (1946), 624–643.
- De Boer, J.B. (1967). *Public lighting*. Eindhoven, The Netherlands: Philips.
- Bommel, W.J.M. van (2009). *The spectrum of light sources and low light levels: the basics*. Lighting Journal, October 2009, 39-43.
- Boyce, P.R. & Rea, M.S. (1990). *Security lighting: Effect of illuminance and light source on the capabilities of guards and intruders*. Lighting Research and Technology, 22, (2), 57-79.
- Bruce, V. and Young, A. (1998). *In the eye of the beholder. The science of face perception*. Oxford University Press.
- Cavanagh, P. and Leclerc, Y. G. (1989). Shape from shadows. Journal of Experimental Psychology: Human Perception and Performance, 15, 3-27.
- Caminada, J.F. & van Bommel, W.J.M. (1980). *New considerations for residential areas*. International Lighting Review, 31, (3), 69-75.
- CIE (1995). *Method of measuring and specifying colour rendering properties of light sources* (Publication CIE 13.3-1995). Vienna, Austria: International Commission on Illumination CIE.
- CIE (2002). *CIE equations for disability glare* (CIE Publication 146, TC 1-50 report, part of CIE Collection on glare, 2002). Vienna: International Commission on Illumination CIE.
- CEN (2003a). *Road lighting - Part 2: Performance requirements* (European Standard EN 13201-2:2003). Brussels: European Committee for Standardisation (CEN).
- CEN (2003b). *Road lighting - Part 3: Calculation of performance* (European Standard EN 13201-3:2003). Brussels: European Committee for Standardisation (CEN).
- CEN (2004). *Road lighting - Part 1: Selection of lighting classes* (Technical Report CEN/TR 13201-1:2004). Brussels: European Committee for Standardisation (CEN).
- CIE (2004a). *Photometry - The CIE system of physical photometry* (Standard CIE S010). Vienna, Austria: International Commission on Illumination CIE.
- CIE (2004b) *Guide for the lighting of road tunnels and underpasses* (Publication CIE 88:2004, 2nd edition). Vienna, Austria: International Commission on Illumination CIE.

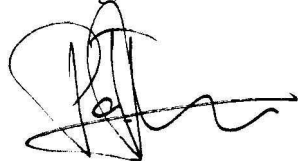
- CIE (2010). *Recommended system for mesopic photometry based on visual performance* (Technical report CIE 191:2010). Vienna, Austria: International Commission on Illumination CIE.
- Eloholma, M., Viikari, M., Halonen, L., Walkey, H., Goodman, T., Alferdinck, J.W.A.M., Frieding, A., Schanda, J., Bodrogi, P., & Várady, G. (2005). *Mesopic models— from brightness matching to visual performance in night-time driving: a review*. Lighting Research and Technology, 37, (2), 155-175
- Fors, C. (2010). *Samband mellan synbarhet och vägbelysningens färg - En litteraturstudie om mätmetoder och synbarhetsexperiment [The relationship between visibility and light source colour - a literature review]* (VTI rapport 687). Linköping, Sweden: Swedish Transport Administration.
- Freiding, A., Eloholma, M., Ketomäki, J., Halonen, L., Walkey, H., Goodman, T., Alferdinck, J.W.A.M., Várady, G., & Bodrogi, P. (2007). *Mesopic visual efficiency I: detection threshold measurements*. Lighting Research and Technology, 39, (4), 319-334.
- Garstang, R.H. (1986). *Model for artificial night-sky illumination*. Publications of the Astronomical Society of the Pacific, 98, 364-375.
- Goodman, T., Forbes, A., Walkey, H., Eloholma, M., Halonen, L., Alferdinck, J.W.A.M., Freiding, A., Bodrogi, P., Várady, G., & Szalmás, A. (2007). *Mesopic visual efficiency IV: a model with relevance to nighttime driving and other applications*. Lighting Research and Technology, 39, (4), 365-392.
- Hall, E.T. (1966). *The hidden dimension*. New York: Anchor Books.
- Hood, D.C. & Finkelstein, M.A. (1986). *Sensitivity to light*. In: K.R. Boff, L. Kaufman, & J. P. Thomas (Eds.), *Handbook of perception and human performance*, (pp. 5-1-5-66). New York: John Wiley and Sons.
- Hulst, H.C. van der (1981). *Light scattering by small particles*, Dover Publications Inc, New York, 1981, ISBN 0-486-64228-3
- IDA (2010). *Visibility, environmental, and astronomical issues associated with blue-rich white outdoor lighting* (Report May 4, 2010). Tucson, Arizona: International dark-sky association.
- Irawan, P., Ferwerda, J.A., & Marschner, S.R. (2005). *Perceptually based tone mapping of high dynamic range image streams*. In: K. Bala & P. Dutré (Eds.), *Eurographics Symposium on Rendering*. Genève, Switzerland: The Eurographics Association.
- Kemp, R., Pike, G., White, P. and Musselman, A. (1996). *Perception and recognition of normal and negative faces: the role of shape from shading and pigmentation cues*. Perception, 25, 37-52.
- Kneizys, F.X., L.W. Abreu, G.P. Anderson, J.H. Chetwynd, E.P. Shettle, A. Berk, L.S. Bernstein, D.C. Robertson, P. Acharya, L.S. Rothman, J.E.A. Selby, W.O. Gallery and S.A. Clough (1996), *The Modtran 2/3 report and Lowtran 7 model*, Philips Laboratory PL/GPOS, Hanscom AFB, MA.
- Knight, C., van Kemenade, J., Deveci, Z. (2007) *Effect of Outdoor Lighting on Perception and Appreciation of End-Users*. Proc. Of 18th Biennial TRB Visibility Symposium, College Station TX, United States.
- Kraats, J. van de, Norren, D. van (2007) *Optical density of the aging human ocular media in the visible and the UV*. J. Opt. Soc. Am. A/Vol. 24, No. 7/July 2007.
- Middleton, W.E.K. (1952). *Vision through the atmosphere*. Toronto: University of Toronto Press.
- Raynham, P. & Saksvikrønning, T. (2003). *White light and facial recognition*. The Lighting Journal (Jan/Feb 2003), 29-33.
- Rea, M.S., Bullough, J.D., Freyssinier Nova, J.P., & Bierman, A. (2004). *A proposed unified system of photometry*. Lighting Research and Technology, 36, (2), 85-111.

- Rogé, J., Pébayle, T., Lambilliotte, E., Spitzenstetter, F., Giselbrecht, D., & Muzet, A. (2004). *Influence of age, speed and duration of monotonous driving task in traffic on the drivers useful visual field*. Vision Research, 44, 2737-2744.
- Rombauts, P., Vanderwyngaerde, H. Magetto, G. (1989). *On residential area lighting and glare*. Lux Europa, Budapest.
- Schmidt-Clausen, H.J. & Bindels, J.T.H. (1974). *Assessment of discomfort glare in motor vehicle lighting*. Lighting Research and Technology, 6, (2), 79-88.
- Schreuder, D.A., Settels, P.J.M., Schmidt, R., & Visser, R. (2008). *Handboek Verlichtingstechniek.[Handbook lighting technology](in Dutch)* The Hague, The Netherlands: SDU Uitgevers.
- Shapley R and Enroth-Cugell C (1984) *Visual Adaptation and Retinal Gain Controls*, In: Progress in Retinal Research, vol. 3, ed. N. Osborne and G. Chader, Pergamon, London, p. 263-346
- Stockman, A. & Sharpe, L.T. (2006). *Into the twilight zone: the complexities of mesopic vision and luminous efficiency*. Ophthalmic and Physiological Optics, 26, (3), 225-239.
- Yao, Q., Sun, Y., & Lin, Y. (2009). *Research on facial recognition and color identification under CMH and HPS lamps for road lighting*. Leukos, 6, (2), 160-178.
- Várady, G., Freiding, A., Eloholma, M., Halonen, L., Walkey, H., Goodman, T., & Alferdinck, J.W.A.M. (2007). *Mesopic visual efficiency III: discrimination threshold measurements*. Lighting Research and Technology, 39, (4), 355-364.
- Walkey, H., Orreveläinen, P., Babur, J., Halonen, L., Goodman, T., Alferdinck, J.W.A.M., Freiding, A., & Szalmás, A. (2007). *Mesopic visual efficiency II: reaction time experiments*. Lighting Research and Technology, 39, (4), 335-354.
- Vos, J.J., Lazet, A., & Bouman, M.A. (1956). *Visual contrast thresholds in practical problems*. Journal of the Optical Society of America, 46, (12), 1065-1068.
- Vos, J.J. (1971). *Do we really wish standardization of acuity testing?* Ophthalmologica, 162, 235-241.
- Wolfe, W.L. & Zissis, G.J. (1978). *The infrared handbook*. Washington, DC, USA: Office of Naval Research, Department of the Navy.
- Walraven, J., Enroth-Cugell, C. , Hood, D., MacLeod, D., Schnapf, J.: *The control of visual sensitivity*. In Visual perception: the neurophysiological foundations., Spillman, L., Werner, J., (Eds.). San Diego: Academic Press, 1990, ch. 5.



## 11 Signature

Soesterberg, december 2010

A handwritten signature in black ink, consisting of a large, stylized 'P' followed by a series of loops and a long horizontal stroke.

Ir. P.A.J. Punte  
Head of department

TNO Defence, Security and Safety

A handwritten signature in black ink, featuring a large, stylized 'J' followed by a series of loops and a long horizontal stroke.

ing. J.W.A.M. Alferdinck  
Author



## A Subject Information

Table A.1 Subject Information.

11-1

| Number | Group | Age group | Subject type  | Sex (m/f) | Age (years) | Visual acuity)* | Glasses/lenses | Remarks         |
|--------|-------|-----------|---------------|-----------|-------------|-----------------|----------------|-----------------|
| 1      | 1     | old       | observer      | f         | 67          | 1.5             | glasses        |                 |
| 2      | 1     | old       | observer      | m         | 69          | 1.5             | glasses        |                 |
| 3      | 1     | old       | observer      | m         | 73          | 1.5             | -              |                 |
| 4      | 1     | old       | observer      | m         | 62          | 2               | glasses        |                 |
| 5      | 1     | old       | observer      | m         | 61          | 2               | -              |                 |
| 6      | 1     | old       | observer      | m         | 59          | 1.5             | glasses        |                 |
| 7      | 1     | old       | observer      | m         | 69          | 2               | glasses        |                 |
| 8      | 1     | old       | observer      | f         | 58          | 2.2             | glasses        |                 |
| 9      | 1     | old       | observer      | m         | 65          | 1               | glasses        |                 |
| 10     | 1     | old       | observer      | m         | 53          | 1.5             | glasses        |                 |
| 11     | 1     | old       | target person | m         | 54          | 2               | glasses        | target person A |
| 12     | 1     | old       | target person | f         | 63          | 0.65            | -              | target person B |
| 13     | 1     | old       | target person | m         | 66          | -               | -              | target person C |
| 14     | 2     | old       | observer      | f         | 51          | 1.5             | no             |                 |
| 15     | 2     | old       | target person | f         | 53          | 1.25            | yes            | target person B |
| 16     | 2     | old       | observer      | f         | 60          | 1.5             | yes            |                 |
| 17     | 2     | old       | observer      | f         | 53          | 1.5             | yes            |                 |
| 18     | 2     | old       | observer      | m         | 66          | 2               | yes            |                 |
| 19     | 2     | old       | observer      | f         | 53          | 1.5             | no             |                 |
| 20     | 2     | old       | target person | f         | 58          | 2               | yes            | target person C |
| 21     | 2     | old       | observer      | m         | 62          | 1.5             | yes            |                 |
| 22     | 2     | old       | observer      | m         | 60          | 1.5             | yes            |                 |
| 23     | 2     | old       | observer      | f         | 58          | 1.5             | no             |                 |
| 24     | 2     | old       | observer      | f         | 49          | 1.5             | yes            |                 |
| 25     | 2     | old       | target person | m         | 63          | 1.5             | no             | target person A |
| 26     | 2     | old       | observer      | m         | 54          | 2.5             | yes            |                 |
| 27     | 2     | old       | observer      | m         | 62          | 1.5             | yes            |                 |
| 28     | 3     | young     | observer      | m         | 16          | 2               | no             |                 |
| 29     | 3     | young     | target person | f         | 17          | 2.5             | yes            | C               |
| 30     | 3     | young     | observer      | m         | 17          | 2               | no             |                 |
| 31     | 3     | young     | observer      | m         | 17          | 2               | no             |                 |
| 32     | 3     | young     | observer      | m         | 17          | 2               | no             |                 |
| 33     | 3     | young     | observer      | m         | 17          | 3               | no             |                 |
| 34     | 3     | young     | observer      | m         | 17          | 2               | yes            | Mild            |

|    |   |       |                  |   |    |      |     |  |                 |
|----|---|-------|------------------|---|----|------|-----|--|-----------------|
|    |   |       |                  |   |    |      |     |  | colour<br>blind |
| 35 | 3 | young | observer         | f | 17 | 1.5  | yes |  |                 |
| 36 | 3 | young | observer         | f | 17 | 2    | yes |  |                 |
| 37 | 3 | young | observer         | f | 16 | 2    | yes |  |                 |
| 38 | 3 | young | target<br>person | f | 17 | 2    | no  |  | B               |
| 39 | 3 | young | observer         | f | 16 | 2    | no  |  |                 |
| 40 | 3 | young | observer         | f | 16 | 2    | yes |  |                 |
| 41 | 3 | young | observer         | f | 16 | 2    | yes |  |                 |
| 42 | 3 | young | target<br>person | m | 17 | 1.5  | no  |  | A               |
| 43 | 3 | young | observer         | m | 16 | 1.25 | no  |  |                 |
| 44 | 3 | young | observer         | m | 18 | 2    | no  |  |                 |
| 45 | 4 | young | observer         | f | 16 | 2    | no  |  |                 |
| 46 | 4 | young | observer         | m | 16 | 2.5  | no  |  |                 |
| 47 | 4 | young | observer         | f | 16 | 2.5  | yes |  |                 |
| 48 | 4 | young | observer         | m | 16 | 2    | no  |  |                 |
| 49 | 4 | young | observer         | m | 16 | 2.5  | no  |  |                 |
| 50 | 4 | young | target<br>person | m | 16 | ?    | no  |  | B               |
| 51 | 4 | young | observer         | m | 17 | 2    | no  |  |                 |
| 52 | 4 | young | observer         | m | 17 | 2    | no  |  |                 |
| 53 | 4 | young | observer         | f | 16 | 2    | no  |  |                 |
| 54 | 4 | young | target<br>person | f | 16 | ?    | no  |  | A               |
| 55 | 4 | young | observer         | m | 17 | 2    | no  |  |                 |
| 56 | 4 | young | target<br>person | m | 17 | ?    | no  |  | C               |
| 57 | 4 | young | observer         | m | 17 | 1.25 | yes |  |                 |

## B Subject instruction and scoring form

### B.1 Subject instruction (in Dutch)

#### *Proefpersooninstructie experiment Gezichtsherkenning*

##### Doel

TNO doet voor de overheid (ministerie van VROM) een onderzoek naar het gebruik van nieuwe soorten openbare verlichting. Momenteel zijn er allerlei nieuwe verlichtingstechnieken (denk aan de LED-lamp) mogelijk, waarmee tegen soms aanzienlijke lagere verbruikskosten hetzelfde lichtniveau op straat gerealiseerd kan worden. Daarbij is één van de onderzoeksvragen, die te maken heeft met maatschappelijke veiligheid: “Kun je met die nieuwe lampen, bij dezelfde lichtsterkte onder dezelfde lichtomstandigheden ’s avonds (als het donker is) op straat, personen even goed herkennen als bij de huidige straatverlichting?” Met een herkenningsexperiment hopen we deze onderzoeksvraag te kunnen beantwoorden.

##### Taak

In de hal van TNO is zijn een rij lantaarnpalen opgesteld. Deze zijn voorzien van verschillende soorten verlichting. Onder de lantaarnpalen zijn zogenaamde doelpersonen opgesteld waarvan het gezicht door u herkend moet worden. U nadert de doelpersoon vanaf ruime afstand. Bij een aantal afstanden (aangegeven door pylonen) houdt u stil en geeft u aan hoe goed het gezicht te herkennen is op een schaal van 0 (absoluut niet te herkennen) tot 100 (zeer goed te herkennen) (Zie bijlage). Het kan zijn dat de persoon een onbekende voor u is. Toch kunt dan wel zeggen of u onder deze omstandigheden het gezicht zou kunnen herkennen.

Op een aantal momenten tijdens het experiment zal u gevraagd worden om de verblinding van de lichtinstallatie te beoordelen. Dit doet u op een schaal van 1 (ondragelijke verblinding) tot 9 (niet noemenswaardig) (Zie bijlage).

Een aantal van u zal uitgekozen worden om dienst te doen als doelpersoon.

##### Duur

Experiment bestaat uit zes delen van elk ongeveer een half uur. Tussen de delen hebt u pauze en zal de experimenteer opstelling aangepast moeten worden.

Als u nog vragen hebt stel deze dan aan de proefleider.

Succes!

Bijlage: Scoreformulier

## B.2 Scoring form

Figure 37 (left) shows the scoring form in Dutch at a A4 paper size that was filled in by the subjects for each lamp and light level condition. The explanation to this sheet is at the right. The translation of this form is shown in Figure 38. Note that the letters that are essential during the experiment are large, because they need to be legible at low illuminance levels.

**Scoreformulier**

|                  |             |                |     |
|------------------|-------------|----------------|-----|
| Proef-persoon:   | ...         | Datum:         | ... |
| Proef-persoonnr: | ...         | Tijd:          | ... |
| Lamp)*:          | 1 2 3 4 5 6 | Lichtniveau)*: | A B |

)\* Omcirkelen

| Stap | Herkenning<br>(0...100%) |   |   | Verblinding<br>(9...1) |   |   |
|------|--------------------------|---|---|------------------------|---|---|
|      | A                        | B | C | A                      | B | C |
| 1    |                          |   |   |                        |   |   |
| 2    |                          |   |   |                        |   |   |
| 3    |                          |   |   |                        |   |   |
| 4    |                          |   |   |                        |   |   |
| 5    |                          |   |   |                        |   |   |
| 6    |                          |   |   |                        |   |   |
| 7    |                          |   |   |                        |   |   |
| 8    |                          |   |   |                        |   |   |
| 9    |                          |   |   |                        |   |   |
| 10   |                          |   |   |                        |   |   |
| 11   |                          |   |   |                        |   |   |

Scoreformulier, 21-6-2010 16:00

**Toelichting**

Hoe beoordeelt u de herkenbaarheid van het gezicht? (0...100%)

| Score | Herkenbaarheid |
|-------|----------------|
| 0     | Absoluut niet  |
| 50    | Matig          |
| 100   | Zeer goed      |

Bijvoorbeeld: 65

Hoe beoordeelt u de verblinding van de verlichtingsinstallatie? (9...1)

| Score | Verblinding         |
|-------|---------------------|
| 9     | Niet noemenswaardig |
| 8     | -                   |
| 7     | Acceptabel          |
| 6     | -                   |
| 5     | Niet toelaatbaar    |
| 4     | -                   |
| 3     | Storend             |
| 2     | -                   |
| 1     | Ondraaglijk         |

Bijvoorbeeld: 5,8

Scoreformulier, 21-6-2010 16:00

Figure 37 Score sheet (paper size A4) in Dutch as presented to the subjects (left) and the explanation at the back (right).

Scoring form

Subject:

...

Date:

...

Subject no:

...

Time:

...

Language:

1 2 3 4 5 6

Light level:

A B

)\* Barcode

Step

Recognition  
(0...100%)

Glare  
(9...1)

A

B

C

A

B

C

1

2

3

4

5

6

7

8

9

10

11

Scoring form 2-15, 16-20/20 15/15

1

Explanation

How do you assess the recognisability of the face? (0...100%)

Score

Recognisability

0

Absolutely not

50

Moderate

100

Very good

Example:

55

How do you assess the glare of the lighting installation? (9...1)

Score

Glare

9

Inappreciable

8

-

7

Acceptable

6

-

5

Just allowable

4

-

3

Disturbing

2

-

1

Unbearable

Example:

5,8

Explanation 2-15, 16-20/20 15/15

2

Figure 38 Score sheet (paper size A4) in English (left) and the explanation at the back (right).



## C Mesopic model

The mesopic luminance divided by the photopic luminance according the mesopic model MES 2 that is proposed by the CIE (2010) is listed in Table C.1 as a function of photopic background luminance and S/P-ratio. This table is a extensive version of Table 11 in CIE (2010).

Table C.1 The mesopic luminance divided by the photopic luminance according the mesopic model MES 2 that is proposed by the CIE (2010) as a function of photopic background luminance ( $L_{\text{photopic}}$ ) and S/P-ratio.

| S/P-ratio | $L_{\text{photopic}}$<br>( $\text{cd/m}^2$ ) => | 0.0001 | 0.003 | 0.01 | 0.03 | 0.1  | 0.3  | 1    | 3    | 10   |
|-----------|---|--------|-------|------|------|------|------|------|------|------|
| 0.25      |   | 0.25   | 0.25  | 0.25 | 0.48 | 0.71 | 0.82 | 0.91 | 0.98 | 1.00 |
| 0.35      |   | 0.35   | 0.35  | 0.35 | 0.58 | 0.75 | 0.85 | 0.93 | 0.98 | 1.00 |
| 0.45      |   | 0.45   | 0.45  | 0.45 | 0.66 | 0.79 | 0.87 | 0.94 | 0.98 | 1.00 |
| 0.55      |   | 0.55   | 0.55  | 0.57 | 0.73 | 0.83 | 0.90 | 0.95 | 0.99 | 1.00 |
| 0.65      |   | 0.65   | 0.65  | 0.69 | 0.80 | 0.87 | 0.92 | 0.96 | 0.99 | 1.00 |
| 0.75      |   | 0.75   | 0.75  | 0.79 | 0.86 | 0.91 | 0.94 | 0.97 | 0.99 | 1.00 |
| 0.85      |   | 0.85   | 0.85  | 0.88 | 0.92 | 0.95 | 0.97 | 0.98 | 1.00 | 1.00 |
| 0.95      |   | 0.95   | 0.95  | 0.96 | 0.97 | 0.98 | 0.99 | 0.99 | 1.00 | 1.00 |
| 1.05      |   | 1.05   | 1.05  | 1.04 | 1.03 | 1.02 | 1.01 | 1.01 | 1.00 | 1.00 |
| 1.15      |   | 1.15   | 1.15  | 1.11 | 1.08 | 1.05 | 1.03 | 1.02 | 1.00 | 1.00 |
| 1.25      |   | 1.25   | 1.25  | 1.18 | 1.13 | 1.08 | 1.05 | 1.03 | 1.01 | 1.00 |
| 1.35      |   | 1.35   | 1.35  | 1.25 | 1.18 | 1.12 | 1.07 | 1.04 | 1.01 | 1.00 |
| 1.45      |   | 1.45   | 1.45  | 1.32 | 1.22 | 1.15 | 1.09 | 1.05 | 1.01 | 1.00 |
| 1.55      |   | 1.55   | 1.55  | 1.38 | 1.27 | 1.18 | 1.11 | 1.06 | 1.02 | 1.00 |
| 1.65      |   | 1.65   | 1.65  | 1.45 | 1.32 | 1.21 | 1.13 | 1.07 | 1.02 | 1.00 |
| 1.75      |   | 1.75   | 1.75  | 1.51 | 1.36 | 1.24 | 1.15 | 1.08 | 1.02 | 1.00 |
| 1.85      |   | 1.85   | 1.85  | 1.57 | 1.40 | 1.27 | 1.17 | 1.09 | 1.03 | 1.00 |
| 1.95      |   | 1.95   | 1.95  | 1.63 | 1.45 | 1.30 | 1.19 | 1.10 | 1.03 | 1.00 |
| 2.05      |   | 2.05   | 2.05  | 1.69 | 1.49 | 1.32 | 1.21 | 1.11 | 1.03 | 1.00 |
| 2.15      |   | 2.15   | 2.15  | 1.74 | 1.53 | 1.35 | 1.23 | 1.12 | 1.03 | 1.00 |
| 2.25      |   | 2.25   | 2.25  | 1.80 | 1.57 | 1.38 | 1.24 | 1.12 | 1.04 | 1.00 |
| 2.35      |   | 2.35   | 2.35  | 1.85 | 1.61 | 1.41 | 1.26 | 1.13 | 1.04 | 1.00 |
| 2.45      |   | 2.45   | 2.45  | 1.91 | 1.65 | 1.43 | 1.28 | 1.14 | 1.04 | 1.00 |
| 2.55      |   | 2.55   | 2.55  | 1.96 | 1.69 | 1.46 | 1.30 | 1.15 | 1.04 | 1.00 |
| 2.65      |   | 2.65   | 2.65  | 2.01 | 1.73 | 1.49 | 1.31 | 1.16 | 1.05 | 1.00 |
| 2.75      |   | 2.75   | 2.75  | 2.07 | 1.76 | 1.51 | 1.33 | 1.17 | 1.05 | 1.00 |
| 2.85      |   | 2.85   | 2.85  | 2.12 | 1.80 | 1.54 | 1.35 | 1.18 | 1.05 | 1.00 |
| 2.95      |   | 2.95   | 2.95  | 2.17 | 1.84 | 1.56 | 1.36 | 1.19 | 1.05 | 1.00 |
| 3.05      |   | 3.05   | 3.05  | 2.22 | 1.88 | 1.59 | 1.38 | 1.19 | 1.06 | 1.00 |
| 3.15      |   | 3.15   | 3.15  | 2.27 | 1.91 | 1.61 | 1.40 | 1.20 | 1.06 | 1.00 |
| 3.25      |   | 3.25   | 3.25  | 2.32 | 1.95 | 1.64 | 1.41 | 1.21 | 1.06 | 1.00 |



## Distribution list

**The following agencies/people will receive a complete copy of the report.**

- 5 ex. Ministry of Infrastructure and Environment (I&M), B.H. Bussemaker
- 2 ex. TNO Defence, Security and Safety, location Soesterberg  
Archief
- 3 ex. TNO Defence, Security and Safety, location Soesterberg  
ing. J.W.A.M. Alferdinck  
dr. M.A. Hogervorst  
ir. P.A.J. Punte
- 2 ex TNO Defence, Security and Safety, Location Den Haag  
prof. dr. A.M.J. van Eijk  
dr. J.T. Kusmierczyk